

Design of slender steel pedestrian bridges

Applying a moving jogger load model including Human-Structure Interaction



Design of slender steel pedestrian bridges

Applying a moving jogger load model
including Human-Structure Interaction

by

T. van de Velde

to obtain the degree of Master of Science
in Structural Engineering

at the Delft University of Technology,

Student number:	4301730	
Chair committee:	Dr. ir. F. P. van der Meer,	TU Delft
Thesis committee:	Prof. Dr. ir. M. Veljkovic,	TU Delft
	Dr. ir. A. Tsouvalas,	TU Delft
	ir. E. Bosman,	Witteveen+Bos

Preface

This master thesis is written as an end to my master Structural Engineering with the specialization Structural Mechanics. During my short period as an intern I came across the engineering problems with the dynamics of slender footbridges. This sparked my enthusiasm and for the last 11 months I learned a lot about this topic, which gave me quite some troubles. Therefore, I would really like to thank Esli Bosman and Wouter Claassen from Witteveen+Bos for helping me during this process. Even during the obligated period of working from home, due to COVID-19, they helped me when it was needed. The biggest thanks goes to Carmen Ramkhelawan, my girlfriend, for keeping up the good spirit and for the often needed talks!

I hope you will enjoy reading my thesis!

Not added in this document are the Matlab codes and animations. These can be requested by sending an e-mail to: t.velde94@gmail.com

*T. van de Velde
Delft, August 2020*

Contents

Abstract	1
I Background and problem statement	2
1 Introduction	3
2 State-of-art Research	4
2.1 Research on dynamic structure characteristics	4
2.2 Research on dynamic load models	5
2.2.1 Dynamic forces	5
2.2.2 Stochastic analysis	9
2.2.3 Human-Structure Interaction (HSI)	13
2.3 Research on the reduction of vibrations	19
2.3.1 Design optimization	19
2.3.2 Additional damping devices	20
3 Research set-up	23
3.1 Problem definition	23
3.2 Scope definition	24
3.3 Research objectives	24
3.4 Methodology	25
4 Literature - Background information	27
4.1 Possible structural designs	27
4.1.1 Chosen cross section type for this research	28
4.2 Dynamics of footbridges	29
4.2.1 Footbridge behaviour	29
4.2.2 Damping	32
4.2.3 Codes and guidelines	33
II Initial design	39
5 Initial design	40
5.1 Design basis	40
5.2 Considered loads	41
5.2.1 Self weight	41
5.2.2 Permanent loads	42
5.2.3 Traffic loads	42
5.2.4 Wind loads	43
5.2.5 Accidental loads	43
5.2.6 Vertical dynamic loads due to humans	44
5.3 Load combinations	44
5.3.1 Ultimate Limit State	44
5.3.2 Serviceability Limit State	46
5.4 Structural design verifications	47
III Jogger load case	49
6 Model description	50
6.1 Basic model	50
6.2 Basic model - verification	54
6.2.1 Static verification	54

6.2.2	Dynamic MF verification	56
6.3	Model including HSI	57
6.4	Model including HSI - verification	60
6.5	Matlab workflow	62
7	Jogger load case - Excluding Human-Structure Interaction	64
7.1	Moving Force model - Input	64
7.2	Moving Force model - Results	65
7.3	Sub-conclusions	68
8	Jogger load case - Including Human-Structure Interaction	69
8.1	Mass-Spring-Dashpot model - Input	69
8.2	Mass-Spring-Dashpot model - Results	70
8.3	Comparison between MF and MSD model results	72
8.4	Sub-conclusions	73
9	Jogger load case - Stochastic analysis	74
9.1	Stochastic analysis - Input	74
9.2	Stochastic analysis - Results	75
9.3	Sub-conclusions	77
10	Jogger load case - Multiple joggers	79
10.1	Multiple joggers - Model description	79
10.2	Multiple joggers - Input	80
10.3	Multiple joggers - Result	81
10.3.1	Research to check MSD model results	83
10.4	Comparison between MF and MSD model for multiple joggers	86
10.5	Sub-conclusions	86
IV	Conclusions	88
11	Discussion	89
12	Conclusion	91
13	Recommendations	93
V	Appendices	94
A	Impulse of force models	95
B	2DOF MSD model stationary - JRC load	97
	Bibliography	98

Abstract

Developments in structural engineering give rise to the ability of increasing the slenderness within the design of footbridges. However, this often results in a fundamental eigenfrequency which coincides with the step frequency range of humans on the bridge. This can lead to uncomfortable vibrations of the structure. In order to maintain the comfortability, the Dutch national annex of the Eurocode prescribes to consider a dynamic jogger load case, which is often governing for the slenderness of a design. In this thesis, a moving model for the dynamic jogger load case with the addition of human-structure interaction (HSI) in vertical direction is considered in order to reduce conservatism. Using a simplified 1-dimensional Finite Element representation of a footbridge consisting of 4 HEA320 profiles, a comparison is made between a moving force (MF) and a moving mass-spring-dashpot (MSD) model representing the jogger. Different analyses of a single jogger case are made to investigate the influence of the following simplifications: 1) applying a stationary instead of a moving dynamic load, 2) applying a load model neglecting the separation between jogger and bridge and 3) neglecting the subject variability. The Dutch national annex prescribes the use of multiple joggers during the load case. Therefore, an initial research is done on the effect of HSI on a multiple jogger case. It is found that the HSI results in a decrease of the maximum accelerations for all load cases. The effect increases when the joggers-to-bridge mass ratio increases. The same holds for the influence of separation. The results show that reduction of the maximum acceleration due to the addition of the HSI is generally not large enough to result in an increase of the maximum slenderness.



Background and problem statement

1

Introduction

Developments in structural engineering give rise to the ability of increasing the slenderness within the design of footbridges. This can lead to the reduction of material which may be cheaper, more environmentally friendly and more aesthetically appealing. A side effect of this is the reduction of the stiffness of the entire bridge, which also lowers the eigenfrequencies. This means a closer look at the dynamic response of the bridge is required. The most common dynamic loads on footbridges, besides wind loading, are forces due to pedestrians and joggers [17]. These dynamic loads introduce vibrations that may become a problem when eigenfrequencies of the bridge coincide with the step frequency range of the pedestrians that make use of the bridge.

There are a lot of uncertainties in the dynamic analysis, both on the loading and the structural side. What is the real dynamic load that a footbridge experiences during its lifetime and how can we correctly model this? Of course codes and guidelines have considered this, but a lot of research claims that the prescribed analyses may be too conservative. On the structural side it is difficult to predict the dynamic characteristics of a specific design prior to the actual built bridge. It is therefore difficult for the engineer to be sure about the structural behaviour of a design. To make sure that the response of the bridge will not exceed the requirements, the design will be made using a conservative approach. This conservatism is included in two different approaches which deal with the uncertainties of the dynamic analysis. The first approach to meet the dynamic requirements is to add changes in the design to make sure that the fundamental frequency of the bridge design does not coincide with the step frequency of the pedestrians. When this is achieved, no resonance can occur and the response will be acceptable. These changes will consider the uncertainties in the loading and structural resistance and will therefore consider the most unfavourable conditions. The 'tuning' of the frequency is often achieved by increasing the stiffness, which can be done by increasing the girders height. This design change will therefore have a lower height-over-span ratio (slenderness). This approach is contradictory to the ambition of slender footbridges. When a high slenderness ratio is desired for a design this first approach may not provide the desired results.

When the slenderness ratio of the footbridges is required to be high it may become impossible to change the characteristics so that no resonance can occur. This is where the second approach can be used. This approach is to include so called vibration mitigation devices which reduce the vibrations by 'absorbing' the energy of the vibrations. Within footbridge designs Tuned Mass Dampers (TMD's) are widely used. However, these devices are sensitive to changes in the dynamic characteristics of the bridge and can therefore be inefficient when the characteristics differ from the design conditions used. This introduces the need of conservatism in this approach. For which vibration modes the TMD is required determines the location of the devices and how many in total are needed. Due to the uncertainties of the structural characteristics and loads the engineer will make sure that for multiple locations dampers can be placed. Which means a conservative amount of measures need to be made and the additional loads due to the weight of the dampers have to be taken into account. So this approach also includes conservatism that can reduce the slenderness of the footbridge design. This master thesis research aims to provide additional knowledge for the dynamic analysis so a footbridge design can become more slender considering the dynamic response due to pedestrian loading.

2

State-of-art Research

Within the field of footbridges dynamics a lot of research is done. This chapter will give a summary of the main research categories. The main focus of this research is finding the maximum slenderness possible for a footbridge design. So for this chapter the objective is to find out what research is done to reduce the amount of conservatism within footbridge dynamics. At the end of this chapter a better understanding is established about the knowledges gaps that are still there and if certain assumptions need further research. Based on this a research goal will be described in chapter 3.

The majority of the research can be divided into the following three fields:

- The structure characteristics
- The load models
- The reduction of vibrations

Obviously these three fields have a big overlap. The loads combined with the structures dynamic characteristics is the essence of the dynamic analysis. However separating these helps to understand how to predict the behaviour of a bridge when it is in use. When the dynamic analysis results in unfavourable results using a certain structure characterization and dynamic load model, additional measures need to be taken to make sure the bridge is comfortable and safe. This results in the third research category in which the vibration reduction is the main goal of the different researches.

2.1. Research on dynamic structure characteristics

When designing a structure there will be assumptions or simplifications. A model is an approximation of the reality, so there will always be a difference which may be unknown during the design phase. The simplifications and assumption will introduce deviations from the reality. However, by using safety factors it is made sure that the design is safe. For example, during the design verification the dimensions and geometry is assumed to be the same as when the structure is build. During construction this may be slightly different due to a lot of reasons. Statistically speaking, this possible lower resistance of the cross section is considered in the safety factor to make sure the structure is safe. However, dynamically this as build structure may behave differently and produce higher vibrations. So there will always be some uncertainties about the dynamic behaviour of a structure after construction.

The estimation of the dynamic properties is however important if the structure is build (almost) perfectly as described. It can be concluded that the dynamic characterization has been improved significantly due to the dynamic analysis ability of Finite Element software. The real stiffness and mass distribution of a design can easily be integrated within this software, which result in a more accurate understanding of the dynamic characteristics of a design.

The biggest knowledge gap in the characterization is found in the determination of the overall damping. Due to the complexity and combination of the large amount of different damping phenomena it is common to assume a linear damping and be conservative about the amount. This is a simplification

that is most certainly not correct all of the time. However, if small deformations, of the vibrations, are considered, this is accurate enough for implementation.

Because of the combination of different damping phenomena it is hard to estimate this linearized damping value. A common way to deal with this in practice is being conservative during the design. So a low damping ratio is used during the design phase. When the results of the calculation prescribe that the maximum acceleration due to comfort levels are (even though some design changes are already made) exceeded, the required space for the possible location of the dampers need to be integrated in the design. After construction the real dynamic characteristics are measured and it is determined if the dampers will be placed. This procedure is the most conservative and will result in a bridge that will meet the serviceability requirements for pedestrian induced vibrations. That is why it is also recommended by the JRC guideline [17].

To improve the knowledge about damping a lot of measurements have to be done, which is not feasible in this master thesis research. So the dynamic structure characterization will not be the field which this research will elaborate on.

2.2. Research on dynamic load models

During the design life of a bridge different load cases can be identified. In the Eurocode including the Dutch national annex it is said that the engineer has to consider crowd loading, joggers and vandalism (jumping). First of all it is important to know what forces these different load cases introduce on the structure. It is clear that the forces differ for a walking or running human being for example. Different researches are done on these different forces and how to model them. The important result they try to achieve is a realistic force model which can be applied on the footbridges design for a walking, running or jumping human beings. It is already known that the walking characteristics of pedestrians can change in crowds due to the limited area due to the surrounding humans. Therefore, when crowd conditions are considered it is possible that the forces change compared to the single human case. These categories considering the dynamic load models will be treated in the following paragraphs.

The research on the dynamic loads on footbridges can roughly be divided into the following categories:

- research on Dynamic forces [2.2.1](#)
- implementation of stochastic analysis [2.2.2](#)
- research on Human-Structure Interaction [2.2.3](#)

2.2.1. Dynamic forces

In this research the focus is on the vertical vibrations of the footbridge, so this part will also be focused on the vertical forces. All the information is based on measurements on a fixed surface, because a flexible surface can introduce changes in the forces. This phenomena on flexible surfaces will be explained in the part about Human-Structure interaction [2.2.3](#).

In order to make a reasonable assessment of the dynamic serviceability of a footbridge design it is necessary that the dynamic loads are predicted accurately. For this a mathematical model of the human-induced loads is needed. It is possible to make these models in the time and frequency domain. In this thesis only the time domain models will be discussed. Within the time domain force models there are in general two types: 1) deterministic and 2) probabilistic. The deterministic models try to find 1 general force model for each load case, which will be discussed here. The probabilistic models depends on stochastic parameters which may influence the force of a load case. A more detailed explanation of how the probability is considered in the stochastic analysis for human induced vibrations can be found in [2.2.2](#).

For the deterministic time domain load models it assumed that the step frequency and the force will be consistent. Therefore the load induced by a human is assumed to be periodic. A common way to deal with a periodic force is to represent it with a Fourier Series. Therefore, the human induced loading can

be expressed as:

$$F_p(t) = G + \sum_{i=1}^n G \alpha_i \sin(2\pi i f_p t - \phi_i)$$

with:

i = the order number of the harmonic (2.1)

n = total number of considered harmonics

G = person weight [N]

α_i = Dynamic Load Factor (DLF) [-]

f_p = step frequency [Hz]

ϕ_i = the phase shift for the i th harmonic

Based on this decomposition a lot of research is done to quantify the DLF (the Fourier's coefficients in a more general sense). The DLF, the factor between the static and dynamic load, is the basis of the time domain load models. To make sure that the possibility of resonance occurring is included within the mathematical load model it is important to use more than 1 harmonic in the force definition. Resonance may occur when an eigenfrequency of the bridge is an integer multiple of the pacing rate, so these harmonics are needed in the model.

Different researchers have done measurements on the forces induced by pedestrians at different types of moving behaviour. It is clear that walking and running produce different loading curves, see figure 2.1. The load curve due to a walking pattern is found to have two peaks. The first peak is due to the heel strike and the second due to pushing off towards the next step. During jogging this pattern is different. Here only a single peak occurs, but the magnitude is significantly larger.

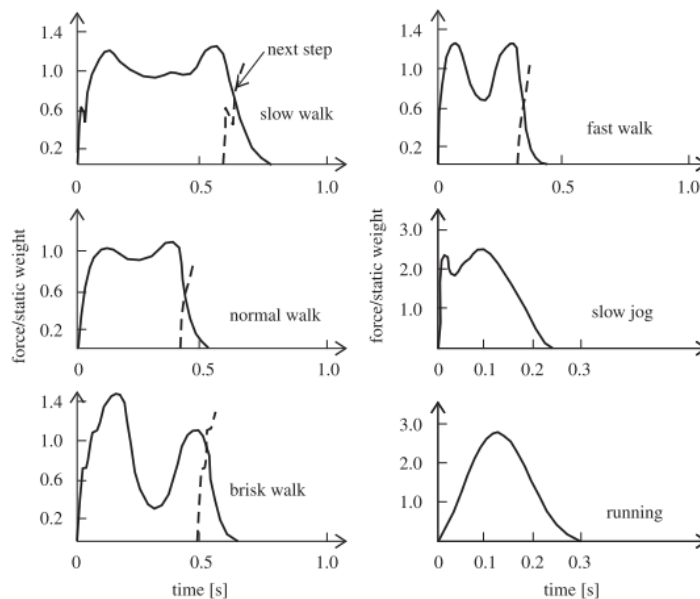


Figure 2.1: Load curves for different types of human movement, displayed as a ratio of the applied force and static weight [24]

Another big difference between the normal walking and running is found when multiple steps are considered for the load cases. During walking there are essentially two different phases: a single foot is in contact with the floor or both feet. This means that before the load curve of a single step ends, the next load curve already starts. During running this is not the case, because there is a "flying" period in between the steps, see figure 2.2.

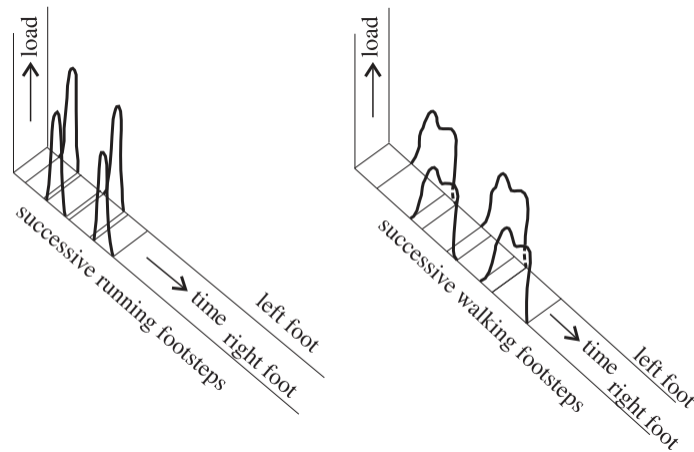


Figure 2.2: The vertical ground reaction force patterns for running and walking [24]

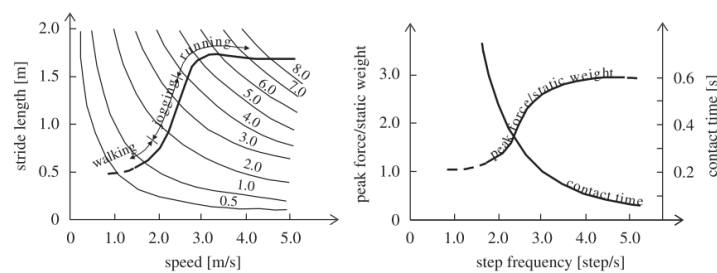


Figure 2.3: Dependency of walking speed, step length, contact duration and peak force as a function of the step frequency [24]

In 1982 Wheeler did research on the contact forces depending on different walking gaits, from slow walking to fast running. He proposed a dependency of the walking speed, step length, contact duration and peak force as a function of the step frequency (see figure 2.3). However, in the basis of load models it is common to assume that the step length is independent of the step frequency. Therefore, a linear relation holds between the step frequency and the walking speed is found [15].

The contact duration is found to have a nonlinear relation with the step frequency. When the load curve for a walking pedestrian is represented by a Fourier series, it is modelled with a continuous contact. So the contact time is not considered in the model, because the next step is already in contact with the structure. When the running behaviour is modelled, the separation that occurs need to be considered, so the contact time will become relevant. The running forces modelled using a Fourier series representation needs to be truncated to zero when there is no contact. So in that load case the contact time needs to be considered.

When the different researches that have been done on the DLF of walking humans are considered, a clear progression of knowledge can be seen. A clear explanation of the researches was made in the literature review by Racic [24].

The biggest progression can be seen in: 1) the number of harmonics considered and 2) the dependency on frequency. An increase in the knowledge of the higher harmonics lead to the recommendation of the first 4 harmonics that needs to be included. There are however some difference in the proposed values for the DLFs for these first 4 harmonics. The research of Rainer suggested that the DLFs depend on the frequency of the activity (walking, running, jumping). Based on this knowledge Kerr made formulas for the DLFs of the first 4 harmonics. Young tried to find more accurate design guidelines and based on the results of Kerr and other a further study was carried out on the DLFs. He again proposed that the DLFs of the first 4 harmonics are frequency dependent and proposed formulas for them. The different Fourier series that describe the vertical load curves of a walking human are illustrated in figure 2.4

When the Fourier series of both Young and Kerr are plotted a small difference can be observed. Both

are valid for the walking frequency range of 1 - 2.7 Hz. When the frequency is below 2.4 Hz the difference is small, but for higher frequencies the difference increases. The occurrence of step frequency describes that the frequencies between 2.4 and 2.7 are not likely. The influence on the response corresponding to the two models will be limited. Therefore, both the Fourier series proposed by Kerr and Young could be used to simulate the loading curve induced by walking humans without large differences in the response.

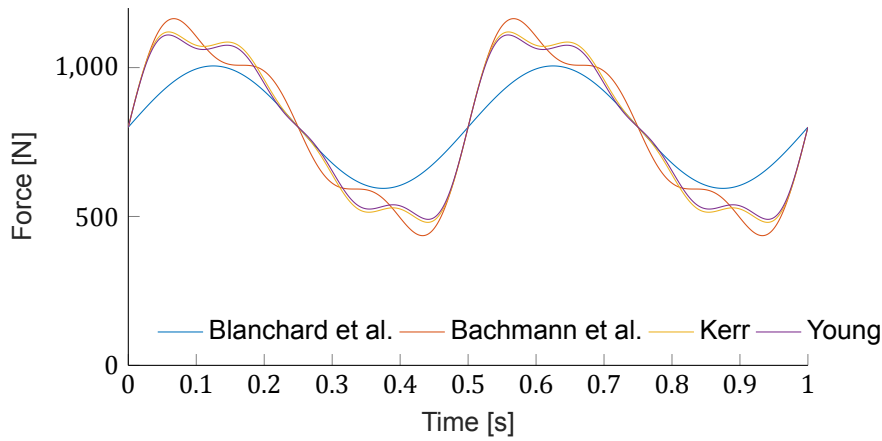


Figure 2.4: Load curves for walking using different Fourier series found by researchers. Step frequency is set to 2 Hz and human weight at 800 N.

Author(s)	DLFs for considered harmonics	Comment	Type of activity and its direction
Blanchard et al. [50]	$\alpha_1 = 0.257$	DLF is less for frequencies from 4 to 5 Hz	Walking—vertical
Bachmann and Ammann [7]	$\alpha_1 = 0.4 - 0.5$	Between 2.0 Hz and 2.4 Hz	Walking—vertical
Schulze (after Bachmann and Ammann [7])	$\alpha_2 = \alpha_3 = 0.1$ $\alpha_1 = 0.37\alpha_2 = 0.10\alpha_3 = 0.12\alpha_4 = 0.04\alpha_5 = 0.08$ $\alpha_1 = 0.039\alpha_2 = 0.01\alpha_3 = 0.043\alpha_4 = 0.012\alpha_5 = 0.015$ $\alpha_{1/2} = 0.037\alpha_1 = 0.204\alpha_{3/2} = 0.026\alpha_2 = 0.083\alpha_{5/2} = 0.024$	At approximately 2.0 Hz At 2.0 Hz At 2.0 Hz At 2.0 Hz	Walking—vertical Walking—lateral Walking—longitudinal
Rainer et al. [51]	$\alpha_1, \alpha_2, \alpha_3$ and α_4	DLFs are frequency dependent (Fig. 10)	Walking, running, jumping—vertical
Bachmann et al. [5]	$\alpha_1 = 0.4/0.5\alpha_2 = \alpha_3 = 0.1/-$ $\alpha_1 = \alpha_3 = 0.1$ $\alpha_{1/2} = 0.1\alpha_1 = 0.2\alpha_2 = 0.1$ $\alpha_1 = 1.6 \dots \alpha_2 = 0.7\alpha_3 = 0.2$	At 2.0/2.4 Hz At 2.0 Hz At 2.0 Hz At 2.0-3.0 Hz	Walking—vertical Walking—lateral Walking—longitudinal Running—vertical
Kerr [44]	$\alpha_1, \alpha_2 = 0.07\alpha_3 \approx 0.06$	α_1 is frequency dependent (Fig. 11)	Walking—vertical
Young [131]	$\alpha_1 = 0.37(f - 0.95) < 0.5$ $\alpha_2 = 0.054 + 0.0044f$ $\alpha_3 = 0.026 + 0.0050f$ $\alpha_4 = 0.010 + 0.0051f$	These are mean values for DLFs	Walking—vertical
Bachmann et al. [5]	$\alpha_1 = 1.8/1.7\alpha_2 = 1.3/1.1\alpha_3 = 0.7/0.5$ $\alpha_1 = 1.9/1.8\alpha_2 = 1.6/1.3\alpha_3 = 1.1/0.8$ $\alpha_1 = 0.17/0.38\alpha_2 = 0.10/0.12\alpha_3 = 0.04/0.02$ $\alpha_1 = 0.5$	Normal jump at 2.0/3.0 Hz High jump at 2.0/3.0 Hz At 1.6/2.4 Hz At 0.6 Hz	Jumping—vertical Jumping—vertical Bouncing—vertical Body swaying while standing—lateral Bouncing—vertical
Yao et al. [92]	$\alpha_1 = 0.7\alpha_2 = 0.25$	Free bouncing on a flexible platform with natural frequency of 2.0 Hz	Bouncing—vertical

Figure 2.5: Recommendations for the DLFs according to different researches [24]. For Kerr: $\alpha_1 = -0.2649f^3 + 1.3206f^2 - 1.7597f + 0.7613$

For the running load case there is a difference compared to the walking case. The most recent values of the DLFs for running are found by Bachmann et al. (see figure 2.5). The forces are similar however, there is a separation of the feet and the structure during the "flying" period. This is added to the load model by truncating the values below zero, so the tension forces are eliminated. If this truncated Fourier series is plotted a clear single peak for every step is found, with a slight influence of the higher harmonics (see figure 2.6). It needs to be mentioned that the contact duration is not an input parameter, but follows by implementing the step frequency into the Fourier series.

An important thing to note is that every person may generate a different load curve, even when walking at the same frequency. There is a variability in the way of walking and so in the DLFs as well. Therefore

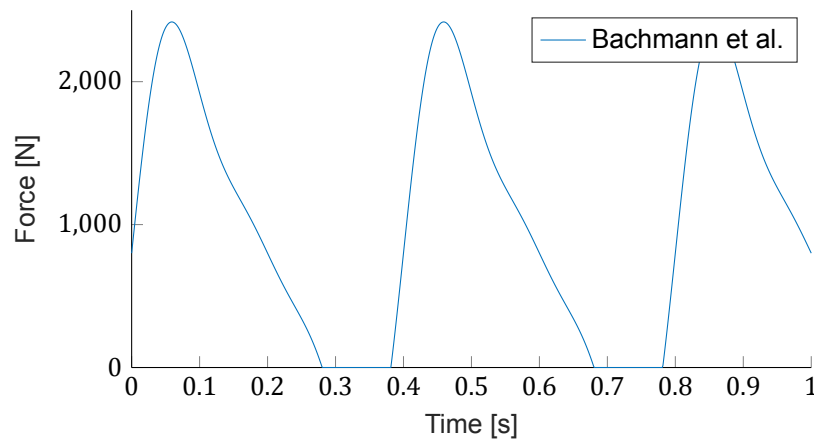


Figure 2.6: Load curve for running at 3 Hz defined by a truncated Fourier series with DLFs proposed by Bachmann et al [24]

all the values that have been given here are the best approximation of the research set, or a mean value to a corresponding probability distribution. If a stochastic approach is used for the assessment of human-induced vibration this may be included as a variable in the analysis. This will be explained in the part about stochastic analysis 2.2.2.

2.2.2. Stochastic analysis

The dynamic loads due to pedestrians on top of the bridge have a random nature. Therefore it is possible to make the reasonable comparison with wind loads, which are often treated using a probabilistic approach. For footbridges the dynamic response is generally calculated using simplified deterministic calculations [23]. Therefore, the question arises if the design codes and guidelines are not too conservative, by prescribing deterministic methods.

It is clear that every human body is different in terms of height and mass. When a more detailed comparison is made a lot of differences can be found such as leg length, foot size etc. Also in the way humans walk differences can be found. Not everyone is walking with the same speed, step size etc. If these two categories are combined, human body characteristics differences and the walking gait differences, it is obvious to conclude that the forces produced by pedestrians will change between individuals. This variability is called the **inter-subject variability**.

If a closer look is taken on the walking gait of a single pedestrian it can also be noted that not every step is exactly the same. A human being will never take precisely the same step length or always walk at the same speed. This can be an effect of the surroundings, for example due to other pedestrians or a walking surface. So there is also a variability over time in the walking gait of an individual. This variability is called the **intra-subject variability**.

In the Eurocode the load model representing the pedestrian forces the Inter and Intra-subject variabilities are not included. A deterministic model is used in which pedestrians are all considered to produce a harmonic force with the same amplitude. The stepping frequency is considered to perfectly match the eigenfrequency of the bridge. In this way the worst-case scenario is considered, but it can be argued that the Eurocode is too conservative because the random nature of the loads due to pedestrians is not considered.

A more realistic model can be found using a stochastic approach. If this approach is used, the inter- and intra-subject variability can be included and thereby represent the load cases more realistically. A stochastic analysis requires to run a big enough amount of different cases so that a conclusion can be made with enough certainty. This approach is based on probability of occurrence and requires different steps in the process.

Different researches have been done on integrating the probability approach into the design of pedes-

trian induced forces. The use of such an approach leads to the ability of finding a probability of exceeding a set maximum vibration level. A more detailed inside can therefore be acquired compared to the deterministic approach which only calculates the maximum acceleration and if it exceeds the set maximum. Zivanovic [33] created a probability based framework for a vibration serviceability check. In this framework the following parameters were treated as variables that have to be described using their probability of occurrence:

- Step frequency
- Walking speed
- Magnitude of the dynamic force
- Intra-subject variability (not exactly the same steps)

For the explanation of the different variables the single pedestrian crossing scenario is considered. Based on this it can be argued if it is useful to consider these parameters stochastically or deterministically. For the single pedestrian case a choice is made which parameters should be modelled stochastically. This choice may be different when multiple pedestrians, in crowd situations, are considered. This will therefore be discussed hereafter.

Single pedestrian situation:

The probability density of the parameters may differ between regions/countries. When the average length of humans change it seems logical that the walking gait will change as well. The way of life in that region/country may also effect the walking gait and so the probability of occurrence of these different parameters. In regions where people are on average more busy, the walking speed may be higher for instance. Therefore, it is concluded that the parameters have to be treated with care and the location for the research has to be considered.

The step frequency is an important parameter from a dynamic response perspective. Significant vibrational response will only occur at situations close to resonance (see figure 4.5). Note that resonance may also occur for higher harmonics of the pedestrian load. Small deviations close to resonance case have big influences on the possible response, so it is very important to model the probability of occurrence of the step frequency correctly. In literature different definitions of the likelihood of step frequencies can be found.

The characteristics of the likelihood that have been found in the different researches is also effected by the different sample sizes. A bigger amount of test subjects which are investigated result in a more realistic likelihood. An extensive research was done by Zivanovic [33] on 1976 subjects. This research has been done in Montenegro. It is assumed that the results of measurements in Montenegro will be applicable for The Netherlands as well. Therefore the choice is made that the likelihood of occurrence of the step frequency applicable in The Netherlands is described with the following function:

$$f_s \sim \mathcal{N}(\mu_f, \sigma_f) = \mathcal{N}(1.87, 0.186\text{Hz}) \quad (2.2)$$

The walking speed is not a straightforward parameter within the walking gait of a pedestrian. The walking speed of a pedestrian depends on the step frequency and on the stride length (step size). Due to this correlation between the frequency, stride length and walking speed it has been a topic in different researches. Due to the findings of these researches different models for the interaction between these three parameter are proposed. The difference between these models consist of the assumption of correlation between the step frequency and the stride length.

In the research of Pedersen [23] a comparison between different models for the walking speed is made. In the three models the walking speed are all defined as $v = f_s l_s$, a multiplication of the step frequency with the stride length. The difference between the models is in the definition of the stride length. However, the comparison of the three different models showed that it had no significant influence on the response, see figure 2.7. For a more detailed description of the different model for the pedestrian speed the author refers to the document of Pederson [23].

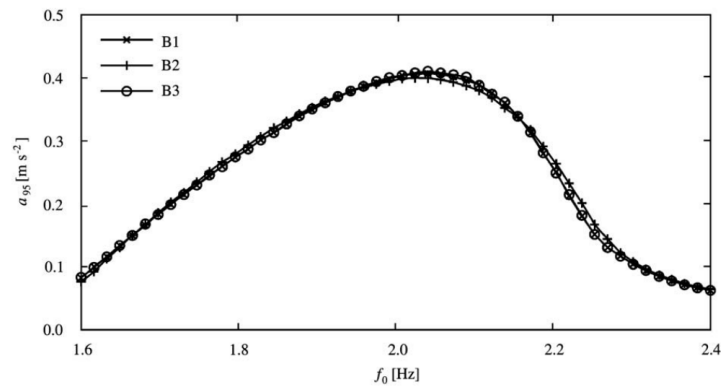


Figure 2.7: The acceleration 95th percentile as a function of bridge frequency f_0 as calculated employing models B1, B2 and B3 for modelling stride length [23]

So by making use of the deterministic stride length of $l_s = 0.71\text{m}$ there is a direct correlation between the walking speed and the step frequency, $v_s = 0.71f_s$.

As previously described is the dynamic force due to the step of a pedestrian of influence on the dynamic response of the footbridge. Multiple researches prescribe different models on how to apply the load and what amplitude has to be used. The magnitude of the dynamic force is also a variable that is effected by variability. As described does the weight of a pedestrian have an influence on the force of a footfall. Obviously, the pedestrian weight is subjected to inter-subject variability and will depend on the region/country. On the other side, the Dynamic Load Factor (DLF) is by some researches seen as a stochastic parameter as well. This is not considered by all researches. Pederson investigated the influence of the variability of the human weight and the dynamic load factor separately [23]. It was found that for both the pedestrian weight and the DLF the mean value has significant influence, but the variance around the mean does not have big influence. The variance is too small to have a significant influence.

Hence, the dynamic force can be modelled deterministically but the mean value must be chosen with care.

In the previously described parameters, the focus was on the inter-variability (difference between different pedestrians). However, a pedestrian will not take every step in exactly the same way and produce the same force every step. Introducing intra-variability into the probabilistic approach results in a more realistic modelling of a pedestrian. However, it was found that the intra-variability does not have a big influence on the response of the bridge [33]. The intra-variability will not be considered in this research in order to exclude unnecessary complexity and needed computational power. This results in the fact that the velocity of a pedestrian is constant when crossing the bridge.

To conclude for the single pedestrian crossing an advise is made in which the need for stochastic parameters is described. This necessity is based on the significance of influence on the vibrational response.

First of all, it is concluded that intra-variability does not significantly influence the vibrational response and so is not useful to be considered in the stochastic analysis. For the inter-variability it is concluded that only the step frequency variability has an influence if modelled stochastically. The stride length, dynamic load factor and pedestrian weight can be used deterministically. However, attention must go to the choice of pedestrian weight because this will directly influence the response.

Crowd situation:

For a footbridge it is more common that more than 1 pedestrian is on the bridge which all apply force to the bridge. This means the response can in general have higher accelerations than for the single pedestrian crossing case. For the crowd cases it is needed to be checked if the conclusion for stochastic parameters still holds.

Firstly, it needs to be questioned if the parameters that can be applied deterministically for the single

pedestrian case can be used the same for crowd situations. Secondly, due to the multiple pedestrians new parameters arise that can influence the response. The distribution of the pedestrians needs to be determined, because the location of a pedestrian is an important parameter for the dynamic response so therefore a good definition is needed. For the crowd situation it is also needed to define the phase shift between the pedestrians, because not everyone is walking in the same phase.

Tubino et al. [26] did research on the effect of these stochastic parameters in crowd loads. The influence of the statistical distribution of step frequency, walking speed, dynamic load factor and pedestrian weight on the maximum dynamic response is analysed. This resulted in the confirmation of the significant influence of the step frequency on the one hand and the insignificant influence of the other parameter distributions on the other hand. So only the step frequency is necessary to be modelled stochastically.

In the research of Caprani et al. [11] the influence of vertical human-structure interaction is investigated. To incorporate this interaction into the model the pedestrians are modelled as Single-Degree-of-Freedom dynamic systems (this will be explained further on in 2.2.3). This will change the influence of the parameter, so this needs to be investigated again. So for these kind of models the influence of a deterministic parameter simplification will be addressed. Even though this is not the main purpose of the research of Caprani, a comparison between a deterministic and random crowd is made so the influence of stochastic approach can be discussed. In the research the following three load case scenarios are described: (1) single pedestrian, (2) deterministic crowd and (3) random crowd.

For the single pedestrian case they used a deterministic model, no variability considered, which describes the worst case scenario in which the step frequency is equal to the fundamental frequency of the bridge. The deterministic crowd model is then generated using this single pedestrian case. An important thing is that the distance between the pedestrians is given to be 1 m and remains constant. However, a normal distribution for the step frequency and a uniform distribution for the phase angle was used. So the pedestrians are deterministic on their own, but the crowd is modelled stochastically. The random crowd load case is modelled with all parameters stochastic. So every pedestrian is characterized using the probability density functions and the crowd is therefore modelled completely stochastic.

- "Deterministic" crowd
 - deterministic mass, velocity and arrival time
 - stochastic step frequency and phase angle
- "fully random" crowd
 - all parameters stochastic
 - pedestrians are free to "pass" each other

In figure 2.8 the change in frequency and damping is shown of 100 random crowds passing the bridge. It can be seen that the mean, upper and lower limits are not symmetrical over time. This is the case for the deterministic load, because of the constant distance between the pedestrians. However, what influence resulted in the asymmetrical changes over time is not stated in the research. A possible reason could be that the arrival of pedestrians is relatively close. Due to the different speeds of the pedestrians the group representing the crowd is more widely spread when it leaves the bridge. This results in a lower departure rate compared to the arrival rate.

Therefore it is unclear what influence the different parameters have on the confidence interval of the results. By increasing the size of the group the influence on the arrival rate on the spread during a steady stream is reduced. When this is done the influence of the other parameters can be better understood.

In this research the 90% confidence interval of the damping as a result of the 100 sampled random crowds is in the range between 2.0 and 2.5%. This is a significant spread if it is compared with the 0.5% damping of the empty bridge. It is however not investigated which parameters introduce these

differences. So when stochastic analysis is used combined with a load model that includes the Human-Structure Interaction using a Single-Degree-of-Freedom it is unclear which parameter necessary have to be modelled stochastically.

In this research it is unclear if the difference between the random crowds is an effect of the distance between the pedestrians (arrival time) or of the stochastically modelled parameters.

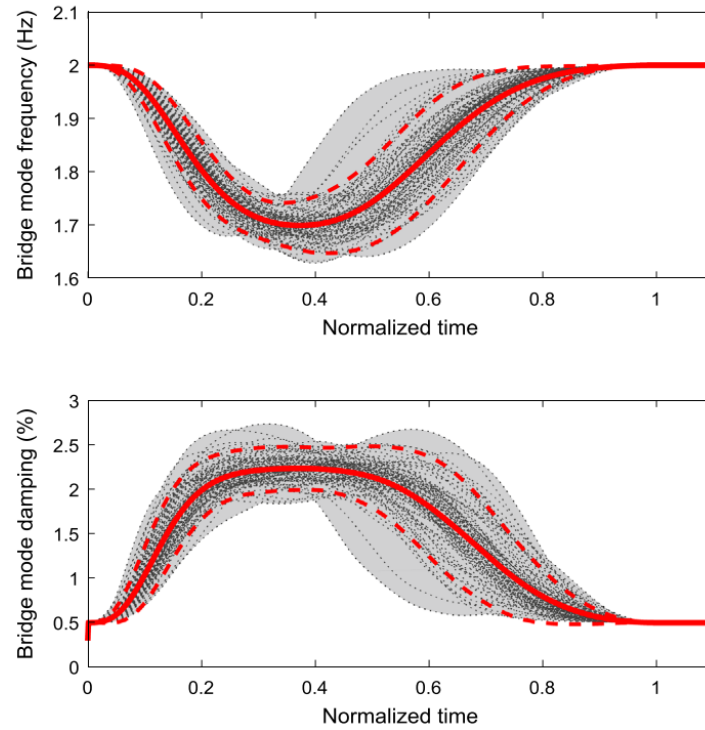


Figure 2.8: Change in frequency and damping due to HSI calculated using 100 random crowds as described below. The solid line is the mean value and the dashed lines are the 5% and 95% values. The time scale is normalized for the time pedestrians are on the bridge. [11].

2.2.3. Human-Structure Interaction (HSI)

The total interaction between the pedestrian and the footbridge is defined as the Human-Structure Interaction (HSI). This interaction can be separated into two phenomena. The humans that are on the bridge can change the dynamic characteristics of the combined dynamic system, compared to the situation of an empty bridge. So the first phenomenon is the influence of the human on the structure (H2SI). The second phenomenon is the opposite. When the vibrations of the bridge become perceptible to the user the force pattern of the human can change. For example, when the bridge starts vibrating the walking human may feel out of balance and will change the step size. This may also happen unconsciously. Therefore, the second phenomenon is the influence of the structure on the human behaviour (S2HI) [8]. The Human-Structure Interaction is illustrated in figure 2.9

The human body can be seen as a complex dynamical system. As a simplification the human body can be described as a single degree of freedom mass-spring-damper system. It influences the total dynamic system by adding mass, stiffness and damping. Using the SDOF approximation of the human body researches are done on how the HSI influences the response of a bridge.

Different measurement studies have shown that humans increase the damping of the total system compared to the empty case. In [32] the impact of standing and walking people on the dynamic characteristics is investigated and resulted in the increasing damping which is higher of standing people. As expected this influences increases with increasing number of people on the bridge.

In [30] the bouncing or jumping on a flexible structure is investigated. In this research a special test

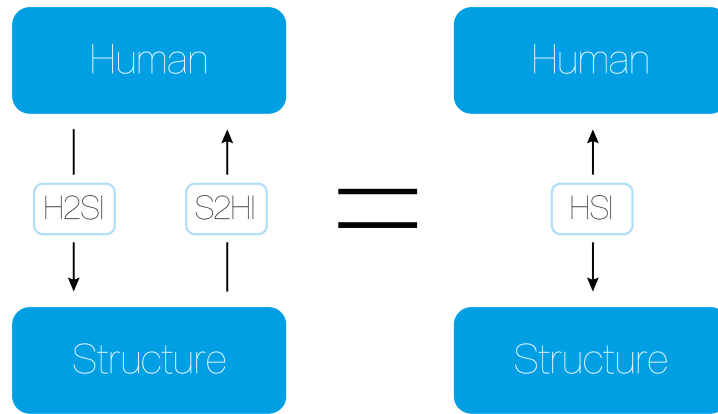


Figure 2.9: Visualization of the Human-Structure Interaction (based on [8])

rig was made which is able to change the fundamental frequency of the structure. The research resulted that a human bouncing or jumping has the potential to change the dynamic properties of the 'joint' human-structure dynamic system. However, this results must be considered carefully because the mass ratio was 0.41 (human mass 75 kg and test rig platform mass 180 kg). Using this information it can be concluded that HSI may also occur when bouncing or jumping humans are considered. However, if this is a significant influence when this is applied in a real bridge structure is not known. In the research on floor vibration done by Ellis et al. [13] it was concluded that HSI interaction during running or jumping has no influence on the response. However, in the research an experimental prestressed concrete simply-supported bridge with a fundamental frequency of 18.68 Hz was used. It is unclear what dynamic parameter resulted in this conclusion. Therefore it can only be said that the HSI due jumping and running may be insignificant for some conditions, using this information.

As described earlier, the Human-Structure interaction consists of Human-to-Structure Interaction (H2SI) and Structure-to-Human Interaction (S2HI). When a study is done aiming to understand the HSI it is difficult to separate the two, because they both occur simultaneously. Ahmadi et al. [8] tried to make this separation using a combination of an experimental and numerical approach. They used a Moving Force model to simulate a single walking human. The amplitude of the load was based on 2 different measurements: 1) Ground Reaction Force on rigid floor (G_{RS}) and 2) Ground Reaction Force during experiment on real life bridge (G_{BS}). They simulate results using these two Ground Reaction Forces (R_{RS} & R_{BS}) and compare them with measured response (R_M). In that way they separated the HSI into the two phenomena. The difference between modelled response with GRF based on rigid floor and modelled response based on real life bridge is a measure for the S2HI. The difference between the modelled response with GRF based on real life bridge and the measured response is due to the H2SI, because this is not included in the model. The procedure is illustrated in figure 2.10. The research concluded that both the S2HI and the H2SI increase as the mass ratio between the human and structure increases. At resonance, the influence is the biggest. For the bridge considered in the research it was also found that the H2SI was far more significant than S2HI.

It is clear that the presence of a human on a flexible structure, in this case a footbridge, consists of 2 parts: 1) Loading and 2) influence due to Human-Structure Interaction. Both parts act simultaneously. In the literature review of Shahabpoor et al. [25] the common approach to deal with both is clearly described. When the human is assumed to be a linear mechanical system it is possible to use the superposition principle to split the total walking GRF into two components:

1. Load as if the surface is rigid - $p_F(t)$
2. the interaction force due to the HSI - $p_H(t)$

In formula these can be represented as:

$$p_P(t) = p_F(t) + p_H(t) \quad (2.3)$$

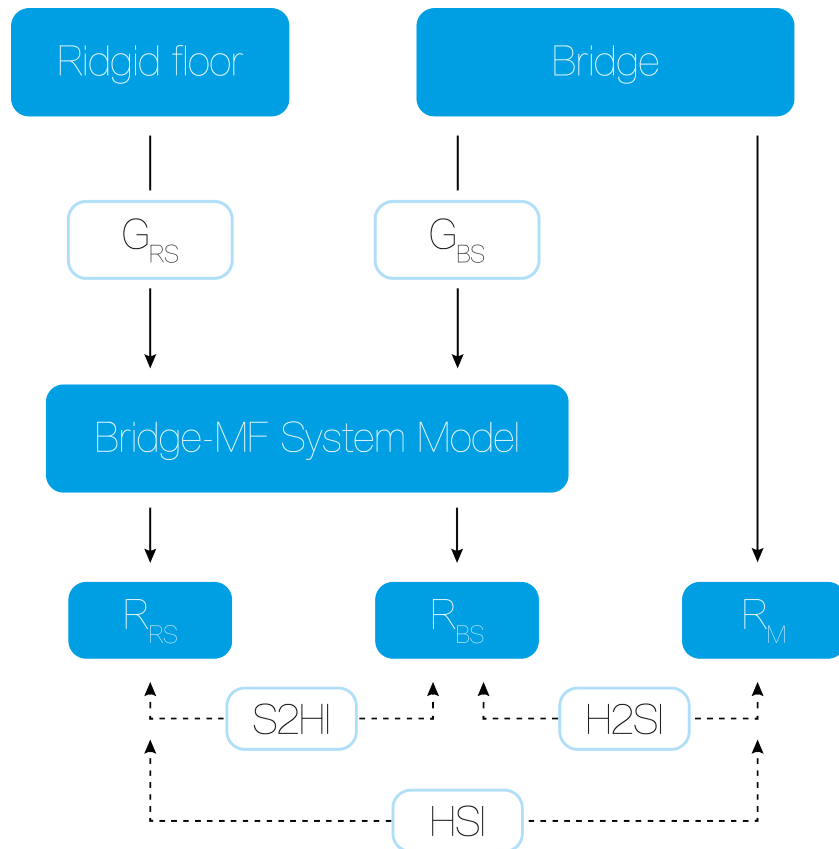


Figure 2.10: Visualization of the HSI separation in [8]

This assumption holds if the walking gait of the pedestrian is not effected by the response of the bridge. In other words, when the S2HI is negligibly small it is possible to assume the human body to behave as a linear mechanical system. Therefore, the assumption can be rewritten as: It is assumed that the response due to the human-induced vibration remains small enough so that the S2HI is negligible. The models that include HSI that are described in the following section are based on this assumption.

There are different models that differ in the amount of detail used to describe the loading, considering the HSI. The most common way to make an assessment of the human-induced vibrations is by applying a load on the structure. The most common used model representing the effect of a pedestrian on the bridge is applying a moving force (MF model) as a moving harmonic point load. This relatively simple model does not consider the HSI ($p_H(t) = 0$). This model is relatively simple to implement, but it may overestimate the response due to neglecting the HSI.

A more complete model is found when the mass of the pedestrians is included in the dynamic analysis. The mass is added directly to the bridge deck at the same location as the moving force to create the Moving Mass model (MM model). By adding the human mass to the dynamic system of the bridge the dynamic properties change. So in the MM model a part of the HSI is added to the MF model. The mass is seen as "passive" because the additional damping that may be present due to the human dynamic characteristics is not introduced [7].

For the crowd load model described in the JRC document [17] the MM model is applied in a modified manner. As described earlier an uniform distributed crowd is considered, so the mass of the humans is also added uniformly. This is done by adding the additional mass of the pedestrians on top to the mass of the deck which is then used to calculate the eigenfrequencies of the total system. There is a minimal threshold of 5% mass ratio added below which the influence of the pedestrians mass is seen as insignificant.

As previously described, different researches have concluded that the presence of humans can add damping to the system. Therefore, research has been done on the modelling of a pedestrian as a Single-Degree-of-Freedom Mass-Spring-Damper system [11] (MSD model). In this MSD the mass is dynamically "active", because of the stiffness and damping between the point mass and the bridge deck. So the HSI is added completely, still assuming the negligibly small influence of the S2HI. The different models (MF, MM and MSD) can be seen in figure 2.11. Multiple researches have shown that the MSD model describes the HSI better than the MM, so the focus will be on the MSD model further on.

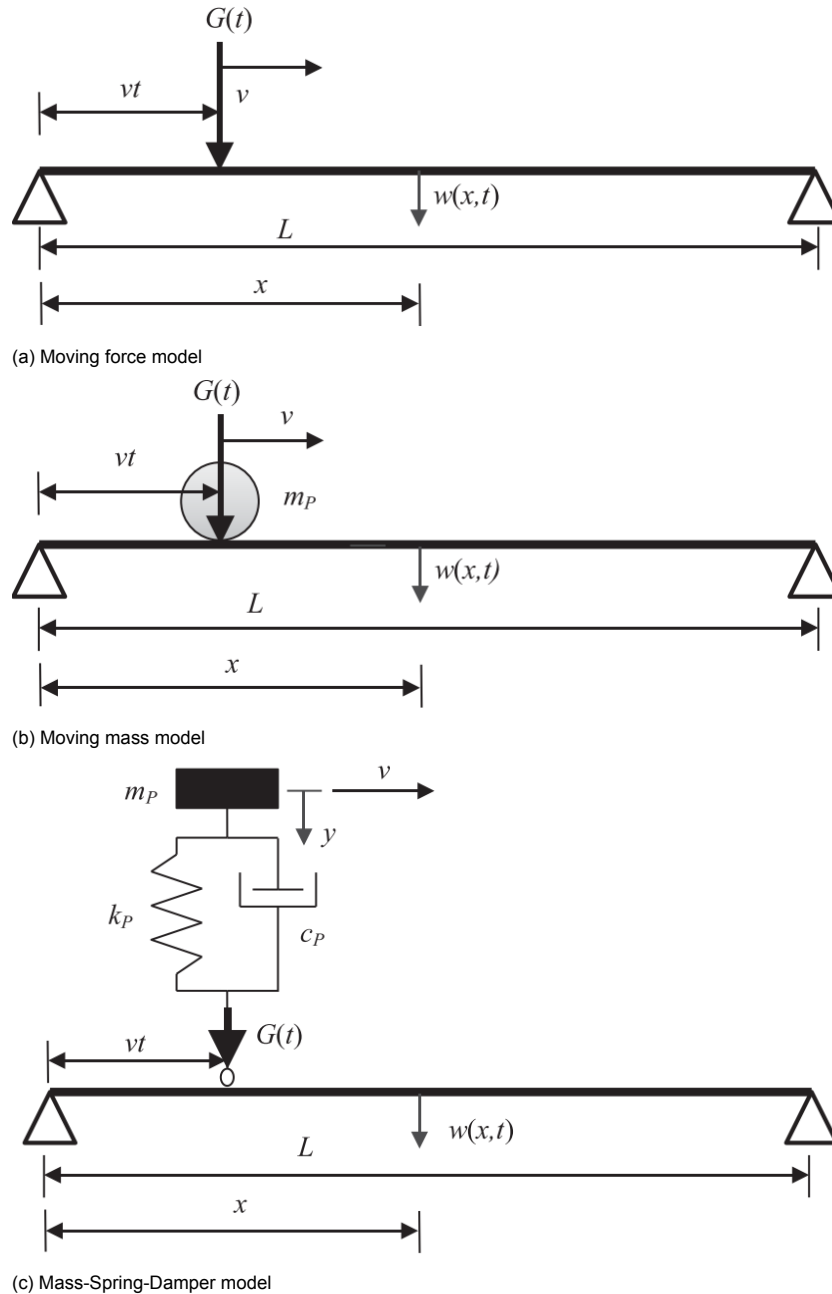


Figure 2.11: The common used and researched models representing the effect of a single pedestrian on a footbridge (illustrated for a simple supported case). Increasing Human-Structure Interaction included from a to c [11]

Next to the described models there are also models that do not separate the GRF as described earlier. The Inverted-Pendulum models (IP models) 2.12a are traditionally used in biomechanics. These models provide a more realistic modelling of the human body dynamics due to the different behavioural phases during the walking process. It is possible to include the difference in behaviour when 1 or 2 legs are connected with the bridge, see figure 2.12b. Therefore the S2HI that may effect the walking gait can be included in this model. Dang and Zivanovic [12] have found that both models predicted the HSI acceptably. However, due to the non-linear behaviour of the inverted pendulum superposition is not possible. So when the assumption of small vibrations holds, it is more efficient to use a MSD model as described before.

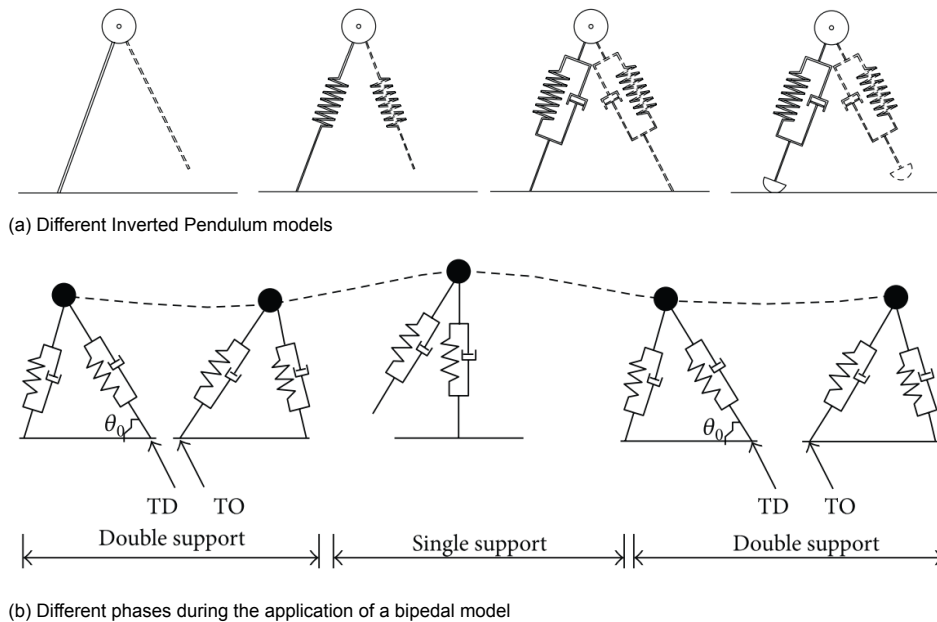


Figure 2.12: Inverted Pendulum model as a representation of the human body walking dynamics [25]

When the human body is represented by a Mass-Spring-Damper system the influence is similar to a Tuned Mass Damper (TMD). A TMD is essentially the physical form of a MSD SDOF model. However, the mass, stiffness, damping and location of the TMD are designed to result in the highest efficiency. This is obviously not the case for the properties of the human body. The biggest difference between the MSD human body representation and a TMD is that the MSD model considers a moving system. To achieve the highest efficiency of a TMD it needs to be located at the location of maximum response (For a single span, at midspan for example). When we transfer this knowledge to the moving human, the influence will change corresponding to the location. This means that the dynamic properties of the combined human-structure system will not be constant.

In the research of Caprani et al. [11] they applied the Moving Mass and Mass-Spring-Damper model and checked the influence on the dynamic properties. They modelled a bridge with a length of 50 m, fundamental frequency of 2.0 Hz, a mass of 500 kg/m, and constant damping of 0.5%. For a single pedestrian crossing (with a step frequency equal to the fundamental frequency) it is clear that the influence of the human changes during crossing, see figure 2.13. Similar to the TMD the biggest influence occurs when the human is at midspan. Note that the MM model only has an effect on the frequency, not on the damping. The single pedestrian can be expanded to a crowd loading situation, as is also done [11] (see figure 2.8). As also mentioned in other literature the influence increases with the number of the pedestrians. A similar increase and decrease can be seen in the crowd load case, but due to the length of a crowd the influence has a constant period in between. Due to the stochastic approach that is applied a range is found, but the mean value shows this behaviour.

By using a MSD model their are new parameters introduced compared to the MF model. The stiffness and damping parameters of the human body are subjectable to changes from human to human. So as already explained in the section about stochastic analysis 2.2.2 it is necessary to implement these

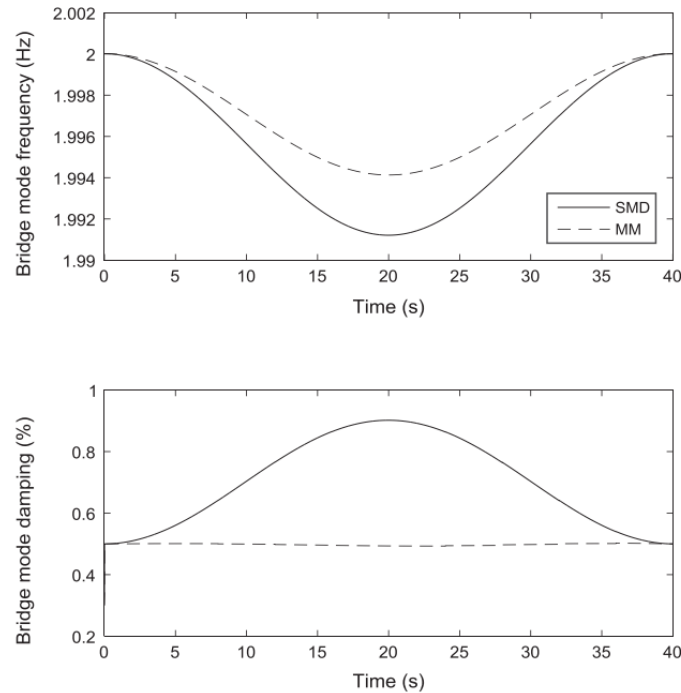


Figure 2.13: The fundamental frequency and damping during a single pedestrian crossing [11] (MM: Moving Mass model, SMD: Mass-Spring-Damper model)

parameters as being stochastic. This will make sure that the HSI is not overestimated due to the exclusion of these variances.

From other researches it can be concluded that Human-Structure Interaction can be implemented in the dynamic analysis for human-induced vibrations using a Mass-Spring-Damper system to represent the human dynamic properties. For a single pedestrian crossing and the crowd case it is shown that the MSD model gives more realistic results when compared to the Moving Force model.

In these walking load cases (single pedestrian or crowd) the dynamical system of the bridge and the pedestrian are always connected. Therefore, it is reasonable to say that the model also needs to be in continuous contact with the structure. However, the stiffness of the MSD model will be constant which is not entirely correct due to the different support phases. This difference is small, because the experiments in which the characteristics of the human body during are measured for walking conditions.

However, when a running behaviour is observed a clear separation is present between the steps. As previously explained this will have an effect on the Ground Reaction Force. The difference between the loading time history of walking and running can be seen in figure 2.2. Due to this separation the time that a force due to the stiffness and damping between the two is present will reduce. It is expected that the influence of the Human-Structure Interaction will decrease compared to the walking case. So applying the same MSD model for the jogger load case will overestimate the HSI influence, which can result in an underestimation of the response. To include the HSI for the jogger load case a change must be made to the previously described MSD model that will allow for the separation of the human and the bridge.

According to the Dutch National Annex of the Eurocode it is required to consider 5 or 10 (depending on bridge span) joggers acting on the bridge. It is mentioned that it may be assumed that the load may be applied as stationary at the location with the biggest value of the considered mode shape. This is however not possible when the HSI is considered using the MSD model, due to the time variation of the dynamic characteristics. Therefore a time history analysis needs to be considered.

Besides that, when multiple joggers are considered it is reasonable to assume that the step frequency

will not be completely equal for every jogger. Next to this a phase shift is also possible. This will mean that the flight phase between the steps is not synchronized for the different joggers. So the time that there is interaction between a jogger and the bridge will depend on the frequency and phase shift. Therefore, it will be necessary to model the multiple joggers individually considering their own frequency and phase shift to make a correct assessment of the Human-Structure Interaction. This will result in a more realistic representation of the response due to joggers.

2.3. Research on the reduction of vibrations

If during the design of a footbridge the vibrations are expected to exceed the requirements there are two possible approaches: 1) optimizing the design based on the dynamic requirements or 2) use additional damping devices. The most common applications and the state-of-art research on the application will be described in the following text.

2.3.1. Design optimization

When a bridge design is found to be governed by the dynamic response due to human-induced vibration it may be possible to change the design in such a way that the response will be reduced. The possibilities to change this may be limited due to the required slenderness, which leads to a small working space. Within the structural dynamics the three important factors are damping, stiffness and mass. Adding damping to the system can only be done by making large changes to the design, such as changing the material (so the material damping). This is not a feasible optimization, so this is not considered here. However, by changing the design it is feasible to change the stiffness and mass of the structure. A problem may arise when the mass is increased that the statistical checks will fail. So there will be an optimal design in which the stiffness is increased so that the response will be reduced without adding too much mass to achieve this. In the research of Jiménez-Alonso et al. [18] such an optimal design was tried to be found. This was achieved by determining the required stiffness distribution while minimizing the self-weight. This optimization method was originally used for wind-induced vibrations in buildings. By using a global discrete optimization method they tried to find the optimum size and shape for a footbridge. The design process is visualized in figure 2.14.

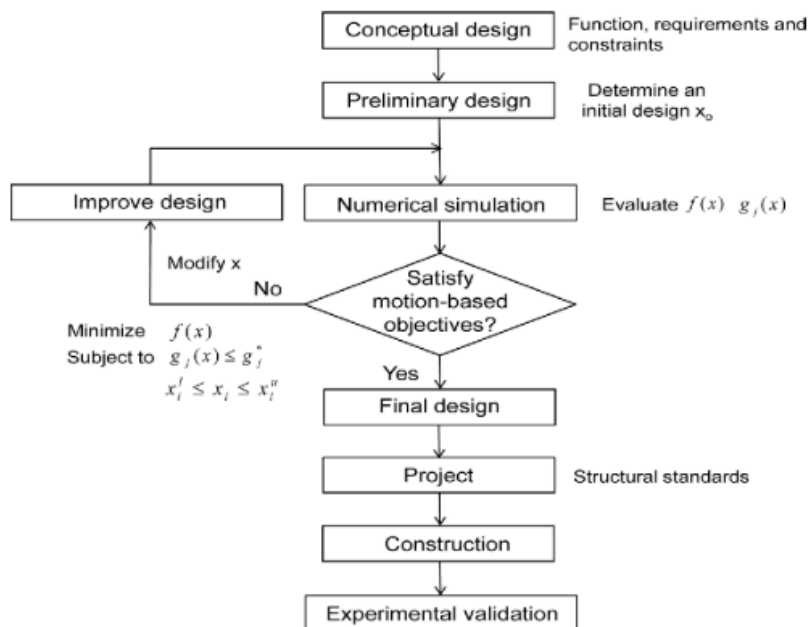


Figure 2.14: Motion based design process as proposed by Jiménez-Alonso et al. [18]

In the research they used a case study to test to optimization protocol. For the Palmas Atlas footbridge a optimization was made by prescribing the following parameters to be changed:

- Deck height over pier
- Deck height central span
- Deck height over abutment
- Lower flange thickness 1
- Lower flange thickness 2
- Lower flange thickness 3

The three lower flange thicknesses are used to apply step-by-step increasing thickness around the piers (thickest over pier). Every parameter has been given a range in which the optimum must be found. As a result of this optimization the bridge is in use without having experienced pedestrian-induced problems.

Therefore it is possible to make a design optimization using a numerical approach based on vibrational response. However, when the span is increasing this will not give the required results at some point. Therefore it is may be necessary to make use of additional measures, which will be described in the next section.

2.3.2. Additional damping devices

If design optimization is not enough to prevent dynamical problems, a useful method to limit the vibrational response of a dynamic system is to increase the damping using additional devices. These devices can be categorized into: 1) passive dampers, 2) controllable (semi-active) dampers, and 3) active dampers (actuators). The passive dampers are defined by fixed damping properties. A controllable, also called semi-active, damper has the possibility of adjusting or controlling the damping characteristic. The last category of active dampers, or so called actuators, go one step further than the other two categories. An actuator is not only able to dissipate energy but also to put energy into the vibrating system. When this is done correctly the response of the system will reduce [28].

Common used damping devices will be explained hereafter combined with the state-of-art research if applicable:

Passive dampers: Viscoelastic damper

The damper force of a viscoelastic damper is composed of a stiffness an viscous part:

$$f_d = k_d \cdot x - c_d \dot{x} \quad (2.4)$$

Which means it can also withstand a constant pressure. This is typical for material dampers, not fluid dampers, since materials can withstand constant deformations. The behaviour of such dampers depend on ambient temperature, material temperature, frequency and shear strain. During the use of the damper the energy is dissipated to heat and therefore it also depends on the number of loading cycles. Especially when larger strains occur. At low temperatures the damper force increase which can become a problem for the damper itself and of course it's effectiveness. These dampers are used in damping of bridge deck by using elastomeric bearings. These bearings are often not primarily used for there damping effect. The damping may be limited because of the fact that the amplitude of the vibrations is limited at the location of these bearings. Therefore, it is assumed that the elastomeric bearings do not have a significant influence on the damping ratio of the entire structure.

Passive dampers: Tuned mass damper

A Tuned Mass Damper (TMD) is an energy dissipation device in the simplest form of a mass attached to the primary system with spring and damper elements. Energy dissipation happens due to the vibration of the TMD relative to the primary system. This can be achieved by tuning the TMD to the fundamental frequency of the system. Since the mass of the TMD is significantly lower than that of the primary system, the TMD will oscillate significantly if the energy is transfer from the structure to the TMD [28]. Most standard dampers described earlier dissipate the energy in a wide frequency band, however the TMD is only effective in a narrow band . It is therefore necessary to tune the damper to the frequency of the primary system. To make an optimum there are different methods described, which are mainly based on the modal displacement theory. This is logical in combination with the narrow band efficiency of the TMD to only be used for a single modal vibration. Bad tuning of the TMD on the frequency has

significant influence. This is not that important for the damping parameter of the TMD, because the influence is way less significant.



Figure 2.15: An example of an implemented TMD for vertical vibration mitigation [28]

The two most common optimization criteria for the tuning of a TMD are the H_∞ and H_2 norm optimization criteria. The H_∞ norm represents the maximum amplitude of the absolute value of the transfer function, which is also known as the dynamic magnification factor. The H_2 norm of a transfer function is a measure of the area between the square of the absolute value of the transfer function and the z-axis. Both norms are sensitive to changes to the frequency ratio (between primary system and TMD) and less sensitive to the damping ratio of the TMD. For loads having mainly a wide band stochastic character (wind, earthquake loads) an optimization on the H_2 norm is more appropriate. An optimization to H_∞ norm is recommended if the loads are mainly periodic. Since the frequency of the loads due to pedestrians is not a wide band process and close to periodic the H_∞ norm can be used [28].

The sensitive character of a TMD consists of two parts: the sensitivity to 1) frequency changes and 2) the mode shape. The two sensitivities are different in the sense of effectiveness. Bad tuning of the TMD to the frequency of the structure can lead to an inactive TMD. When the tuning is done correctly the TMD will have an effect on a single vibrational mode. At this modal frequency the structure vibrates in the corresponding mode shape. When the TMD is located at the maximum amplitude of that mode shape it will be most effective. If this is not the case, the response reduction will be lower. This can happen due to the following two reasons. Firstly, the maximum location may not be suitable for the TMD implementation and will therefore be placed at a less effective location dynamically speaking. Secondly, the mode shape may be different than estimated during the design phase. The sensitivity to the mode shape is lower than to the frequency, but to implement an effective damper the combination needs to be correct.

The TMD design is usually based on the assumption that the response is governed by a perfect harmonic loading causing resonance. However, as explained earlier this is not entirely true. Especially when crowd load case is considered this assumption may not be correct and the TMD design is not very effective. On the basis of the uncertainties in the modal parameters and the uncertainties in the loading a research was done by Lievens et al. [19] and [20]. They used a uncertainty level to define a range for the frequency and damping characteristics for the bridge. So with increasing level of uncertainty the range around the assumed values will increase. For the level of uncertainty an α -level is defined as: $\alpha = 1$ means no uncertainty and $\alpha = 0$ is largest uncertainty. The frequency and the modal damping are modelled as effected by the uncertainty. At the level of $\alpha = 0$ the frequency interval is $\pm 10\%$ and the damping $\pm 50\%$, see figure 2.16.

By designing the TMD in such a way that maximum response is below the requirement threshold for the entire ranges of modal parameters a robust design is found. This robust design is made for different α uncertainty levels. It was found that when the uncertainty increases the mass and the damping of the



Figure 2.16: Modal parameter ranges at different levels of uncertainty α for fundamental frequency (left) and modal damping (right) [20]

TMD increases as well. The mass of a TMD is seen as the biggest influence on the building cost [19]. Therefore, it is shown that it is possible to implement a robust TMD design including the uncertainty during the design phase by increasing the mass and damping of the TMD itself. To make sure the TMD is tuned as effectively as possible measurements after construction are still necessary. But using the information of the robust design it is possible to include the TMD in the design conservatively based on the values as found by Lievense et al. [19].

(Semi) active dampers:

Controlling the damper characteristics requires measurements of the system that have to be updated in the damper itself. Especially for fully active dampers this requires some sort of computer based system based on real life measurements. Different researches have been done and have proven that using these kind of dampers can results in significant reduction of the vibrational response of footbridges. This will not be considered in this thesis, because this is not a structural problem but a computer based problem statement.

3

Research set-up

3.1. Problem definition

A lot of research has already been done in the field of footbridges and the main focus lies on the dynamic response, since it was found to be governing in the design. The majority of this research is divided into the following three fields: (1) the structure characteristics, (2) the load models, and (3) the reduction of vibrations.

In the State-Of-Art literature study it has been found that the identification of the dynamic characteristics of the structure has increased due to the practical implementation of software, such as the Finite Element (FE) model programs. However, errors in this dynamic analysis are a common occurrence. The biggest uncertainty in the dynamic structure characterization is the damping. Therefore, it is necessary to make measurements on the bridge when it is constructed, so that dynamic characteristics can be correctly assessed. Based on these measurements the FE model can be updated and possible further actions can be correctly designed. The options to reduce the vibrations by changing the design or implementing additional devices are effective only when the dynamic properties are modelled correctly. Therefore, the structure characterization and reduction of vibration will not be the research direction of this master thesis.

The identification of the load models has been found to be another research field of interest. During the design life of a structure it is possible to identify different load cases, which have their own specifications. The loads induced by the pedestrians are obviously more important for pedestrian bridges than for road traffic bridges. The pedestrians give rise to vertical, horizontal and longitudinal directional forces (in decreasing order). Due to cases of extensive horizontal vibrations in built bridges, a lot of research is done on this subject. However, this is not the case for the vertical direction. The conservatism in the often used models, described by Eurocode, are researched and updated. These updates are based on the research on the dynamic load factors (DLFs), the implementation of stochastic analysis and the implementation of Human-Structure Interaction (HSI). In the State-of-Art literature study it was found how the DLFs are best used to describe different pedestrian motions. Research on the stochastic analysis shows what parameters are useful to be implemented with their probability of occurrence. The flexibility of the bridge deck is found to have an influence on the interaction forces between the pedestrian and the bridge itself. This HSI can be implemented in the dynamic models by modelling the pedestrian as a Mass-Spring-Dashpot (MSD) system. For walking behaviour it is possible to use this method to more accurately predict the response of a bridge design, which is found to be lower.

The application of this MSD model to investigate the potential HSI during jogging has not yet been researched. For jogging/running behaviour a clear separation between the deck and the pedestrian occurs, which means that the HSI will decrease. In current practice it is often found that the jogger load case (as described by Dutch National Annex of the Eurocode) is governing for the design slenderness. Therefore, this research will be focused on reducing the conservatism in the jogger load case by analysing the Human-Structure interaction.

3.2. Scope definition

Due to the relatively low live loads on footbridges a large variety of possible designs can be made. They all have their own structural characteristics, both statically and dynamically. Therefore, it is impossible to provide a guideline for a completely general footbridge design. To be able to provide information on the maximum slenderness, a typical footbridge design basis will be chosen in the literature study in chapter 4.

To make a clear scope definition the following boundaries have been defined:

- Steel is used as the structural material
- A single span is considered
- A straight alignment is considered
- A constant cross section is considered
- No vertical and horizontal curvature of the bridge is considered
- No collision with the structure can occur
- Structural influence of parapets is neglected for the bridge as a whole
- Fatigue behaviour is not included
- Dynamic analysis is done using beam elements
- Only vertical vibrations are considered
- Dynamic response due to wind is assumed to be non existing
- Human-Structure Interaction is only investigated for the jogger load case
- Eurocode combined with the Dutch national annex is applied

3.3. Research objectives

The main objective is to provide knowledge for future steel footbridge designs, based on the described typical design. By including the Human-Structure Interaction in the jogger load case, a better representation of the loads is provided. Using this better representation the possibility of a more slender design may be possible. The design basis will be checked on static and dynamic requirements. Therefore, the design can be considered to be realistic and the results may be useful for a typical bridge design.

Based on this goal the main research question is defined as follows:

“Is it possible to increase the maximum slenderness for a typical single span steel foot-bridge design when the dynamic jogger load case is considered as a moving model including separation and Human-Structure Interaction?”

In order to find a suitable answer to this main research question it is divided in a set of sub-questions. The research will follow these questions during the entire process:

- What typical cross section can achieve high slenderness ratios?
- Which loads and checks have to be considered in footbridge design?
- Which check is governing for a certain length?
- What is the influence of applying a 'stationary' jogger compared to the moving case?
- What is the influence of neglecting the separation when applying the jogger load?
- How big is the reduction in the effect of the Human-Structure Interaction due to the separation during running?

- What is the influence of the stochastic parameters when the jogger is modelled using the Mass-Spring-Dashpot Model?
- What is the influence of the distribution of multiple joggers on the Human-Structure Interaction?
- Is the Human-Structure Interaction of joggers significant?

3.4. Methodology

1) Making an "Initial" design:

As a start, the original codes and guidelines will be used to make an initial design. Thus, the Eurocode combined with the Dutch national annex and JRC document will be used to do the ULS (Maximum stress) and SLS (deflection and dynamic) checks. This will be done for different span lengths. The important outcome for this step are answers to the following questions:

- Which check is governing for a certain length?
- For what combination of parameters is the dynamic jogger load case governing? (This will be used as an input for the further steps)

The objective of the research is to investigate if this initial design can be more slender by implementing the HSI for the dynamic jogger load case. This can only be done for the set of parameters where the jogger load case is governing.

2) Setting up the dynamic model:

The dynamic model is created through a script in Matlab. It will be a 1-D model, so the bridge will be represented as a beam supported on both ends. The beam behaviour will be based on the Euler-Bernoulli beam theory. The partial differential equation of the dynamic behaviour of the Euler-Bernoulli beam will be solved using the Finite Element Method and numerical time integration. First the Moving Force model will be made, without additional Human-Structure Interaction. To model the Human-Structure Interaction, additions to the model have to be made. This is based on the separation of the force in a forcing term (equal to that on a rigid floor) and the interaction term. The vertical location of the mass of the human body is an extra degree of freedom and the relative motion between the human mass and the bridge deck will introduce the HSI.

The following steps will be taken to verify the Moving Force model:

1. Static check
 - (a) point load and uniformly distributed load (Based on analytical solutions)
2. Dynamic check: MF - 'stationary'
 - (a) applying sinusoidal load (JRC: $F(t) = 1250 \sin(2\pi f_p t)$)
3. Dynamic check: MF - moving
 - (a) by comparing with result of Caprani et al. [11]

To verify the Mass-Spring-Dashpot model including the Human-Structure Interaction, the following is done:

1. Dynamic check: MSD - moving
 - (a) by comparing with results of Caprani et al. [11]
 - (b) change in properties including separation 'floating time'

3) First investigation of the Human-Structure Interaction influence:

For the Moving Force (MF) and Mass-Spring-Dashpot (MSD) there are 4 different load cases considered. These consist of the combinations of stationary-moving with 'no separation'-'with separation'. To see what effect the Human-Structure Interaction has on the response of the bridge the results of the MF and MSD models are assessed at these 4 load cases:

1. 'Stationary' jogger - JRC load (sinusoidal with tension)
2. 'Stationary' jogger - Bachmann load (including separation/'floating time')
3. Moving jogger - JRC load
4. Moving jogger - Bachmann load

Note: When the MSD model without separation is used, the HSI will be larger than in real life. Therefore, it can be seen as an unrealistic model. However, the influence of the separation on the HSI is of interest.

4) Stochastic analysis for the moving jogger models (MF and MSD):

Until now the models used deterministic values for all the parameters, which resulted in a first investigation of the HSI is made. However, the subject variability between pedestrians has an influence on the response of the bridge. This influence is expected to be bigger for the MSD model, because the HSI is additionally depending on these stochastic parameters.

To make a correct assessment of the HSI for joggers a Monte-Carlo analysis will be done for the following models:

1. MF - moving jogger. With stochastic parameters:
 - (a) Step frequency
 - (b) Mass of the pedestrian
2. MSD - moving jogger. With stochastic parameters:
 - (a) Step frequency
 - (b) Mass of the pedestrian
 - (c) Stiffness of the pedestrian
 - (d) Damping of the pedestrian

It is important to note that the step frequency affects the walking speed. So every pedestrian will have a different step frequency, speed and therefore also a different time on the bridge.

5) Applying the MSD model for a multiple jogger load case:

In the Eurocode it is prescribed that multiple joggers need to be considered during the dynamic analysis. Therefore, it needs to be considered for MSD model as well. A lot of different research on multiple joggers can be done. As a first insight in the MSD model, including HSI, for the jogger load case the influence of the spatial distribution will be checked. Therefore, the following situations will be considered:

- 1 giant jogger, representing 10 joggers at the same location
- 5 jogger pairs, 2 side-by-side with a gap of 1.5 m to the next two joggers
- 10 single joggers, one after the other with a gap of 1.5 m between every jogger

4

Literature - Background information

4.1. Possible structural designs

Bridges for pedestrian or bicycle traffic, also known as footbridges, are characterized by relatively low loads compared to road and railway bridges. This means more different structural designs are possible. Therefore, a client or even an architect has more freedom leads to more aesthetically driven design process in which the structural system can vary a lot. Figure 4.1 shows different structural designs of pedestrian bridges.



(a) Footbridge in Lourdes [16]



(b) Footbridge in Venette [5]

Figure 4.1: Two examples of footbridge design

In this research the most slender designs are considered, which limits the possible structural systems. The definition of a slender design is referred to as the ratio of structural height over length of the span. If we compare the designs of the footbridge in Lourdes 4.1a and Venette 4.1b we clearly see that the bridge in Lourdes has a higher slenderness.

The possible designs that can achieve a high span over height ratio for a footbridge design is therefore restricted in this research to beam bridges. There are different kind of beam bridges which can be separated into four categories:

- set of beams with a non-structural deck
- set of beams with a structural deck
- box girder
- plate girder beams

The first two categories are defined by a set of regular beams in longitudinal direction and therefore provide the initial structure of the bridge. The difference between these categories is the function of the

decking. The initial function of a deck is to provide a surface for the traffic on the bridge. Additionally a deck can be designed to contribute to the overall structural resistance of the bridge by acting as a top flange of the girders. In that case the transfer of forces between the deck and the girders needs to be sufficient. This extra function influences the choice of the decking material. An example of a deck without a structural function for the whole bridge is made of timber planks and a steel plate can be used as a top flange of the girders thus adding resistance.

The box girder can be seen as an upgraded set of beam girders with a structural deck, but the bottom flanges are also connected to make a closed cross section. A big difference is the construction of a box girder, because it needs to be fabricated specifically for that bridge. To prevent instabilities of a box girder stiffeners will be necessary. The project specified construction increases the cost of the bridge, but more complex cross sections and alignments are possible for box girders. For example: T-box girders, triangular box girders or squared box girders. An example of a really slender boxgirder footbridge is build in Ljubljana, see figure 4.2.



Figure 4.2: A slender boxgirder footbridge in Ljubljana [3]

Plate girder bridges are a category of beam bridges in which two plate girders with a relatively large height are used as the main load bearing system. The slenderness ratio of this type of bridge will not be low because of this height. Nevertheless, no additional guardrails are necessary which is the case with the first three categories. There are already some plated girder bridges constructed that have an open web of the girders which result in a bridge that looks like a beam bridge with a unusual parapets. This gives the illusion of a high slenderness level, which is according to the above described definition not really the case.

4.1.1. Chosen cross section type for this research

The scope of this research is on footbridges with a high span of structural height ratio. It is already shown that a set of beams and box girder bridge designs can achieve really slender bridges (see bridge in Lourdes figure 4.1a and Ljubljana 4.2). In this research the set of beams is chosen due to the more clear structural system in comparison with the box girder. The deck will be used as a structural component of the global bridge behaviour. This is done using the simple reason that less material is needed, so a higher slenderness ratio is possible. This can result in a design guide in which a more clear understanding can be created of the possible failure mechanisms. An example of such is bridge can be seen in figure 4.3.

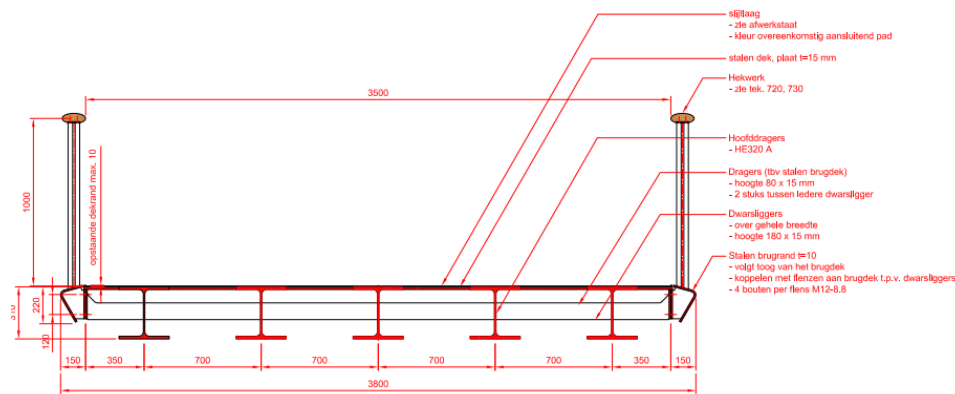


Figure 4.3: Cross section of tuinveld brug [4], example of a set of beams with a structural deck

4.2. Dynamics of footbridges

4.2.1. Footbridge behaviour

The relatively low loads that act on a footbridge does not only mean a lot of different structural designs are possible, but the mass of the bridge can be relatively low as well. Not a lot of material is needed to resist the loads that act on the bridge. However, this means that the dynamic forces have an increase effect on these bridges. The main dynamic loads that act on footbridges are wind loading and pedestrian loading.

The response of a footbridge under dynamic loading depends on two main parts: the load characteristics and the structural dynamic characteristics. The dynamic characteristics of the footbridge depends on the stiffness, mass, material, boundary conditions etc. This means for a proposed structural design a dynamical calculation needs to be made. An important thing to notice is that these calculations include uncertainties. This is because the assumptions that have been made on the boundary conditions, geometry of the cross section or damping for example. The difficulty with the damping characteristic of a bridge will be discussed further on. However, even when important parameters for the dynamic characteristics have to be assumed it is recommended to do the calculations to get an early inside in the possible dynamic problems [17].

The dynamic characteristics of a footbridge can be estimated as a first step using hand calculations and simplified methods. The result is a rough estimation which may lead to the necessity of a more sophisticated model, a Finite Element (FE) model. The general basics of the dynamic analysis will be discussed here.

When we look at the simple case of a single span bridge, the following equation for free vibration holds if the bridge is assumed to behave as a Euler-Bernoulli beam with a constant cross section and without damping:

$$\rho A \frac{\partial^2 w}{\partial t^2} + EI \frac{\partial^4 w}{\partial x^4} = 0 \quad \text{for } x = 0..L \quad (4.1)$$

In which:

w is the vertical displacement at location x and time t

A completely defined problem also needs initial conditions and boundary conditions. In the governing partial differential equation we have a second derivative with respect to time and a fourth derivative with respect to the location. This means we need two initial conditions and 4 boundary conditions to defined the complete problem. When we assume the solution in the following form we can transform

the problem to the frequency domain:

$$w(x, t) = W(x) \exp(i\omega t)$$

Which results after substitution in:

$$-\omega^2 \rho A W(x) \exp(i\omega t) + EI \frac{d^4 W(x)}{dx^4} \exp(i\omega t) = 0 \quad (4.2)$$

Now the time component can be eliminated which results in:

$$\frac{d^4 W(x)}{dx^4} - \beta^4 W(x) = 0 \quad \text{with} \quad \beta^4 = \frac{\rho A \omega^2}{EI}$$

For this differential equation a general solution can be written in the following way:

$$W(x) = A \cosh(\beta x) + B \sinh(\beta x) + C \cos(\beta x) + D \sin(\beta x) \quad (4.3)$$

In which A,B,C,D are constants that have to be solved using the boundary conditions.

The most general support cases are pinned or clamped. The following two boundary conditions at the support locations result from this support:

at Pinned support:

$$W = \frac{d^2 W}{dx^2} = 0 \quad (4.4)$$

at Clamped support

$$W = \frac{\partial W}{\partial x} = 0$$

With these two boundary conditions at each support we are able to determine the constants A to D in the general solution. However in this problem the beam is considered as a continuous system, which means there are an infinite number of degree of freedom and therefore an infinite number of eigenfrequencies and mode shapes. This means equation 4.3 has an infinite number of solutions, because there are an infinite number of beta values. It is possible to solve the equation for a specified eigenfrequency. Note that a with a summation of the infinite number of modes shapes describes the vibration of the beam.

We can determine three support situations for a single span beam: simply supported (pinned-pinned), clamped (clamped-clamped) or combined (clamped-pinned). This results in the following definitions for the n_{th} mode shape (Also plotted in figure 4.4):

- Pinned-Pinned

$$\Phi_n = \sin(\beta_n x)$$

- Clamped-Clamped

$$\Phi_n = \cosh(\beta_n x) - \cos(\beta_n x) - \alpha(\sinh(\beta_n x) - \sin(\beta_n x))$$

with:

$$\alpha = \frac{\cosh(\lambda) - \cos(\lambda)}{\sinh(\lambda) - \sin(\lambda)}$$

$$\lambda_n \approx \frac{1}{2}(2n + 1)\pi$$

- Clamped-Pinned

$$\Phi_n = \cosh(\beta_n x) - \cos(\beta_n x) - \alpha(\sinh(\beta_n x) - \sin(\beta_n x))$$

with:

$$\alpha = \frac{\cosh(\lambda) - \cos(\lambda)}{\sinh(\lambda) - \sin(\lambda)}$$

$$\lambda_n \approx \frac{1}{4}(4n + 1)\pi$$

In these equation λ is the wavelength of the corresponding mode shape, which is also defined as follows: $\lambda = \beta_n/L$. It is possible to substitute this into the mode shape equation.

It is important to note that the equations are based on Euler-Bernoulli equation for the definition of a beam, which does not take into account shear deformation. Besides that the rotational inertia is not taken into account. The consequence of these bases is that the found equations can be unreliable for higher order modes.

Using the same differential equation it is possible to calculate the eigenfrequencies as well. For an Euler-Bernoulli beam with a constant mass and stiffness this results in the following definition, which can be used for the different boundary conditions possible:

$$f_n = \frac{1}{2\pi} \sqrt{\frac{k_n^*}{m_n^*}} = \frac{C}{2\pi} \sqrt{\frac{EI}{\rho AL^4}} \tag{4.5}$$

NOTE: $\omega_n = f_n \cdot 2\pi$

In equation 4.5 the frequency f_n is first written in the general case, which states the well known relation between the frequency, stiffness and mass. In the considered case with a constant stiffness EI and mass ρA over the length this expression can be written in the second manner. In here the constant C is present, which depends on the mode shape and the boundary conditions, see figure 4.4.

		$n = 1$	$n = 2$	$n = 3$	$n = 4$	$n = 5$
clamped	free	C = 3.52	C = 22.4	C = 61.7	C = 121.0	C = 200.0
simply supported	simply supported	C = 9.87	C = 39.5	C = 88.9	C = 158.0	C = 247.0
clamped	clamped	C = 22.4	C = 61.7	C = 121.0	C = 200.0	C = 296.0
free	free	C = 22.4	C = 61.7	C = 121.0	C = 200.0	C = 298.0
clamped	simply supported	C = 15.4	C = 50.0	C = 104.0	C = 178.0	C = 272.0
simply supported	free	C = 15.4	C = 50.0	C = 104.0	C = 178.0	C = 272.0

Figure 4.4: Eigenfrequency and mode shape of a beam with constant EI , ρ and A for combinations of the well known boundary conditions (free, simply supported, clamped) for the first 5 modal vibrations [6]

When the eigenfrequency of a footbridge is close to the frequency of the dynamic load, in this case the pedestrian or wind loading, resonance can occur. When the excitation is acting on the bridge for a long period the vibrations can become quite significant and therefore cause problems. The period of time is of importance, because it may take some time to develop significant vibrations even when the frequencies of the load and structure are similar. In the theoretical case where no damping is present in the system resonance can cause an infinite response. However in a real situation there is always damping within the system. This damping lowers the response amplitude, as we can see from the graph in figure 4.5. It is clearly visible that the damping has a big influence on the response of a dynamic system.

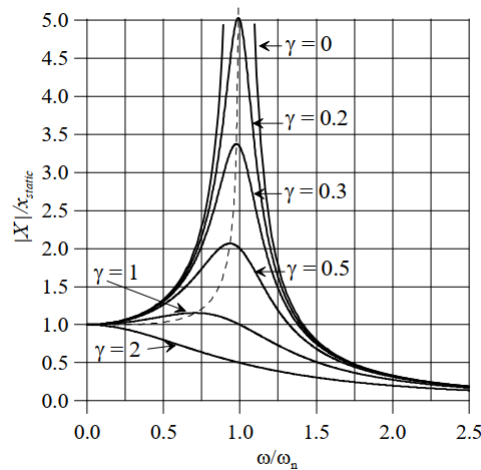


Figure 4.5: The dynamic amplification factor of a single degree of freedom system. Horizontal axis denotes the ratio between loading frequency and eigenfrequency and the vertical axis the ratio between dynamic and static amplitude (γ is the damping ratio in this graph [6])

4.2.2. Damping

Damping is the characteristic that dissipates the energy of the vibration of the structure. This overall damping can initially be separated in two different parts: material damping and structural damping. Material damping is the amount of energy that dissipates due to the deformations of the material itself. During stressing and distressing of a material energy will be 'absorbed' by the material and so dissipated from the vibration energy. The structural damping can be seen as the dissipation of energy due to other phenomena than material properties, for example friction in a connection. Besides these two initial parts there are many more possible energy dissipation mechanisms present in a system. The environment of a system can also influence the amount of energy that is dissipated. An clear example is aerodynamic damping. Most of the time the energy dissipation increases when the amplitude of vibration increases, which also brings more complexity into the concept of damping.

Due to the vast amount of phenomena that dissipate vibrational energy it is difficult to predict. Usually the entire concept of damping is simplified into a single damping principles. Therefore it can be related to the total vibrational energy dissipation of a structure that is measured. For a simplified model this is shown in figure 4.6.

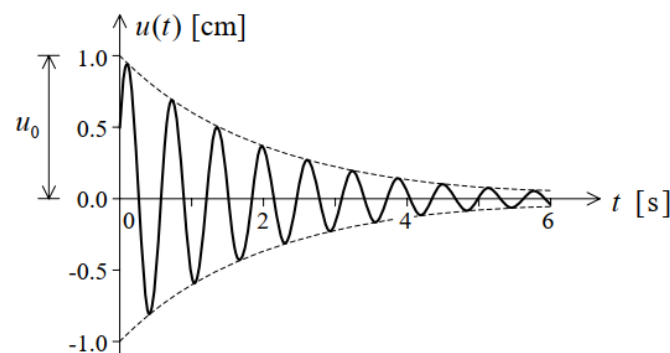


Figure 4.6: The vibrational energy dissipation can be clearly seen in the decreasing amplitude. Such a graph does not hold any information on how this energy is dissipated, but it contains the amount of energy that is dissipated from the vibrational behaviour [6]

A common way to model the damping is by assuming linear viscous damping behaviour. This means that damping forces are proportional to the velocity, which is a accepted assumption for small vibrations. Another assumption for the damping model is that damping is distributed over the entire structure. The implementation of this damping behaviour leads to a linear set of equations which solutions can be

easily found. For example, multi degree of freedom systems can be dealt with using separated modes when this linear equations are derived. this damping model will also be used in this research.

In the explanation of resonance the influence of damping on the amplitude of the response has already been described. Theory also describes that the damping also adds a shift to the eigenfrequency. However, the damping ratio of the footbridges that are considered in this research are small. Therefore, the change of frequency is neglected.

4.2.3. Codes and guidelines

Dutch codes and guidelines

Eurocode and Dutch national annex

In Eurocode NEN-EN 1991-2 the traffic loads on bridges are defined. In this document a general description of the dynamic serviceability assessment is given. In paragraph 5.7 it is stated that the dynamic characteristics of the structure must be defined using an appropriate dynamical model. This information needs to be combined with the frequency ranges of the loading due to pedestrians to check for the occurrence of resonance. For the more specific description of the dynamic models and comfort requirements the document refers to the National Annex and NEN-EN 1990 A2. The comfort criteria are defined as a limitation of the maximum acceleration of a arbitrary part of the bridge deck. For these the following values are recommended:

- 0.7 m/s^2 in vertical direction for regular use and wind loading
- 0.2 m/s^2 in horizontal direction for regular use and wind loading

These values are midrange value of comfort class 2 as defined in the JRC (Joint Research Centre) document *Design of Lightweight Footbridges for Human Induced Vibrations* ([17]). For a project other comfort criteria may be used, but the values in the JRC document are recommended.

In the Dutch national annex of NEN-EN 1991-2 the dynamic load models are described in more detail. These load models are derived from the JRC. There are 2 different load cases defined, namely for crowd loading and joggers. The Dutch national annex requires for regular user situations the use of Traffic Class 3 for crowd loading. For the regular user situation the jogger loading is depending on the span of the bridge: for a span $\leq 20 \text{ m}$ 5 joggers have to be considered, for a span of $> 20 \text{ m}$ 10 joggers have to be considered. It is allowed to model them stationary on the normative location.

The before mentioned load and comfort requirements are a serviceability limit states. However Eurocode NEN-EN 1991-2 also prescribes to check the ultimate limit state of vandalism loading. For this Traffic class 5 have to be used (if not specified otherwise for the project) combined with a damping ratio equal to 50% of the nominal damping value for large vibrations.

JRC document: *Design of Lightweight Footbridges for Human Induced Vibrations* [17]

As previously mentioned, this document describes the load models for crowds and joggers. Different calculation methods are explained to find this maximum acceleration. These accelerations can be checked with the in this document defined comfort classes.

The first step in the JRC document is the assessment of the eigenfrequencies. This can be done using hand calculations, as described before, and with a Finite Element model. The FE models has to be used whenever the eigenfrequencies are close to the load frequencies to make sure the correct behaviour is checked.

When the bridge is loaded the mass of the people on the bridge may alter the eigenfrequencies. Therefore it is recommended to take into consideration during the calculation of the eigenfrequencies when the modal mass of the pedestrians is more than 5 % of the modal mass of the deck.

The critical ranges for the eigenfrequencies are defined to be the following. This is defined using the frequency ranges of the load frequencies and result in:

- Vertical and longitudinal vibrations:
 - 1.25 to 2.3 Hz;
 - 2.5 to 4.6 Hz for the 2nd harmonic;

- Lateral vibrations:
 - 0.5 to 1.2 Hz;
 - (2nd harmonic no effect in lateral vibrations)

A dynamic analysis must be done when the eigenfrequencies coincide with these critical ranges.

The following step is to define the design situations. A design situation is an event that has a certain load and certain acceptable maximum acceleration.

For crowd loading the Traffic Classes are defined. The Traffic Classes (TC1 to TC5) describe a density of the pedestrian stream on the bridge, see figure 4.7.




Traffic Class	Density d (P = pedestrian)	Description	Characteristics
TC 1*)	group of 15 P ; $d=15 P / (BL)$	Very weak traffic	(B =width of deck; L =length of deck)
TC 2	$d = 0,2 P/m^2$	Weak traffic 	Comfortable and free walking Overtaking is possible Single pedestrians can freely choose pace
TC 3	$d = 0,5 P/m^2$	Dense traffic 	Still unrestricted walking Overtaking can intermittently be inhibited
TC 4	$d = 1,0 P/m^2$	Very dense traffic 	Freedom of movement is restricted Obstructed walking Overtaking is no longer possible

Figure 4.7: Pedestrian traffic classes for crowd loading. It is important in the design stage to make a realistic assumption for loading during the design life.

To be able to assess the comfort during a certain response Comfort Classes (CL1 to CL4) are defined as an range of maximum acceleration, see figure 4.8.

Comfort class	Degree of comfort	Vertical a_{limit}	Lateral a_{limit}
CL 1	Maximum	< 0,50 m/s ²	< 0,10 m/s ²
CL 2	Medium	0,50 – 1,00 m/s ²	0,10 – 0,30 m/s ²
CL 3	Minimum	1,00 – 2,50 m/s ²	0,30 – 0,80 m/s ²
CL 4	Unacceptable discomfort	> 2,50 m/s ²	> 0,80 m/s ²

Figure 4.8: The different Comfort Classes defined as ranges of maximum accelerations. Note that the lock-in phenomena is not checked in this comfort classes

As already described plays the damping an important role in the response. In this JRC document the assumption of linear viscous damping is also made. Some damping ratios are defined for different construction materials. For regular service conditions the following damping ratio are prescribed for steel footbridges:

- Minimum damping ratio $\xi = 0.2\%$
- Average damping ratio $\xi = 0.4\%$

When the amplitude of vibrations increase the damping ratio will also increase. This means that when the bridge is intentionally excited the maximum acceleration can be calculated with an higher damping ratio than for service conditions: For steel welded joints $\xi = 2.0\%$

There are different methods recommended that calculated the maximum acceleration of the footbridge under the prescribed loads and damping (see figure 4.9). It is possible to apply the dynamic loads directly into the FE model. It is also possible to simply the structure to multiple Single-Degree-Of-Freedom systems using modal analysis. The last method that the document recommends is the Response spectra method, in which the problem is solved using the frequency domain. In this research the SDOF method will be used.

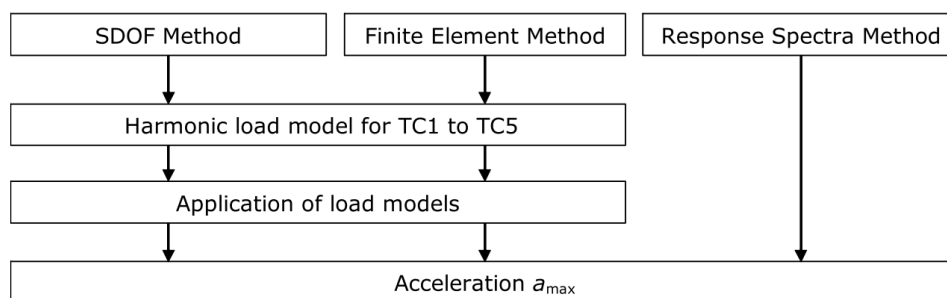


Figure 4.9: The different methods and steps to calculate the maximum acceleration under a prescribed load and damping

The load on the SDOF method requires the load to be harmonic. For a stream of n "random" pedestrians each individual pedestrian load can be model harmonically, but combining them to calculate the response can be a lot of effort. This problem is solved by simulating the result using a harmonic model with a equivalent number of perfectly synchronized pedestrians n' . This equivalent load stream is supposed to have the same effect on the structure. This 'equivalent' load can be used for the SDOF method deterministically.

Using this approach the uniformly distributed harmonic load can be defined as:

$$p(t) = P \times \cos(2\pi f_s t) \times n' \times \Psi$$

with :

- P The force due to a single pedestrian with step frequency f_s (4.6)
- f_s Step frequency which is assumed to be the same as the eigenfrequency
- n' The number of equivalent pedestrians
- Ψ the reduction coefficient

For the reduction coefficient the probability that the footfall frequency approaches the critical range of eigenfrequencies under consideration is taken into account. The values for the parameters are given in figure 4.10:

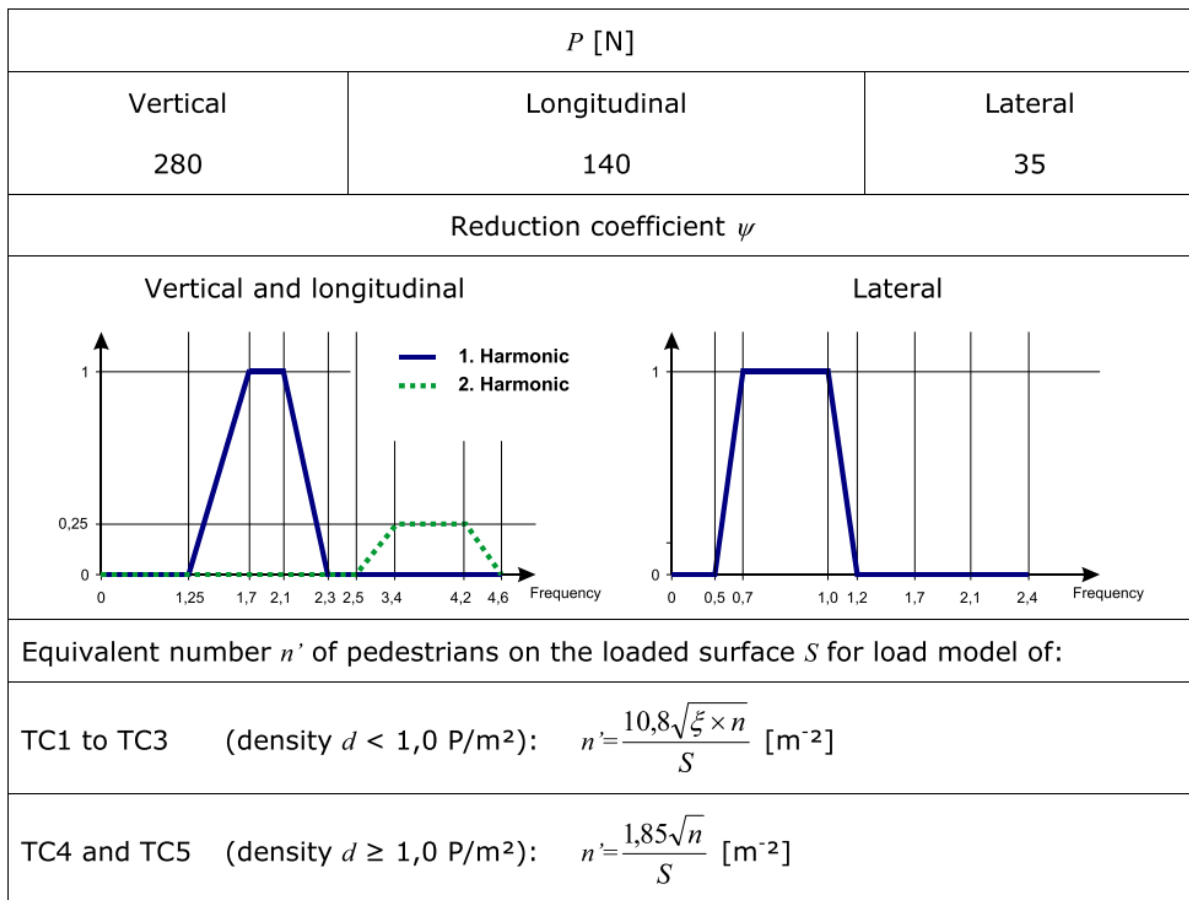


Figure 4.10: Parameters for uniformly distributed harmonic load to model the crowd loading

For joggers the dynamic load is modelled in a similar way, because the jogger loading is also modelled harmonically. Together with the simplification that the load is applied stationary at the location with the biggest amplitude of the considered mode shape it uses the same formula, see equation 4.6. The parameters are given in figure 4.11.

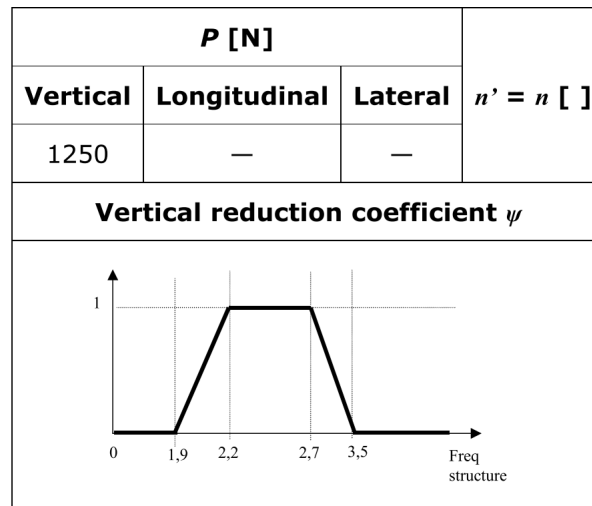


Figure 4.11: Parameters for the harmonic load to model the jogger loading. stationary at the maximum amplitude of the considered mode shape. Note that n' is equal to n .

The Single Degree Of Freedom method is based on a modal analysis in which every mode shape with corresponding eigenfrequency is modelled as a SDOF mass-spring-dashpot system. In that way it is fairly simple to derive the maximum acceleration of a system:

$$a_{max} = \frac{p^*}{m^*} \frac{1}{2\xi}$$

with:

$$p^* = \int_L p(x)\Phi(x)dx \quad , \text{ the modal equivalent load} \quad (4.7)$$

$$m^* = \int_L \mu(\Phi(x))^2 dx \quad , \text{ the modal mass}$$

Note in the calculation $p(x)$ is the amplitude of the applied harmonic uniformly distributed load $p(t)$ of equation 4.6.

Codes in other countries

In this subsection of the literature study a quick comparison is made between the codes and guidelines that are set for The Netherlands and other countries. Only the big differences will be mentioned, such as different methods or load cases.

Code used in France - SETRA document [10]: Assessment of vibrational behaviour of footbridges under pedestrian loading

The SDOF method used in the JRC document is also used in the SETRA document, so there are a lot of similarities between the two guidelines. For the crowd load case, the step frequency ranges are slightly different, namely 1 to 5 Hz. The reduction factor for the second harmonic of the step frequency $\Psi = 1$ is significantly different since the JRC document prescribes $\Psi = 0.25$.

The biggest difference is for the jogger load case. In the SETRA document it is prescribed that jogger load case should not be systematically retained. This is due to the fact that the duration of joggers on the bridge is relatively short. The time for resonance to build up and the time other pedestrian are annoyed is therefore limited. Note that this jogger load case does not consider events such as a marathon.

However, the document still describes the forces due to a jogger. For the vertical direction the Bachmann load model is prescribed to be considered.

British Standards National Annex of EN 1991-2

In the UK the national code is considering different load cases. Which load cases have to be considered is defined by different bridge classes, see figure 4.12. The group of walking pedestrians is an extra load case compared with the JRC and SETRA documents.

For the three load cases a moving pulsating force defined as a sinusoidal load has to be applied. This is similar to the prescribed load in the JRC and SETRA document, however the simplification of a stationary application is only allowed for crowd loading, not for group or jogger loading. For the jogger load cases the force has an amplitude of 910 N, which is lower than the prescribed 1250 N in the other codes.

Bridge class	Bridge usage	Group size (walking)	Group size (jogging)	Crowd density ρ (persons/m ²) (walking)
A	Rural locations seldom used and in sparsely populated areas.	N = 2	N = 0	0
B	Suburban location likely to experience slight variations in pedestrian loading intensity on an occasional basis.	N = 4	N = 1	0.4
C	Urban routes subject to significant variation in daily usage (e.g. structures serving access to offices or schools).	N = 8	N = 2	0.8
D	Primary access to major public assembly facilities such as sports stadia or major public transportation facilities.	N = 16	N = 4	1.5

Figure 4.12: Table NA.7 recommended crowd densities for design, BS NA EN 1991-2

Another big difference for the British Standards is the maximum acceleration criteria. The design acceleration limit is given by:

$$a_{\text{limit}} = 1.0 k_1 k_2 k_3 k_4 \text{ [m/s}^2\text{]} \quad (4.8)$$

and

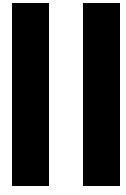
$$0.5 \leq a_{\text{limit}} \leq 2.0 \text{ [m/s}^2\text{]}$$

The four k factors are so called response modifiers in which:

- k_1 = site usage factor
- k_2 = route redundancy factor
- k_3 = height of structure factor
- k_4 = exposure factor

So the limit of the maximum acceleration is based on location, alternatives, height and other conditions that may affect the users perception towards the vibrations. These project specific factors are not considered in the other codes.

It is worth mentioning that all codes use the acceleration of the bridge as a criterium. For other dynamic analysis the velocities and displacements are often used. It is found that the velocities and displacements are related to the damage due to vibrations. However, the dynamic analysis under human induced vibrations is a serviceability, comfort, check. Since the perceptibility of vibrations by pedestrians is found to be related to accelerations this is used.



Initial design

5

Initial design

This chapter will describe the structural system that is chosen for this research. This structural system will form the basis of the dynamic analysis of the jogger load case (see part III). The most important result of this chapter will therefore be the parameters of the structural system for which the jogger load case will be governing. Since these structural system is used as a indication of the parameters, the checks are limited to the vertical direction. So for the Ultimate Limit State: the maximum stresses will be checked. For the Serviceability Limit State: the maximum deformation and the vertical vibrational comfort will be checked.

The design must also be capable of supporting non-uniform loads in transverse direction. This will probably lead to the necessity of cross girders to distribute the forces towards the main girders. However, the corresponding checks are not done in this research. The presence of these additional girders will be added in the self weight.

In the first section of this chapter the design basis will be explained, based on the chosen cross section type (see 4.1.1) and general scope boundaries. Thereafter, the considered loads on the bridge will be discussed which leads to a set of load combinations. On this basis of the set boundary and loads the structural systems a proposed design will be checked using the applicable codes for a bridge design in The Netherlands.

5.1. Design basis

When a footbridge design process is started it is important to make a list of requirements. The potential design needs to fulfil these requirements which can involve the dimensions and loads on the bridge for example. For this research the following framework is described which influence the implementation of the results. The following requirements and/or conditions are used in the design:

- The cross section is made using a set of beams
- A constant cross section is used
- The width is 3 m
- Type of deck: Steel with an anti-slip wear layer
- Steel grade S355 is used for the design
- Location of the bridge does not introduce high expectation of fully loaded case due to pedestrians (see 5.2.3).
- Location of the bridge does not introduce collision probabilities

The initial design is based on the information of the literature study which shows the possible structural design possibilities to achieve a high slenderness ratio. Together with the set requirements and

boundary conditions described above the following design is chosen.

The design is simplistic because it is composed out of regular known I-sections in a grid. On this grid a steel sheeting is placed that functions as a decking and as the top flange of the girders. This design can quite simply be changed to different spans and width due to the simple beam grid basis. This offers a more direct comparison if the design parameters are changed for different lengths.

The cross section used, shown in figure 5.1 consists of the following beams and deck (it is based on the design of the Tuinveld bridge [4]):

- HEA 320 used as girders
- 4 girders
- deckplate thickness $t_{deck} = 15$ mm



Figure 5.1: Cross section of footbridge used in thesis. Cross beams may be needed, but not considered at this stage except for increase in self weight

5.2. Considered loads

In the Eurocode the loads on the structures are defined in NEN-EN 1991. Part 1.1 to 1.7 define the general loads that may act on a structure and in part 2 the loads due to traffic are discussed. On the basis of these Eurocode part the loads that shall be considered in this initial design are listed. In this section the loads that are considered will be shortly mentioned and the relevant loads will be determined for this case. These loads are initially described individually after which the required load combinations are defined. In the Eurocode the following loads are described that can act on the footbridge:

- Self weight
- Permanent loads on the bridge
- Traffic loads
- Wind load
- Accidental loads
- Vertical dynamic loads due to humans

5.2.1. Self weight

The self weight is simply derived by the amount of the steel parts multiplied with a volumetric of 78.5 kN/m^3 . The additional cross girders that are possibly needed have an extra weight of approximately 10%. The extra weight due to painting and additional steel works (added in later design stage) are taken into account by adding 5% of the calculated load due to the steel. So this results in a characteristic line load:

$$q_{\text{self weight steel}} = A_{\text{cross}} \cdot (1 + 0.05 + 0.10) \cdot 78.5 \text{ kN/m}$$

Where A_{cross} is the cross sectional area in m^2 .

5.2.2. Permanent loads

On top of the steel deck a wearing anti-slip surface is applied made of an epoxy resin. Split stones are used to provide traction and prevent the degradation of the steel of the deck. This layer is assumed to result in a uniformly distributed load of 0.15 kN/m^2 (Based on epoxy layer weighing approximately 15 kg/m^2 [1]).

The parapets that are present on the bridge to protect the pedestrian or cyclists from falling off are applied as a line load of 1 kN/m on the structure.

$$q_{\text{wearing layer}} = 0.15 \cdot B = 0.45 \text{ kN/m}$$

$$q_{\text{parapets}} = 1 \text{ kN/m}$$

Where $B = 3 \text{ m}$ is the width of the deck.

5.2.3. Traffic loads

Eurocode NEN-EN 1991-2 5.3.2 states that 3 mutually exclusive models need to be considered:

- a uniformly distributed load, q_{fk}
- a concentrated load, Q_{fvd}
- loads representing a service vehicle, Q_{serv}

However, since a service vehicle is considered in this design this concentrated load does not have to be applied.

Uniformly distributed load, q_{fk}

A uniformly distributed load needs to be applied that covers the static effect of a dense crowd. This is the same as load model 4 (BM4) for every bridge case which describes a recommended value of $q_{f;k} = 5 \text{ kN/m}^2$. However, if the continuously loaded surface length exceeds 10 m the following formula may be applied:

$$q_{fk} = 2.0 + \frac{120}{L + 30} \quad \text{if } 2.5 \text{ kN/m}^2 \leq q_{fk} \leq 5.0 \text{ kN/m}^2 \quad (5.1)$$

With L is the continuous length of the influence length in m . The formula is also illustrated in figure 5.2.

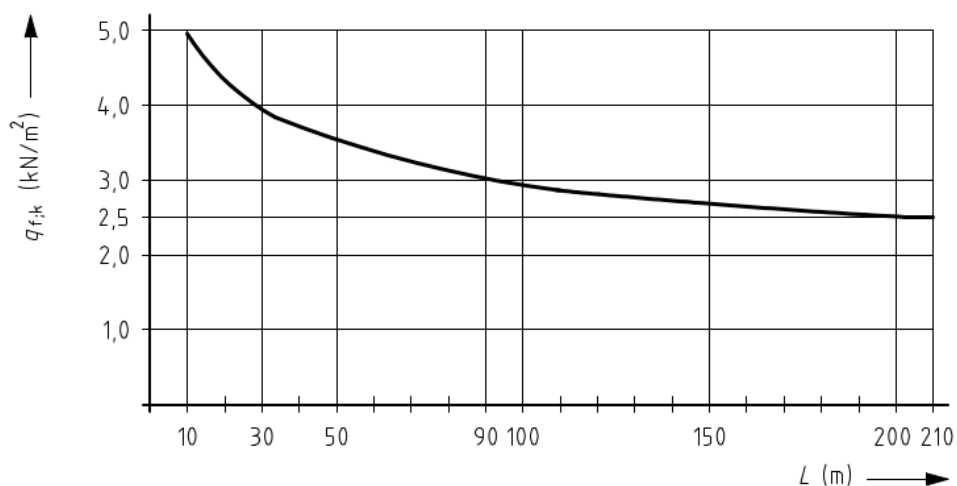


Figure 5.2: The characteristic value of the uniformly distributed load due to crowd loading depending on influence length

If it can be expected that the bridge may be fully loaded, for example close to a stadium, $q_{f;k} = 5.0 \text{ kN/m}^2$ must be considered. NOTE: This will not be considered in this design.

Service Vehicle, Q_{serv}

NEN-EN 1991-2 5.3.2.3 states when service vehicles are to be carried by the footbridge, one service vehicle shall be taken into account. This vehicle may be a vehicle for maintenance, emergencies or other services. The characteristics of this loading are given in the Dutch national annex as:

- two axels with a wheel base of 3 m
- characteristic value of the axle load is 25 kN
- every axle has two wheels with a track of 1.75 m
- 0.25×0.25 m contact area per wheel

The two traffic loads, q_{fk} and Q_{serv} , have to be considered using groups of loads. Since, the horizontal forces are not checked the groups are found to be, according to Dutch national annex:

gr1: q_{fk}

gr2: $0.8 \cdot q_{fk}^a$ combined with Q_{serv}

^a Not at the location of the service vehicle, including a space of 5 m in front and behind.

5.2.4. Wind loads

We only consider vertical wind loads. Eurocode NEN-EN 1991-1-4 states the wind perpendicular to the bridge must be considered. The coefficient $c_{f,z}$ for the loads in vertical direction is 0.9 according to 8.3.3. The factor $c_s c_d = 1$ since the spectrum of the wind fluctuations is lower than the fundamental frequency of the bridge. The distributed vertical wind load is found to be:

$$P_{w,z} = c_s c_d c_{f,z} q_p = 0.9 q_p$$

With q_p = extreme wind pressure at height z in meters.

In the Dutch national annex the values for q_p depending on wind area and surroundings is given in table NB.5. To be conservative: The general location of a footbridge is chosen to be area I, in a Rural area at a height om 8 m. A realistic conservative situation is thereby used: a footbridge crossing a road, at a rural area with high average winds. Table NB.5 prescribes $q_p = 0.94$ kN/m². However, this table is based on a return period of 50 years. Since a footbridge is designed for a return period of 100 years, the value must be changed.

The probability factor for the basic wind velocity is given as:

$$c_{prob} = \left(\frac{1 - K \cdot \ln(-\ln(1 - p))}{1 - K \cdot \ln(-\ln(0.98))} \right)^n \quad (5.2)$$

With $K = 0.2$ and $n=0.5$.

For a return period of 100 years ($p = 0.01$) this means $c_{prob} = 1.038$. This value is multiplied with the basis wind velocity. The value of the peak wind pressure is calculated according to:

$$q_p(z) = (1 + 7l_v(z)) \cdot 1/2 \cdot \rho \cdot v_m^2(z) \quad (5.3)$$

So by multiplying peak wind pressure from table NB.5 with c_{prob}^2 the return period of 100 years is used. Which results in:

$$P_{w,z} = 0.9 \cdot 1.038^2 \cdot 0.94 = 0.99 \text{ kN/m}^2$$

5.2.5. Accidental loads

As described in the scope definition (see chapter 3) no collision of any kind shall occur. This means the only accidental load case that shall be considered is the possibility of a vehicle on the bridge. This is a different, heavier, vehicle than the one considered in the maintenance vehicle load case.

Accidental presence of vehicles on a bridge

In the Eurocode NEN-EN 1991-2 5.6.3 a load model is prescribed that has to be considered for the accidental vehicle. The model is described as follows (see figure 5.3):

- a wheel base of 3 m
- 80 kN at the front and 40 kN at the back axle
- every axle has two wheels with a track of 1.3 m
- a square contact area of 0.2×0.2 m per wheel

No other variable loads should be applied together with this accidental vehicle.

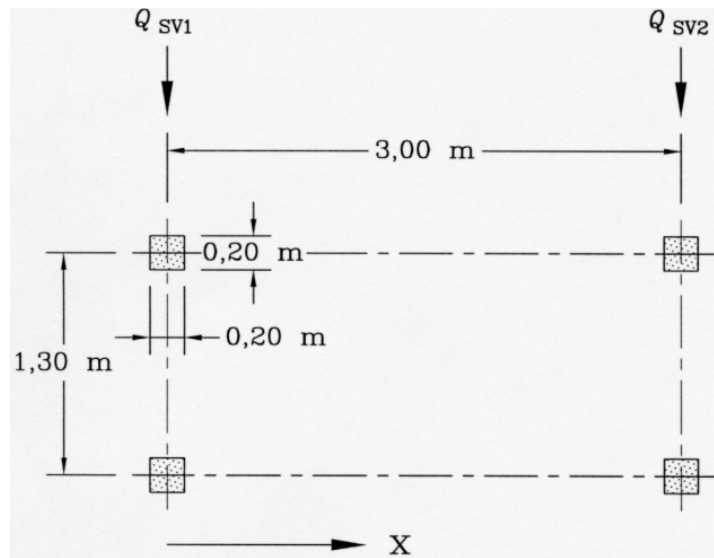


Figure 5.3: Illustration of the vertical load model for accidental presence of vehicles on the bridge (X is the bridge axis direction)

5.2.6. Vertical dynamic loads due to humans

The dynamic loads will be considered as described in the literature background 4. The accelerations will be calculated using the SDOF-method. For the crowd loading case Traffic Class TC3 will be used.

5.3. Load combinations

The load combinations are depending on the Limit State and design situation. For the Ultimate Limit State (ULS) is related to the safety of the structure and humans using it. The Serviceability Limit State is related to the functioning of the structure and the comfort of the humans using it. To check these limit states, the load combination related to design situation are made.

5.3.1. Ultimate Limit State

For the Ultimate Limit State (ULS) the checks will consider the following design situation:

1. permanent and temporary design situation
2. accidental design situation

They will introduce different load cases that have to be considered for the maximum stresses in the design.

Load combinations for permanent and temporary design situation

The least favourable of the following two formulas should be used for the loads (derived from NEN-EN 1990 6.10 (a) and 6.10(b) respectively):

$$\sum_{j \geq 1} \gamma_{G,j} G_{k,j} + \gamma_{Q,1} \Psi_{0,1} Q_{k,1} + \sum_{i > 1} \gamma_{Q,i} \Psi_{0,i} Q_{k,i}$$

or

$$\sum_{j \geq 1} \xi_j \gamma_{G,j} G_{k,j} + \gamma_{Q,1} Q_{k,1} + \sum_{i > 1} \gamma_{Q,i} \Psi_{0,i} Q_{k,i}$$
(5.4)

Load combinations for accidental design situation

For the accidental load case the formula for the load is given by (NEN-EN 1990 6.11(b)):

$$\sum_{j \geq 1} G_{k,j} + A_d + (\Psi_{1,1} \text{ or } \Psi_{2,1} Q_{k,1}) + \sum_{i > 1} \Psi_{2,i} Q_{k,i}$$
(5.5)

In the equation for the accidental design situation, 5.5, there is a variable load added. The only accidental load case that is considered describes the accidental presence of a vehicle on the bridge. It is stated that this should not be combined with other traffic loads and wind load. This means that the last two parts of equation 5.5 are zero.

Partial factor γ for the ULS

For structural ULS checks for slow traffic and footbridges the partial factors are given in table NB.13 - A2.4(B) of the Dutch national annex. For a footbridge the consequence class CC2 is applied. This leads to the following:

Table 5.1: Partial load factors for slow traffic and footbridges for structural ULS checks

Consequence Class	G		Traffic loads	Other variable loads
	$\gamma_{G,j}$		γ_Q	γ_Q
	6.10(a)	6.10(b) (incl. ξ)		
CC2	1.3	1.2	1.35	1.5

Ψ -factors

The combination factors Ψ for the variable loads for footbridges are given by the Dutch national annex to be:

Load combinations for the Ultimate Limit State

Since we need to find the least favourable for the equations of 5.4 and combination of leading variable loads

1. wind and gr1 - (based on 6.10(a))
2. wind and gr2 - (based on 6.10(a))
3. gr1 leading combined with wind - (based on 6.10(b))
4. gr2 leading combined with wind - (based on 6.10(b))
5. wind leading combined with gr1 - (based on 6.10(b))
6. wind leading combined with gr2 - (based on 6.10(b))
7. accidental load case

The factors γ and Ψ are combined in the table 5.2 to show what factors are applied in which load case. Note that for the load combinations with traffic load gr2, the restrictions on the applied uniform load need to be applied:

Loads	Symbol		ψ_0	ψ_1	ψ_2
Traffic loads	gr1	Uniformly distributed load q_{fk}	0,4	0,8 ^c	0,4
		Horizontal load Q_{fk}			
	gr2	Uniformly distributed load q_{fk}	0,4	0,8 ^b	0
		Service vehicle Q_{serv}			
		Horizontal load Q_{fk}			
		Concentrated load Q_{fwk}		0	0,8 ^b
	Accidental vehicle (see 5.6.3)		0	0,8 ^b	0
Wind loads	F_{Wk}	Lasting design situation Construction	0,3 0,8	0,6 ^b 0	0
Thermal loads	T_k		0,3	0,8	0,3 ^a
Snow loads	$Q_{Sn,k}$	Lasting design situation	0	0	0
		Construction	0,8	0	
Loads during construction	Q_c		1,0	0	1,0
^a In ultimate limit state ψ_2 for thermal loads can be used as 0 ^b In the event of a collision on or under the bridge $\psi_1 = 0$. ^c In the event of a collision on or under the bridge $\psi_1 = 0,4$. NOTE groups of traffic loads do not have to be combined.					

Figure 5.4: NEN-EN 1990 Table NB.10 - A2.2 - Ψ -factor for footbridges

Table 5.2: Combined factors for the Ultimate Limit State load combinations

Load	ULS - Load Combination						
	1	2	3	4	5	6	7
Permanent, G	1.3	1.3	1.2	1.2	1.2	1.2	1
uniform traffic	$0.4 \cdot 1.35$	$0.4 \cdot 1.35^a$	1.35	1.35^a	$0.4 \cdot 1.35$	$0.4 \cdot 1.35^a$	0
service vehicle	0	$0.4 \cdot 1.35$	0	1.35	0	$0.4 \cdot 1.35$	0
wind	$0.3 \cdot 1.5$	$0.3 \cdot 1.5$	$0.3 \cdot 1.5$	$0.3 \cdot 1.5$	1.5	1.5	0
accidental	0	0	0	0	0	0	1

^a Note the restrictions described by 5.2.3

5.3.2. Serviceability Limit State

The Serviceability of the structure will be tested for the static and dynamic behaviour. For the static behaviour, the maximum deflection of the bridge will be considered. For this the frequent load combination will be used, which is defined as (derived from NEN-EN1990 6.15(b)):

$$\sum_{j \geq 1} G_{k,j} + \Psi_{1,1} Q_{k,1} + \sum_{i > 1} \Psi_{2,i} Q_{k,i} \quad (5.6)$$

The Ψ values are already described in figure 5.4. The load combinations, see table 5.3 for the Serviceability Limit State are found as:

1. gr1 leading variable load combined with wind
2. gr2 leading variable load combined with wind
3. wind leading variable load combined with gr1
4. wind leading variable load combined with gr2

It is assumed that the deflection due to the permanent loads can be countered by an small upward curvature during construction. Therefore, the permanent loads (self weight and additional loads) are not considered in the SLS load combinations for the deflection check. The combined factors for the serviceability Limit State load combinations are shown in tabel 5.3.

Table 5.3: Factors for the Serviceability Limit State load combinations

Load	SLS - Load Combination			
	1	2	3	4
Permanent, G	0	0	0	0
uniform traffic	0.8	0.8 ^a	0.4	0.4 ^a
service vehicle	0	0.8	0	0.4
wind	0	0	0.6	0.6
Accidental	0	0	0	0

^a Note the restrictions described by 5.2.3

5.4. Structural design verifications

As already mentioned, the structural design verification will be done according to the following checks:

- $\sigma_{max}/f_y \leq 1.0$, maximum stress in ULS
- $w_{max} < L/500$ m, maximum deformation in SLS
- $a_{max} < 0.7$ m/s², maximum accelerations in SLS for crowd and jogger loads

These checks are considered for different span lengths. The goal is to find the length for which the maximum acceleration due to the jogger loads is failing the design. At that length, it is useful to better examine the jogger load case. Which will be done in the remainder of the thesis.

The checks are done for the design basis described in 5.1, for span lengths between 14 and 30 m. In figure 5.5 the 4 checks for the different span lengths are shown. In this figure the value of 1 represents the check that failed, and 0 the check that passed. In the top graph it can be seen that for a span length below 18 m or between 23.1 and 24.1 m the stress, deformation and dynamic crowd checks are passed. In the bottom graph it can be seen that the dynamic jogger test fails between 20.3 and 28 m. Therefore, it can be concluded that in between 23.1 and 24.1 (indicated by the vertical lines) the jogger load case is causing the design to fail.

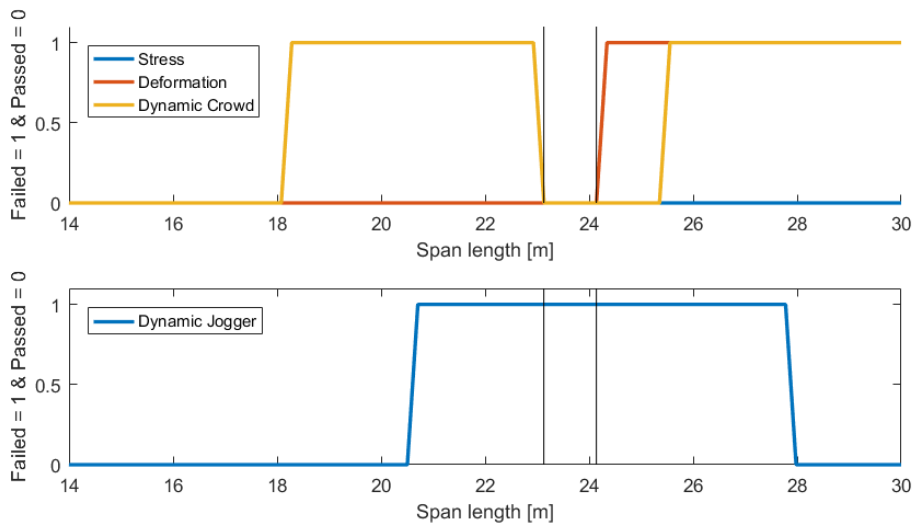


Figure 5.5: Graph that shows the pass/fail of the 4 different checks according to different span lengths

The result of the jogger load case is considered more closely to make a choice for 1 span length in the interval 23.1 and 24.1. In figure 5.6 the value of the check can be seen. The ratio of calculated maximum acceleration over the maximum allowed value (0.7 m/s²) is shown for different span length. The highest value of this check is found at L = 23.5 m, which is within the previously found interval. At this span length the highest maximum acceleration is found and the other checks are passed.

To conclude, as an input for the remainder of the thesis the following characteristics for a beam representation of the bridge will be used:

- $L = 23.5$ m, span length
- $\mu = 925.9$ kg/m, self weight
- $I_y = 3.9273 \cdot 10^9$ mm⁴, vertical moment of inertia

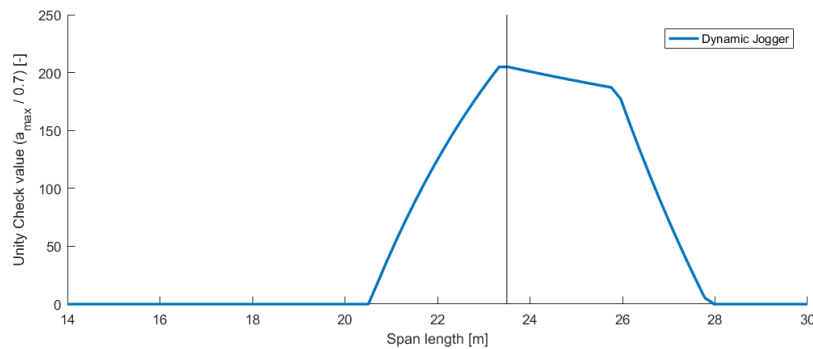
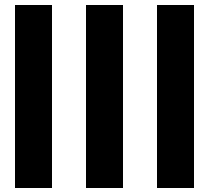


Figure 5.6: Unity Check values for the maximum acceleration due to jogger loading for different span length, vertical line at $L = 23.5$ m

The 1-dimensional simplification means that only the global design checks can be done. The transverse direction is not considered, statically and dynamically. For the static checks, the design must also be capable of supporting non-uniform loads. For the considered design this will be done using cross girders that distribute the forces towards the main girders. The presence of these additional girders is added in the self weight and so added to the vertical checks considered. However, the 1-dimensional simplification results in neglecting the torsional dynamical modes. The distribution of the joggers will have an effect on the bridge response when it is modelled as a 2-dimensional problem, since the torsional modes will also be affected by the loading. The 1-dimensional simplification is conservative for the vertical vibrations, but the torsional dynamic checks are not considered. If the torsional modes have a eigenfrequency that may coincides with the step frequency, they must be checked additionally.



Jogger load case

Model description

In this chapter a description is made of the dynamic numerical model. This model is made in Matlab. The general model that is used here will be adapted so it is applicable for the MF and the MSD models. This chapter will first describe the general dynamic model. Some general checks on the behaviour of the model are done to verify its behaviour. The difference in the model due to the application of the dynamic load models will be explained and checked hereafter. The models that are constructed in this research are based on the same approach as used in the research of Caprani et al. [11].

6.1. Basic model

The dynamic model that is used for this research is based on the Finite Element (FE) Method. This means that the beam is discretized in a number of elements and nodes. The displacement field is approximated using 1-dimensional beam elements, that are based on the Euler-Bernoulli beam equation. To use this beam equation every node in the FE model has two degrees of freedom (DOF): displacement (w) and rotation (ϕ), see figure 6.1. Thus, the beam is modelled with the following characteristics:

- n_e , number of elements
- $n_N = n_e + 1$, number of nodes
- $N = 2(n_e + 1)$, number of DOFs

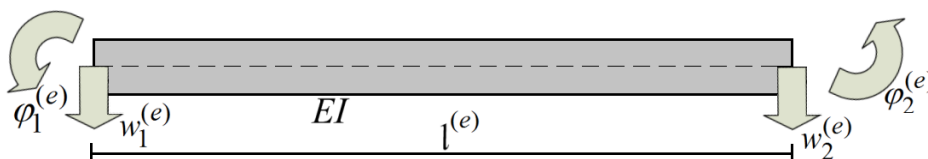


Figure 6.1: Beam element with two degrees of freedom per node to model an Euler-Bernoulli beam

Using this discretization the dynamic model of the beam can be formulated as:

$$\mathbf{M}\ddot{\mathbf{u}} + \mathbf{C}\dot{\mathbf{u}} + \mathbf{K}\mathbf{u} = \mathbf{P} \quad (6.1)$$

The \mathbf{M} , \mathbf{C} , and \mathbf{K} are the mass, damping, and stiffness matrix respectively (all of size $N \times N$). The vector \mathbf{P} is the force vector. The vector \mathbf{u} (size $N \times 1$) contains the degrees of freedom, and the dot refers to the time derivative.

The vector \mathbf{u} contains the displacement and rotation of each node in the following manner:

$$\mathbf{u} = \begin{bmatrix} w_1 \\ \phi_1 \\ w_2 \\ \phi_2 \\ \vdots \\ w_N \\ \phi_N \end{bmatrix} \quad (6.2)$$

For the construction of the matrices the shape functions are needed. Due to the two degrees of freedom per node the cubic Hermitian shape functions are needed. The shape functions are collected in the row vector \mathbf{N} . The shape functions are dependent on a dimensionless local coordinate ζ , so that they can be used for every element length. They are defined as follows:

$$\begin{aligned} \mathbf{N} &= [N_1 \quad N_2 \quad N_3 \quad N_4] \\ N_1 &= 1 - 3\zeta^2 + 2\zeta^3 \\ N_2 &= (\zeta - 2\zeta^2 + \zeta^3)l_e \\ N_3 &= 3\zeta^2 - 2\zeta^3 \\ N_4 &= (-\zeta^2 + \zeta^3)l_e \end{aligned} \quad (6.3)$$

for:
 $0 \leq \zeta \leq 1$

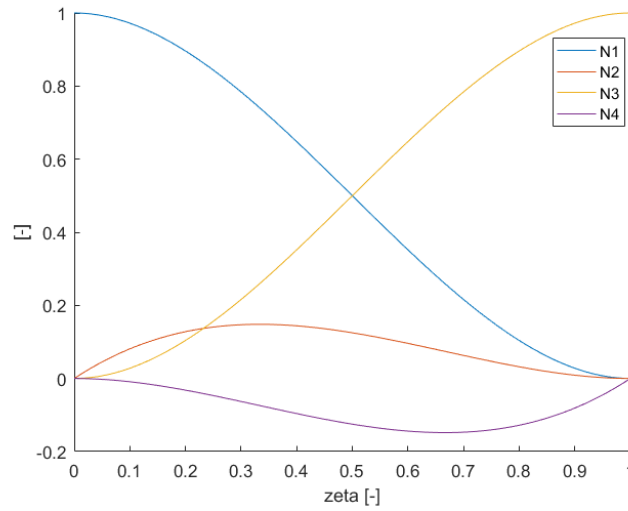


Figure 6.2: Shape function for each element. Defined as unity at location of the node and zero for all the other DOFs.

The element mass matrix is then defined as:

$$\mathbf{M}^e = \int_{l_e} \mathbf{N}^T \rho A \mathbf{N} = \frac{\rho A l_e}{420} \begin{bmatrix} 156 & 22l_e & 54 & -13l_e \\ 22l_e & 4l_e^2 & 13l_e & -3l_e^2 \\ 54 & 13l_e & 156 & -22l_e \\ -13l_e & -3l_e^2 & -22l_e & 4l_e^2 \end{bmatrix} \quad (6.4)$$

The element stiffness matrix is then defined as:

$$\mathbf{K}^e = \int_{l_e} \mathbf{B}^T E I \mathbf{B} = EI \begin{bmatrix} \frac{12}{l_e^3} & \frac{6}{l_e^2} & -\frac{12}{l_e^3} & \frac{6}{l_e^2} \\ \frac{6}{l_e^2} & \frac{4}{l_e} & -\frac{6}{l_e^2} & \frac{2}{l_e} \\ -\frac{12}{l_e^3} & -\frac{6}{l_e^2} & \frac{12}{l_e^3} & -\frac{6}{l_e^2} \\ \frac{6}{l_e^2} & \frac{2}{l_e} & -\frac{6}{l_e^2} & \frac{4}{l_e} \end{bmatrix} \quad (6.5)$$

In equation 6.5 the \mathbf{B} is defined as the spatial derivative of the shape functions in \mathbf{N} .

At this point the mass and stiffness matrices are known at element level. To construct the global problem, the element matrices need to be combined to form the global matrices. In this model the nodes are named in increasing order. Consequently, the global mass and stiffness matrices are skyline matrices. This means that only close to the diagonal values will have a non-zero value.

As an example the stiffness matrix (before implementation of boundary conditions) for a beam with 3 elements with $l_e = 1$ is found to be:

$$\mathbf{K} = EI \begin{bmatrix} 12 & 6 & -12 & 6 & 0 & 0 & 0 & 0 \\ 6 & 4 & -6 & 2 & 0 & 0 & 0 & 0 \\ -12 & -6 & 24 & 0 & -12 & 6 & 0 & 0 \\ 6 & 2 & 0 & 8 & -6 & 2 & 0 & 0 \\ 0 & 0 & -12 & -6 & 24 & 0 & -12 & 6 \\ 0 & 0 & 6 & 2 & 0 & 8 & -6 & 2 \\ 0 & 0 & 0 & 0 & -12 & -6 & 12 & -6 \\ 0 & 0 & 0 & 0 & 6 & 2 & -6 & 4 \end{bmatrix} \quad (6.6)$$

To specify the general equation of motion 6.1 the boundary conditions need to be implemented. In this model we look at the simply supported case, which means the following for a beam from $x = 0$ to $x = L$:

$$\begin{aligned} w &= 0 \text{ at } x = 0 \rightarrow w_1 = 0 \\ w &= 0 \text{ at } x = L \rightarrow w_N = 0 \end{aligned} \quad (6.7)$$

So the degrees of freedom w_1 and w_N are zero at every point in time. This means we can erase them from the set of equations. This is done by removing these DOFs from the vector \mathbf{u} . For the matrices \mathbf{M} and \mathbf{K} this means that the corresponding row and column need to be removed. To visualize this, the same example with a 3 element beam stiffness matrix as in 6.6 is used. After implementing the boundary conditions due to the simply supported case the stiffness matrix looks like:

$$\mathbf{K} = EI \begin{bmatrix} 4 & -6 & 2 & 0 & 0 & 0 \\ -6 & 24 & 0 & -12 & 6 & 0 \\ 2 & 0 & 8 & -6 & 2 & 0 \\ 0 & -12 & -6 & 24 & 0 & 6 \\ 0 & 6 & 2 & 0 & 8 & 2 \\ 0 & 0 & 0 & 6 & 2 & 4 \end{bmatrix} \quad (6.8)$$

with:

$$\mathbf{u} = \begin{bmatrix} \phi_1 \\ w_2 \\ \phi_2 \\ w_3 \\ \phi_3 \\ \phi_4 \end{bmatrix}$$

After the implementation of these 2 boundary conditions, the order of the system is reduced: $N = 2(n_e + 1) \rightarrow N_{\text{new}} = 2(n_e + 1) - 2$.

The derivation of the damping matrix is different compared to the stiffness and mass matrices. In this model proportional damping (Rayleigh damping) is used. Using this method the damping matrix is proportional to the global mass and stiffness matrix. The proportional damping matrix is then defined as follows:

$$\mathbf{C} = \alpha_0 \mathbf{M} + \alpha_1 \mathbf{K} \quad (6.9)$$

The calculation methods prescribed by Eurocode and JRC are based on modal analysis. In these calculations the modal damping matrix is diagonal and shows the damping per vibrational mode. A useful property of the Proportional damping is that the modal damping matrix will be diagonal by definition, as can be seen from:

$$\mathbf{C}^* = \mathbf{E}^T \mathbf{C} \mathbf{E} = \alpha_0 \mathbf{E}^T \mathbf{M} \mathbf{E} + \alpha_1 \mathbf{E}^T \mathbf{K} \mathbf{E} = \alpha_0 \mathbf{M}^* + \alpha_1 \mathbf{K}^* \quad (6.10)$$

In this \mathbf{E} is the eigenvector matrix of the dynamic system and the 'star' matrices are modal properties. To be able to verify the model a comparison is made with the results of Caprani et al. [11]. Since in that model proportional damping is applied, this is also done here.

In the proportional damping equation 6.9, α_1 and α_0 are unknown. However, in this case we want to make the comparison to the modal analysis and therefore the damping ratios of the modes are already defined. Using the first two principal modes to calculate the alpha values, the damping matrix can be found:

$$\alpha_0 = \frac{2\omega_1\omega_2(\xi_1\omega_2 - \xi_2\omega_1)}{\omega_2^2 - \omega_1^2} \quad (6.11)$$

$$\alpha_1 = \frac{2(\xi_2\omega_2 - \xi_1\omega_1)}{\omega_2^2 - \omega_1^2}$$

In this model the numbering of the eigenfrequencies is in increasing order. Together with the modal damping ratios that is assumed to be constant for every mode, this means that the damping ratio is always positive. Because the α -values are based on the first two modes, the higher modes will have higher damping ratios. Which means that the frequencies outside the step frequency range are damped out.

The last thing to be implemented in the model is the right hand side of the general equation, the loading. Due to the discretization the load also needs to be translated to the degrees of freedom of the beam. By using the shape functions as described in 6.3, a force on an element can be transformed to equivalent nodal forces. It is important to note that the displacement and rotation at a node result in a force and a moment per node.

The first thing that needs to be known is the location of the load on the element, denoted as ζ . By multiplying the force with the element shape function vector \mathbf{N} at that location the nodal forces are calculated:

$$\mathbf{P}^e = \mathbf{N}^T(\zeta) F(t) = \begin{bmatrix} N_1(\zeta) \\ N_2(\zeta) \\ N_3(\zeta) \\ N_4(\zeta) \end{bmatrix} F(t) = \begin{bmatrix} F_1(t) \\ M_1(t) \\ F_2(t) \\ M_2(t) \end{bmatrix} \quad (6.12)$$

This element level forcing vector \mathbf{P}^e needs to be translated to the global problem. This is done by constructing the global forcing vector with $2(n_e + 1)$ entries. All entries will be zero except the ones of the element on which the force is acting. The entries corresponding to that element can be filled using the equation in 6.12. So the global location of the force on the beam, denoted as x , shows on which element the force is acting. This is transformed to the local coordinate ζ to translate the force to equivalent nodal forces. These nodal forces can then be added to the global forcing vector. To clarify the procedure, figure 6.3 shows the different coordinates x and ζ depending on the location of the force on the bridge. This is a general representation of the global forcing vector \mathbf{P}_{glob} , which can be time dependent when the force is moving across the bridge. It is also possible to use this for the case of multiple loads on the bridge, which can be added individually to the global shape function.

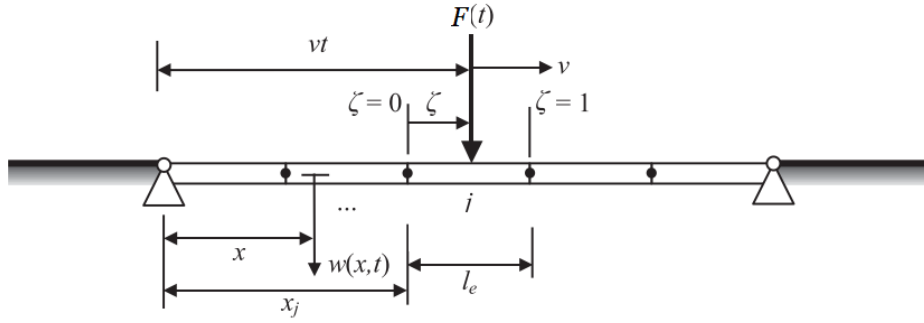


Figure 6.3: Finite Element model of the beam, showing global coordinate x and local coordinate ζ to calculate global forcing vector \mathbf{P}_{glob} [11]

Since the initial conditions are zero, the dynamic problem is complete. The spacial discretized set of equation will be solved numerically in the time-domain. To be able to do this the time will be discretized as well. At every time step we are capable of calculating 'accelerations' $\ddot{\mathbf{u}}$, because the 'displacements' \mathbf{u} and 'velocities' $\dot{\mathbf{u}}$ are known:

$$\ddot{\mathbf{u}} = \mathbf{M}^{-1}(\mathbf{P} - \mathbf{C}\dot{\mathbf{u}} - \mathbf{K}\mathbf{u}) \quad (6.13)$$

Using a time integration scheme it is possible to now calculate the displacement en velocity at the following time step. Continuing this allows to numerically solve the equation of motion. In Matlab this is done using the built in ODE45 solver function. A more detailed explanation of this solver can be found in 6.5.

The basic model that is described here is applicable for the moving force model, because the mass, damping, and stiffness matrices are constant over time. However, in MSD model the dynamic properties of the pedestrian will effect the stiffness and damping matrix. How this is implemented in the Matlab model is described in 6.3.

6.2. Basic model - verification

The model that is made in the Matlab should simulate the behaviour of a Euler-Bernoulli beam. To check this the response to static loading is verified with the analytical solution. After this a dynamic verification for a load at midspan will be verified with the steady-state solution. Finally, a comparison will be made with the results found by Caprani et al. [11] and thereby verifying the moving dynamic loading case.

6.2.1. Static verification

When applying a static load, the vibration of the beam will decrease due to the damping and will approach a equilibrium. In general this means we will check the the stiffness matrix and the loading vector. For this static verification two loads are considered and compared to the analytical solution:

- Point load at midspan
- Uniformly distributed load on entire length

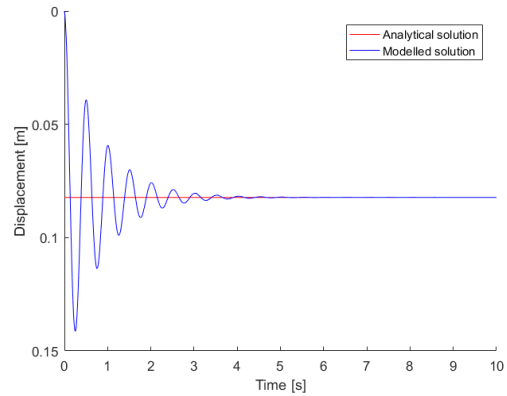
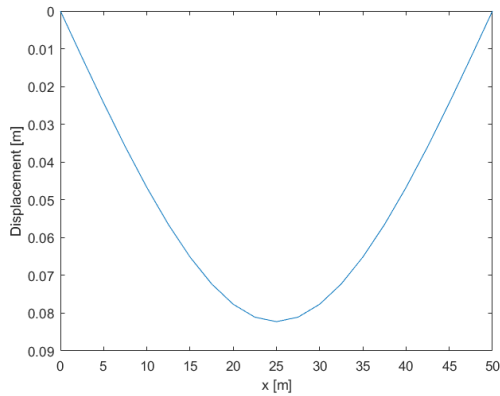
Since a steel bridge has really low damping ratio (minimum of 0.2 % and mean of 0.4%) it will take a long time to reach the equilibrium situation. For these checks the damping ratio is increased significantly, to reduce the calculation time. As this is a check to verify the stiffness matrix, this will not influence the results.

From the general differential equation of the stiffness problem of a Euler-Bernoulli beam the analytical solutions for these standard load cases are:

- Point load F at midspan: $w_{\text{mid}} = \frac{1}{48} \frac{FL^3}{EI}$
- Distributed load q : $w_{\text{mid}} = \frac{5}{384} \frac{qL^4}{EI}$

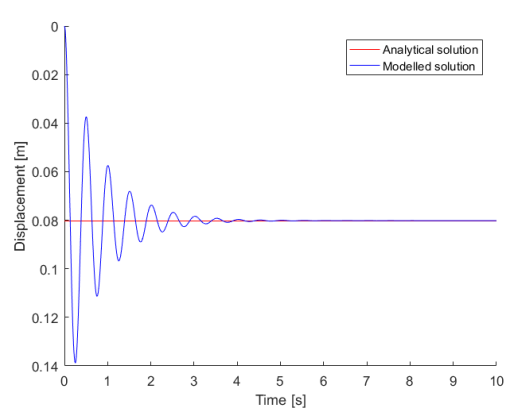
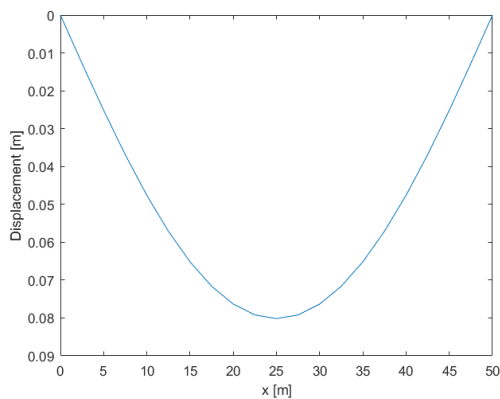
For this static verification the following parameters are used:

- $L = 50$ [m]
- $EI = 5.0660 \cdot 10^9$ [N/m²]
- $F = 160 \cdot 10^3$ [N]
- $q = 5 \cdot 10^3$ [N/m]
- $n_e = 10$ [-], number of elements
- $\xi = 10.0$ [%]
- $\mu = 500$ [kg/m], mass per meter



(a) Shape of the modelled beam in equilibrium state due to point load F (b) Deflection at midspan using model and analytical solution

Figure 6.4: Static verification for point load at midspan based on deflection shape and maximum



(a) Shape of the modelled beam in equilibrium state due to distributed load q (b) Deflection at midspan using model and analytical solution

Figure 6.5: Static verification for uniform distributed load at midspan based on deflection shape and maximum

In figures 6.4 and 6.5 it can be seen that the model converges towards the analytical solution. It can also be seen that the shape of the beam is consistent and does not show distortions. Therefore, it can be concluded that the stiffness matrix \mathbf{K} is correct.

6.2.2. Dynamic MF verification

To verify the Mass and damping matrix a dynamic verification is needed. This is done following the 'Stationary' jogger load case as used in the JRC guideline [17]. In here the analytical solution is calculated based on modal analysis and a harmonic load. Since a single span bridge with a constant cross section is considered and no significant camber or arc in the beam is applied, the first eigenmode will have a extremely high influence. In combination with the jogger frequency that will be equal to the first eigenfrequency, it is accurate to compare this analytical solution with the model.

Since the analytical solution considers a Steady-State solution and the damping of the bridge is low, the model needs to be run for a long period. The analytical solution is defined as 4.7. For a single 'stationary' jogger represented as a harmonic point load at midspan for the first eigenmode means:

$$a_{max} = \frac{p^*}{m^*} \frac{1}{2\xi}$$

with:

$$p^* = 1250 \quad [\text{N}], \text{ the jogger load amplitude}$$

$$m^* = \frac{\mu L}{2} \quad [\text{kg}], \text{ the modal mass}$$
(6.14)

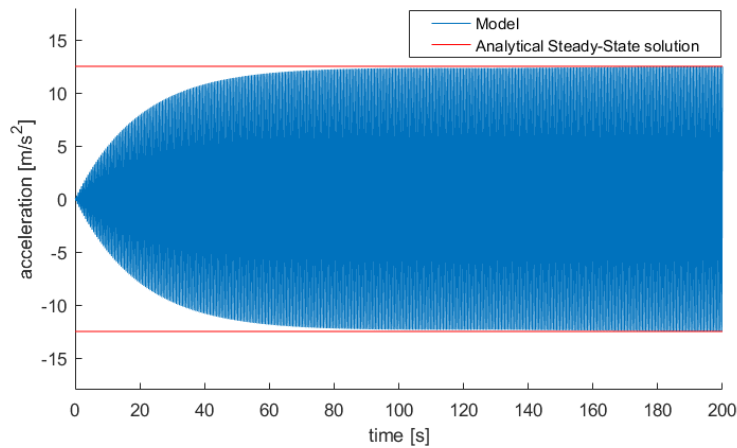


Figure 6.6: Dynamic verification of the 'Stationary' jogger. The accelerations of the model converge towards the analytical steady-state solution of the maximum acceleration

As can be seen the FEM model convergence towards the steady-state analytical solution. So for the 'stationary' jogger case the model performs as wanted. Which is a sign that the Mass **M** and Damping **C** matrices are correct.

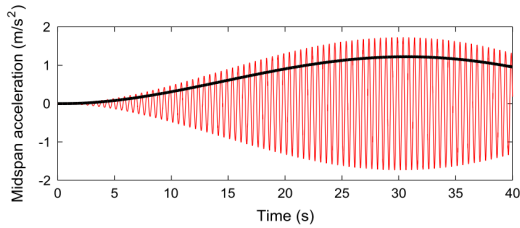
The last thing that needs to be checked to verify the Moving Force (MF) FEM model is the moving jogger case. The difference between the application of the 'stationary' and moving case is the global shape vector (see figure 6.3). For the moving jogger case the global shape vector is depending on the location of the jogger. To show the verification of the model in this document the results of Caprani et al. [11] are recreated. In the research of Caprani et al. They conducted a FEM vibrational analysis on a walking human across a single span bridge. To be able to compare different results they used the 1 s-RMS value of the accelerations. This is the 1 second Root Mean Square value, which is defined as:

$$x_{RMS} = \sqrt{\frac{1}{n}(x_1^2 + x_2^2 + \dots + x_n^2)} \quad \text{for every } x \text{ that is within 1 second of considered time} \quad (6.15)$$

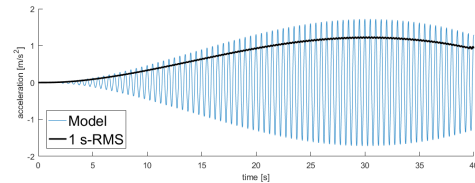
So if the 1 s-RMS is calculated for the accelerations at time $t = t_0$, all accelerations in time frame $[t_0 - 0.5; t_0 + 0.5]$ have to be used. The maximum 1 s-RMS is often used as a human perception criteria [11].

To recreate the results the same input is used, which is:

- $L = 50$ [m]
- $\mu = 500$ [kg], mass per meter
- $f_n = 2.0$ [Hz]
- F [N] is based on DLFs for walking by Young
- $P_v = 1.25$ [m/s], pedestrian speed
- $f_p = f_n$, [Hz] pacing frequency of the pedestrian
- $\xi = 0.5$ [%], Rayleigh Damping based on mode 1 and 3
- $n_e = 10$ [-], number of elements



(a) Accelerations as found by Caprani et al. [11]



(b) Accelerations as calculated by FEM model

Figure 6.7: Accelerations due to pedestrian walking across the bridge calculated using the Moving Force model with DLFs according to Young

When we compare the results in figure 6.7 we see similar behaviour over time. In this thesis the absolute maximum acceleration will be used, but this information is not mentioned in the paper by Caprani et al. [11]. To better compare the two results the maximum 1 s-RMS needs to be compared.

- Caprani et al. [11]: 1.223 m/s^2
- Matlab model: 1.221 m/s^2

The small difference can be explained with the numerical integration time steps. Caprani did not mention what time steps sizes (can also be variable) were used. A small difference in this can cause a difference in the 1 s-RMS value. However, since this difference is extremely small it can be neglected. To conclude, the 'stationary' model converges towards the steady-state analytical solution and the moving model produces similar results as Caprani et al [11]. Therefore, it can be said that the Moving Force Matlab code works.

6.3. Model including HSI

To include the Human-Structure Interaction in the dynamic model the Mass-Spring-Dashpot model is used (see figure 6.8). The introduction of the Mass-Spring-Dashpot oscillator to simulate the dynamic effect of the jogger requires to update the Equation of Motion (EoM). It is important to note that the EoM of the entire system needs to be considered. The entire system is a combination of the EoM of the bridge and the EoM of the human. These systems are coupled due to the interaction force. In this part the matrix equation of this coupled system of equations will be derived.

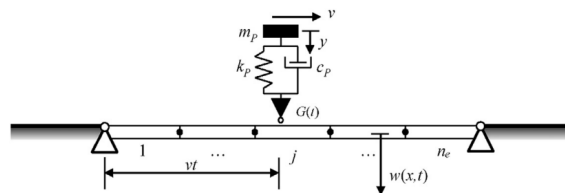


Figure 6.8: Finite Element Mass-Spring-Dashpot model as a representation of a human crossing a bridge

The equation of motion of the bridge is similar to the equation 6.1 given previously. Here denoted with subscript b to clarify the property of the bridge:

$$\mathbf{M}_b \ddot{\mathbf{u}} + \mathbf{C}_b \dot{\mathbf{u}} + \mathbf{K}_b \mathbf{u} = \mathbf{P} = \mathbf{N}^T F(t) \quad (6.16)$$

The difference with the equation for the MF is in the force $F(t)$. This is the interaction force between the human and the bridge. Since this model includes the HSI the force consists out of the force due to the footfall and the force due to the HSI (to be more precise H2SI, since we assumed small vibrations so the walking gait is constant.) These two parts of the force are also included in the model:

$$F(t) = G(t) + c_p(\dot{y} - \dot{w}) + k_p(y - w) \quad (6.17)$$

In this equation $w(x, t)$ is the displacement of the beam at the location of the human. So it is dependent on location x and time t . Therefore, the time derivative is defined as:

$$\dot{w}(x, t) = \frac{\partial w}{\partial x} \dot{x} + \frac{\partial w}{\partial t} \quad (6.18)$$

Note that the location x is directly related to time t because the velocity is constant. This explains the two terms in the time derivative of $w(x, t)$.

In the Finite Element Method the displacement $w(x, t)$ is expressed using the global shape function vector and the degrees of freedom. The notation of $\mathbf{N}(x)$ is remained here, because the global shape function is initially dependent on location x :

$$\begin{aligned} w(x, t) &= \mathbf{N}(x) \mathbf{u}(t) \\ \frac{\partial w}{\partial x} &= \mathbf{N}_x(x) \mathbf{u}(t) \\ \text{so:} \\ \frac{\partial w}{\partial t} &= v \mathbf{N}_x \mathbf{u} + \mathbf{N} \dot{\mathbf{u}} \end{aligned} \quad (6.19)$$

Note that the subscript x means the derivative with respect to x .

When equation 6.19 is substituted in 6.17, the interaction force is written as:

$$F(t) = G(t) + c_p \dot{y} + k_p y - v c_p \mathbf{N}_x \mathbf{u} - c_p \mathbf{N} \dot{\mathbf{u}} - k_p \mathbf{N} \mathbf{u} \quad (6.20)$$

Now the force on the bridge is defined, it can be substituted in the EoM of the bridge 6.16. Note that the force is depending on the DoF vector \mathbf{u} and y , which is the DoF of the human. These are rewritten to the left hand side of the equation, because we want to solve for \mathbf{u} and y :

$$\mathbf{M}_b \ddot{\mathbf{u}} + (\mathbf{C}_b + c_p \mathbf{N}^T \mathbf{N}) \dot{\mathbf{u}} + (\mathbf{K}_b + k_p \mathbf{N}^T \mathbf{N} + v c_p \mathbf{N}^T \mathbf{N}_x) \mathbf{u} - c_p \mathbf{N}^T \dot{y} - k_p \mathbf{N}^T y = \mathbf{N}^T G(t) \quad (6.21)$$

The equation of motion of the human, the Mass-Spring-Dashpot oscillator, is given as:

$$m_p \ddot{y} + c_p(\dot{y} - \dot{w}) + k_p(y - w) = 0 \quad (6.22)$$

In which m_p, c_p and k_p denote the mass, damping and stiffness of the pedestrian. y is the displacement relative to the equilibrium location of the pedestrian. So in comparison with the MF model there is an additional degree of freedom, that of the human.

The EoM of the human is discretized in a similar way as for the equation of the bridge. Substitution of 6.19 in 6.22 gives:

$$\begin{aligned} m_p \ddot{y} + c_p \dot{y} + k_p y - c_p \dot{w} - k_p w &= 0 \\ m_p \ddot{y} + c_p \dot{y} + k_p y - (v c_p \mathbf{N}_x + k_p \mathbf{N}_x) \mathbf{u} - c_p \mathbf{N} \dot{\mathbf{u}} &= 0 \end{aligned} \quad (6.23)$$

These two coupled equations can be combined into the following EoM of the entire system:

$$\begin{bmatrix} \mathbf{M}_b & \mathbf{0}_{N \times 1} \\ \mathbf{0}_{1 \times N} & m_p \end{bmatrix} \begin{Bmatrix} \ddot{\mathbf{u}} \\ \ddot{y} \end{Bmatrix} + \begin{bmatrix} \mathbf{C}_b + \mathbf{c}^* & -c_p \mathbf{N}^T \\ -c_p \mathbf{N} & c_p \end{bmatrix} \begin{Bmatrix} \dot{\mathbf{u}} \\ \dot{y} \end{Bmatrix} + \begin{bmatrix} \mathbf{K}_b + \mathbf{k}^* & -k_p \mathbf{N}^T \\ -c_p v \mathbf{N}_x - k_p \mathbf{N} & k_p \end{bmatrix} \begin{Bmatrix} \mathbf{u} \\ y \end{Bmatrix} = \begin{Bmatrix} \mathbf{N}^T G(t) \\ 0 \end{Bmatrix} \quad (6.24)$$

in which:

$$\begin{aligned}\mathbf{c}^* &= c_p \mathbf{N}^T \mathbf{N} \\ \mathbf{k}^* &= c_p v \mathbf{N}^T \mathbf{N}_x + k_p \mathbf{N}^T \mathbf{N}\end{aligned}\quad (6.25)$$

The Equation of Motion of the entire system is now complete. However, in the paper of Lin et al. [21] a small change is proposed which may improve the calculation speed. This approach will be shown in the following steps. Note that this will not change the result, because the equation is equivalent. The first step is to rewrite equation 6.22 so that we have the equivalent of mass times acceleration equals force:

$$\begin{aligned}m_p \dot{y} &= -c_p (\dot{y} - \dot{w}) - k_p (y - w) \\ -m_p \ddot{y} &= c_p (\dot{y} - \dot{w}) + k_p (y - w)\end{aligned}\quad (6.26)$$

This can be substituted into the equation of the interaction force on the bridge 6.17. This will reduce the equation into:

$$F(t) = G(t) - m_p \ddot{y}\quad (6.27)$$

After substitution into the EoM of the bridge 6.16:

$$\mathbf{M}_b \ddot{\mathbf{u}} + \mathbf{C}_b \dot{\mathbf{u}} + \mathbf{K}_b \mathbf{u} - m_p \mathbf{N}^T \ddot{y} = \mathbf{N}^T G(t)\quad (6.28)$$

The discretized EoM of the pedestrian is not changed. So after combining 6.23 & 6.28 the EoM of the entire system is found to be:

$$\begin{bmatrix} \mathbf{M}_b & m_p \mathbf{N}^T \\ \mathbf{0}_{1 \times N} & m_p \end{bmatrix} \begin{Bmatrix} \ddot{\mathbf{u}} \\ \ddot{y} \end{Bmatrix} + \begin{bmatrix} \mathbf{C}_b & \mathbf{0}_{N \times 1} \\ -c_p \mathbf{N} & c_p \end{bmatrix} \begin{Bmatrix} \dot{\mathbf{u}} \\ \dot{y} \end{Bmatrix} + \begin{bmatrix} \mathbf{K}_b & \mathbf{0}_{N \times 1} \\ -c_p v \mathbf{N}_x - k_p \mathbf{N} & k_p \end{bmatrix} \begin{Bmatrix} \mathbf{u} \\ y \end{Bmatrix} = \begin{Bmatrix} \mathbf{N}^T G(t) \\ 0 \end{Bmatrix}\quad (6.29)$$

The EoM for the MSD model, so including HSI, is found to be 6.29. An important difference compared to the basic model is the time dependency of the M, K, and C matrices. The MSD oscillator introduces the global shape vector \mathbf{N} in these matrices. This vector is time dependent in two cases:

- When the human is moving across the bridge
- When the separation during running is included

The first reason why the global shape vector is time dependent is already explained in the basic model description 6.1, namely moving of the jogger. The second reason is introduced due to the MSD oscillator. As the goal is to use the MSD model for the jogger load case the model needs to include the separation between the bridge and the human. In the load model the force $G(t)$ is truncated so no tension is applied between the human and the bridge. In that way there is a time frame in which there is no load applied on the bridge. This simulates the 'floating' period characteristic during running. To include the 'floating' period in the HSI the MSD oscillator needs to be disconnected from the bridge. This is done using an additional statement for the global shape vector. When the force $G(t) = 0$ (during the 'floating' period), the global shape vector is set to zero. The off-diagonal terms in the M, C, and K matrices are zero. This means that the two systems are decoupled, which is the case during the 'floating' period.

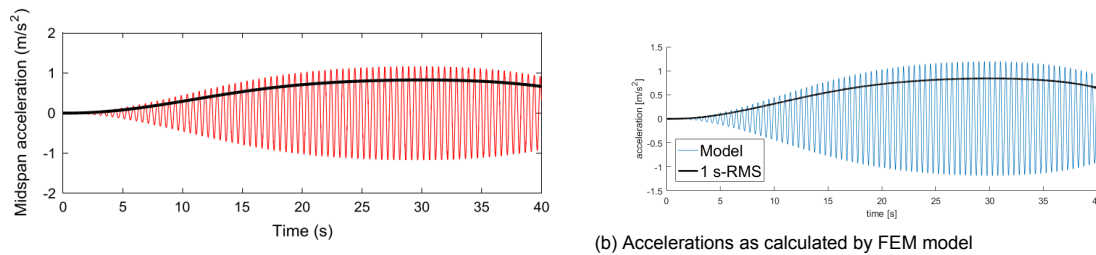
A result of the time dependency of the matrices is that every time step the matrices needs to be evaluated again. Due to the large amount of time steps this results in a large increase of calculation time. Therefore, the Moving Force model will always be faster than the Mass-Spring-Dashpot model.

6.4. Model including HSI - verification

The model including HSI, the MSD model, as defined in 6.29, is based on the general equation that is already verified. To verify the additional parts to include the HSI the following verification checks are made.

The first verification is again based on a comparison. Since Caprani et al. [11] also added the MSD model for the walking human case, this is recreated with the Matlab model. As input for the human dynamic properties the following are used:

- $m_p = 73.85$ [kg]
- $c_p = 612.5$ [Ns/m]
- $k_p = 14.11 \cdot 10^3$ [N/m]



(a) Accelerations as found by Caprani et al. [11]

(b) Accelerations as calculated by FEM model

Figure 6.9: Accelerations due to pedestrian walking across the bridge calculated using the Mass-Spring-Dashpot model with DLFs according to Young

The 1 s-RMS of both results is found to be:

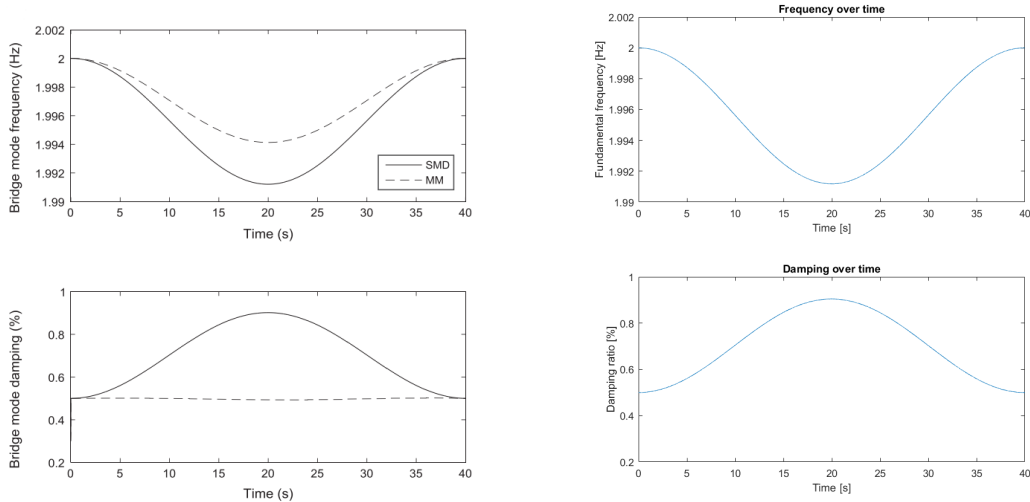
- Caprani et al. [11]: 0.826 m/s^2
- Matlab model: 0.822 m/s^2

Again the difference can be explained because of the possible time step difference between Caprani and the used model. However, the difference is still insignificantly small.

The human oscillator influences the dynamic characteristics of the entire system. When the jogger is 'stationary' the additional effect of the human oscillator is constant and therefore similar to a tuned mass damper. However, when the moving jogger is considered, the influence also changes over time. In the moving case the frequency and damping of the first vibrational mode changes over time due to this effect. To check if this effect is captured correctly in the model this is compared with the results found by Caprani et al. As can be seen in figure 6.10 the Matlab model produces the same results. The frequency is slightly lowered from 2.0 to 1.991 Hz and the damping is significantly increased from 0.5 % to 0.9 %.

There are 2 reasons why the MSD model results in lower maximum accelerations of the bridge: 1) change in frequency and damping of the bridge modes and 2) the energy dissipation in the damping of the jogger. The first reason results in a lower maximum acceleration since the loading frequency is not identical to the eigenfrequency of the bridge. For the second reason it is important to note that the eigenfrequency of the human in this model is 2.2 Hz. This is close to the fundamental frequency of the bridge. Therefore, the energy transmitted into the human oscillator is relatively high. When this phenomena is consider from the physical aspect of the human, it can be mentioned that a human is capable of actively damping a vibration. Subconsciously this can already result in high damping ratio's. This is not incorporated in the model using the Mass-Spring-Dashpot representation, but it shows that the large increase in damping can be realistic.

As a second verification, the 'floating' time for the jogger load case is considered. For both cases the 'floating' time has an effect on the mass, damping, and stiffness matrices. To verify if the 'floating' time

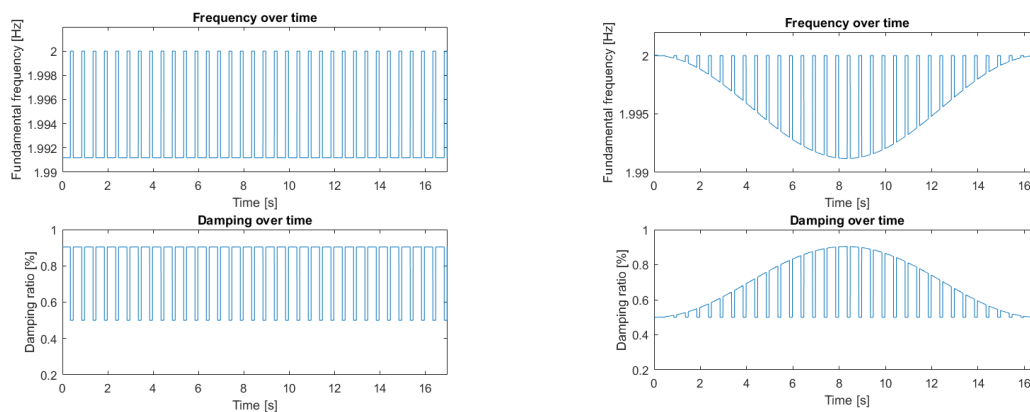


(a) Fundamental frequency and damping as found by Caprani et al. [11]

(b) Fundamental frequency and damping as calculated by FEM model

Figure 6.10: Fundamental frequency and damping due to pedestrian walking across the bridge calculated using the Mass-Spring-Dashpot model with DLFs according to Young

is added, the Bachmann load model (including 'floating' time) is applied for the stationary and moving jogger case. Since the global shape vector is set to zero, the oscillator is disconnected as well.



(a) 'Stationary' jogger

(b) Moving jogger

Figure 6.11: The fundamental frequency and damping of the bridge with a 'stationary' and moving jogger over time for the Bachmann load model. The human characteristics are for this example the same as in [11]

In figure 6.11 a clear difference can be seen between results of the JRC and Bachmann load model. Due to the 'floating' time that is considered in the Bachmann load model, the frequency and damping of the entire system changes. A clear difference between the contact and 'floating' time can be seen.

It can be concluded that the influence of the human oscillator on the fundamental vibration mode is correctly modelled, based on the results by Caprani et al. [11]. To implement the human oscillator for the jogger load case the separation of the two systems needs to be implemented as well. This is seen to be effective by setting the global shape vector to zero during zero force periods.

6.5. Matlab workflow

In the previous sections the different models are described and verified. This is all collected in the Matlab code, so that every combination of model (MF or MSD), load (JRC or Bachmann) and location (stationary or moving) can be calculated. To clarify what is done within the code the following workflow diagram is made, see figure 6.12. In the Annex, the Matlab code can be found.

The given input must contain (c_p and k_p only if MSD model is used):

- Model (MF or MSD)
- Load (JRC or Bachmann)
- Location ('Stationary' or Moving)
- Time the model needs to run
- Bridge parameters (EI, μ, L)
- Element input (n_e , shape functions)
- Pedestrian input (m_p, c_p, k_p)

Using the input the model can be prepared. Step 1) First the bridge Mass and Stiffness matrix are constructed. Step 2) The eigenfrequencies can be calculated using the M and K matrices. Step 3) The bridge damping matrix is constructed using the eigenfrequencies, mass and stiffness matrix. These bridge matrices are time independent so therefore can be calculated as a preparation.

Step 4) when the 'stationary' model is considered, the global shape function is time independent and so can be calculated as a preparation. This will speed up the solver, since it will not be calculated each time step. Step 5) if the MF model is considered, the M, C and K will be time independent. To again speed up the solver it is therefore efficient to calculate the Inverse multiplications in advance.

After the preparation the build in numerical solver of Matlab will be called: ODE45. This numerical solver is a robust numerical solver based on the explicit Runge-Kutta formula. It is a single step solver, so it calculates the solution on the next time step based on information of the current time step. The solver uses a time string at which the state-vector \mathbf{q} is calculated as output. The state-vector is defined as:

$$\mathbf{q} = \begin{bmatrix} \mathbf{u} \\ \dot{\mathbf{u}} \end{bmatrix} \quad (6.30)$$

In this \mathbf{u} is the column vector containing the degrees of freedom. So the state-vector at time t_0 contains values of the degrees of freedom and the first time derivatives.

ODE45 needs information about the first time derivative of the state-vector, $\dot{\mathbf{q}}$ at the current time step to calculate the state-vector of the next time step. Therefore, it calls ODE-FUNC every time step to calculate $\dot{\mathbf{q}}$.

The purpose of ODE-FUNC is to calculate the first derivative of the state-vector at the current time step. \mathbf{u} is already known, so only $\dot{\mathbf{u}}$ needs to be calculated. This is calculated using equation 6.13. Therefore, at every time step \mathbf{M} , \mathbf{C} , \mathbf{K} and \mathbf{P} also need to be known. In the ODE-FUNC function the following steps are taken

Step 1) If moving jogger, calculate global shape vector \mathbf{N}_{glob} . Step 2) Calculate the force of the human on the bridge \mathbf{f} at current time step. Step 3) If the MSD model is used the global shape vector needs to be filled with zero's when there is no force to remove the oscillator influence. Step 4) the force vector $\mathbf{P} = \mathbf{N}_{\text{glob}}\mathbf{f}$ is constructed. Step 5) if the MSD model is used the matrices \mathbf{M} , \mathbf{C} , and \mathbf{K} are time dependent, so they must be calculated at current time step. Step 6) extract information from state-vector. Step 7) calculate $\dot{\mathbf{u}}$ using equation 6.13. Step 8) Construct $\dot{\mathbf{q}}$ so ODE45 can calculate the state vector at next time step.

As output of ODE45 the state-vector is known at every time step given as input. The $\dot{\mathbf{u}}$ are not given as output, but these are of interest for the dynamic checks. Therefore, the output (\mathbf{q}) and time vector is inserted in ODE-FUNC to extract $\dot{\mathbf{u}}$. This is not extracted during the first call to ODE-FUNC, because the ODE45 solver uses a variable time step and possible recalculates some steps to make sure the required accuracy is reached. By calculating the output $\dot{\mathbf{u}}$ after using ODE45 no errors due to this are present.

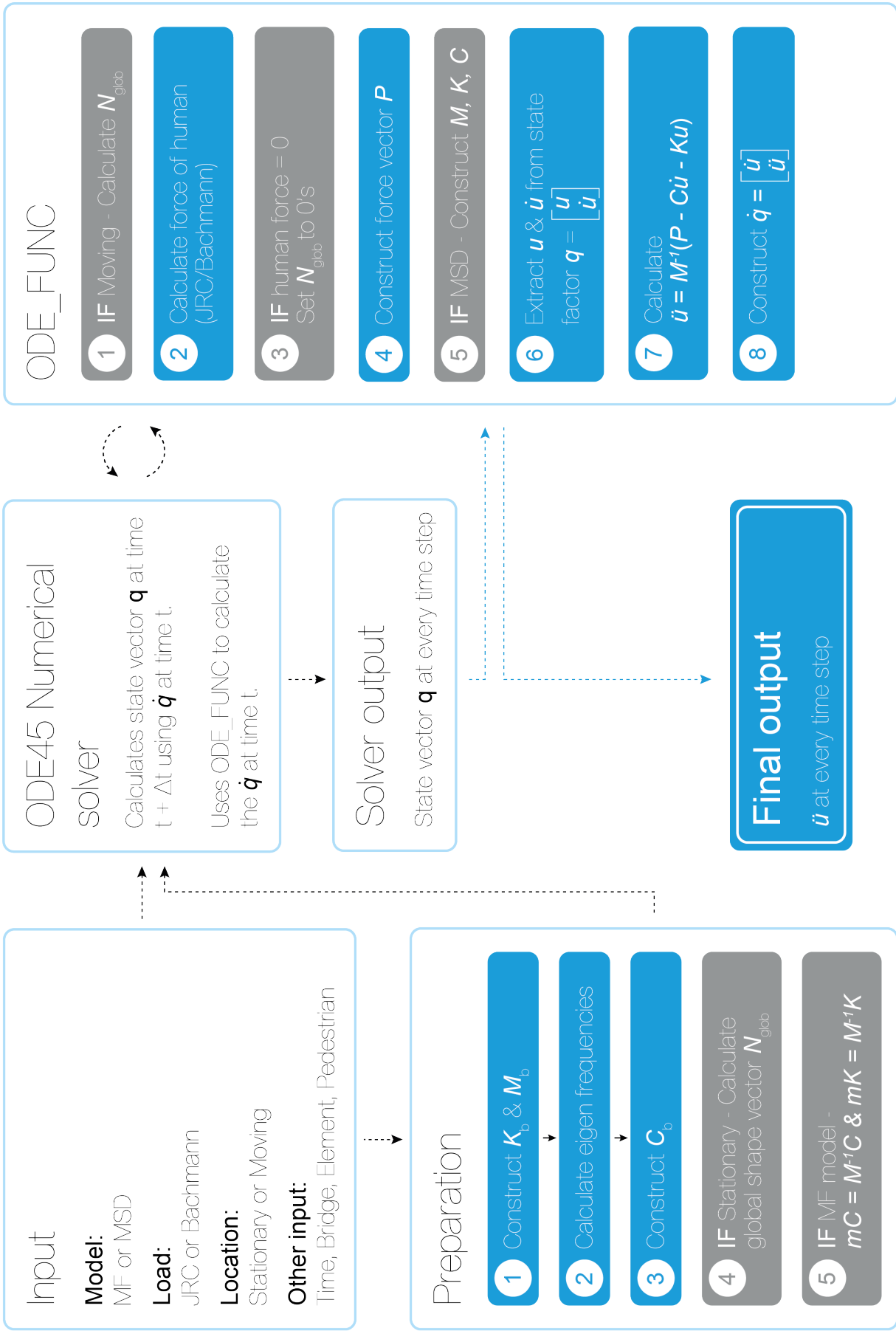
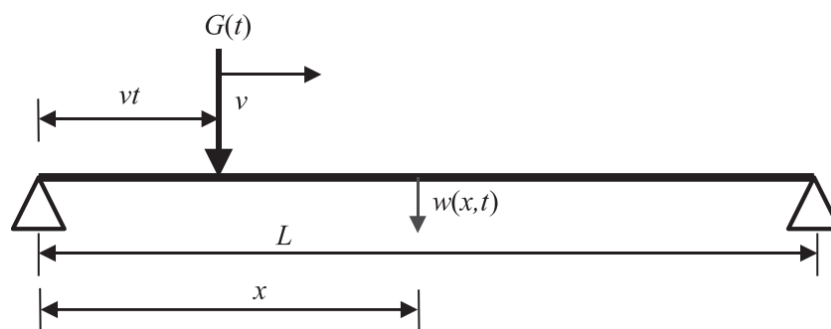


Figure 6.12: Matlab workflow. The blue coloured steps are always done, the grey ones depend on the model input

Jogger load case - Excluding Human-Structure Interaction



The aim of this chapter to get a better understanding of the Moving Force model to represent a jogger on a footbridge. As described before, two big assumptions in the dynamic analysis with jogger loading are often used: 1) load is applied stationary at midspan and 2) the separation between jogger and deck is neglected in the loading. To completely understand what influence these assumptions have on the results all 4 possible combinations will be tested:

1. 'Stationary' jogger - JRC load (sinusoidal with tension)
2. 'Stationary' jogger - Bachmann load (including separation 'floating time')
3. Moving jogger - JRC load
4. Moving jogger - Bachmann load

7.1. Moving Force model - Input

The input of the Moving Force model consists only of the information about the velocity of the pedestrian and the force itself. The velocity prescribed by the JRC document [17] as $v = 3$ m/s. This is found by using the average values for the relation between velocity, step length and step frequency. The step frequency is set to be equal to the fundamental frequency of the bridge which is 2.68 Hz. So running with 3.0 m/s leads to a step length of $3.0/2.68 = 1.11$ m. This is considered to be a normal step size for average running. Therefore:

$$v = 3 \text{ m/s}$$

The two load models: sinusoidal load & Bachmann load, are already described in 2.2.1. So here only the mathematical formulations are given:

$$F_{\text{JRC}} = 1250 \cdot \sin(2\pi f_s t)$$

&

$$F_{\text{Bachmann}} = 800 \cdot (1 + 1.6 \cdot \sin(2\pi f_s t) + 0.7 \cdot \sin(4\pi f_s t) + 0.2 \cdot \sin(6\pi f_s t))$$

with:

$$F_{\text{Bachmann}} = 0 \quad \text{if} \quad F_{\text{Bachmann}} < 0$$

Note that in the Bachmann equation the pedestrian weight is 800 N, which is also used for the derivation of the sinusoidal load.

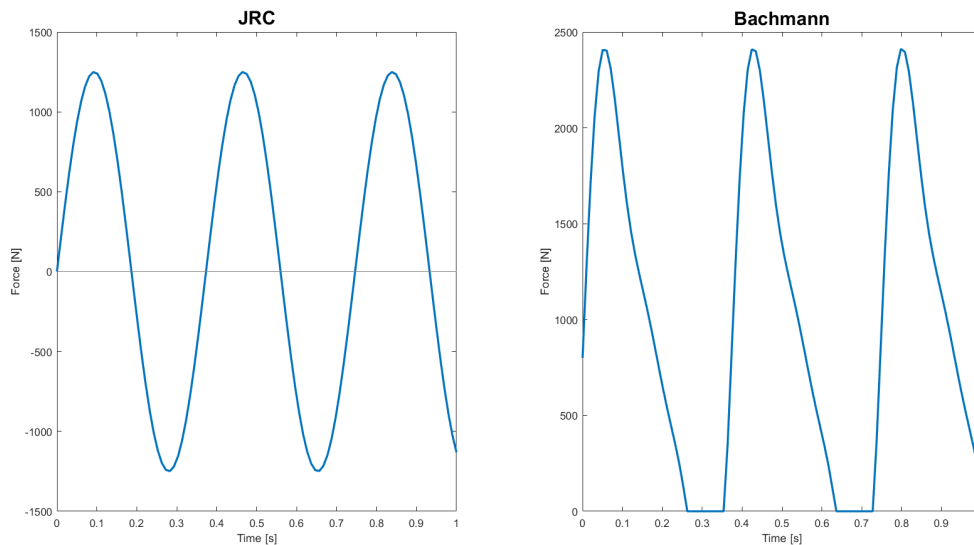


Figure 7.1: Sinusoidal and Bachmann load for the jogger load case displayed for 1 second ($f_n = f_s = 2.68$ Hz)

7.2. Moving Force model - Results

The four combinations of the Moving Force model have been calculated for the initial designed bridge. The following comparisons have been made:

- 'Stationary' jogger with JRC and Bachmann load, see figure 7.2a
- JRC load with 'stationary' and moving jogger, see figure 7.2b
- Bachmann load with 'stationary' and moving jogger, see figure 7.2c
- Moving jogger with JRC and Bachman load, see figure 7.2d

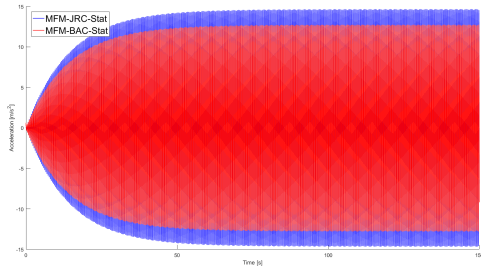
To answer the sub-questions about the moving force model the results of the four combination will be compared on maximum acceleration and the acceleration over time. It is known that the 'stationary' jogger convergence towards a steady-state solution while the moving jogger will return to it's initial state. Therefore, the comparison based on behaviour over time between these two cases only illustrates the difference in time to reach the maximum acceleration.

The four combinations result in four maximum accelerations:

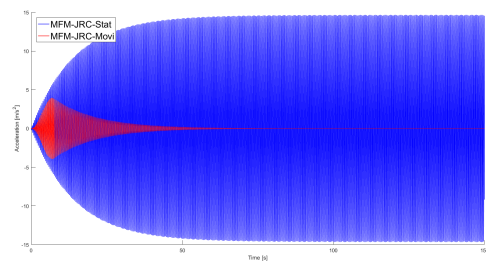
- | | |
|--|---|
| • JRC load - 'Stationary' jogger
→ $a_{max} = 14.36 \text{ m/s}^2$ | • JRC load - Moving jogger
→ $a_{max} = 3.78 \text{ m/s}^2$ |
| • Bachmann load - 'Stationary' jogger
→ $a_{max} = 11.96 \text{ m/s}^2$ | • Bachmann load - Moving jogger
→ $a_{max} = 3.13 \text{ m/s}^2$ |

Table 7.1: Difference in maximum acceleration for **MF** models = $a_{\max}(\text{model } i)/a_{\max}(\text{model } j)$

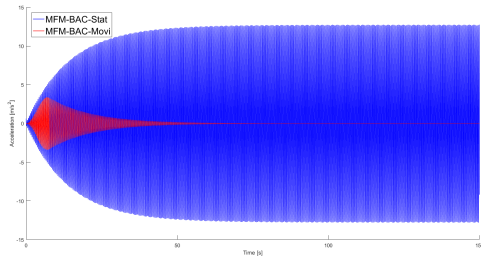
model i	model j			
	JRC - Stat	BAC - Stat	JRC - Movi	BAC - Movi
JRC - Stat	1,00	1,20	3,80	4,59
BAC - Stat	0,83	1,00	3,16	3,82
JRC - Movi	0,26	0,32	1,00	1,21
BAC - Movi	0,22	0,26	0,82	1,00



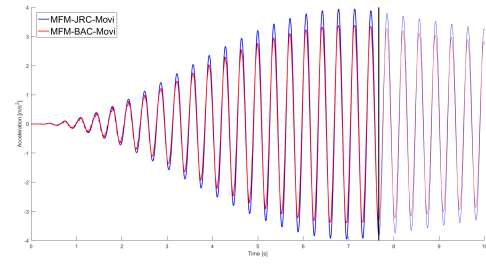
(a) JRC and Bachmann load for a 'stationary' jogger



(b) JRC load for a 'stationary' and moving jogger



(c) Bachmann load for a 'stationary' and moving jogger



(d) JRC and Bachmann load for a moving jogger. Vertical line indicates the time where the jogger has left the bridge

Figure 7.2: Comparison of accelerations over time according to the **MF** model for the initial design**'Stationary' jogger with JRC-Bachmann (see 7.2a)**

When the 'Stationary' jogger case, it can be seen that the Bachmann load results in a reduction of $(1 - 0.83) \cdot 100 = 17\%$ on the maximum acceleration compared to the JRC load. The time until the steady-state response is similar.

To get a better understanding why the Bachmann load results in a lower maximal acceleration the energy of both load models are compared. This is done by calculating the impulse of 1 load period ($T = 1/f_s$). Which is calculated by integration of the load over the period (see figure 7.1). The calculation can be found in the annex A.

The impulse energy for a step frequency of 3 Hz are found to be:

- $J_{\text{JRC}} = 265.3 \text{ N}\cdot\text{s}$
- $J_{\text{Bachmann}} = 309.0 \text{ N}\cdot\text{s}$

So the energy of the Bachmann load model is higher than of the JRC load model. However, in the Bachmann load model the first four harmonics of the step frequency are included. This means that the Bachmann load will have an additional effect on the higher eigenmodes of the bridge. The response of the bridge is not only effected by the amount of energy and the frequency of the load, but the location of the load is an important aspect as well. Every eigenmode corresponds with different locations where the force has the biggest influence (at the biggest displacement of the mode, see figure 7.3). For the moving jogger case the location of the forces is moving across the bridge. The JRC load only excites

the first eigenmode of the bridge, while the Bachmann load excites the first four modes. Especially for the moving case this will lead to a different response due to influence of the higher eigenmodes. The type of loading is also different in the two models. Since the Bachmann load includes the separation, the response is a free vibration of the system between each step. This is not the case for the JRC load which is always applying a force on the beam.

As a result of the difference between the JRC and Bachmann load model, it is not directly known where the difference in response of the bridge originates. However, both models have found to be applicable as a representation of the jogger load. Therefore, in this thesis the difference in results

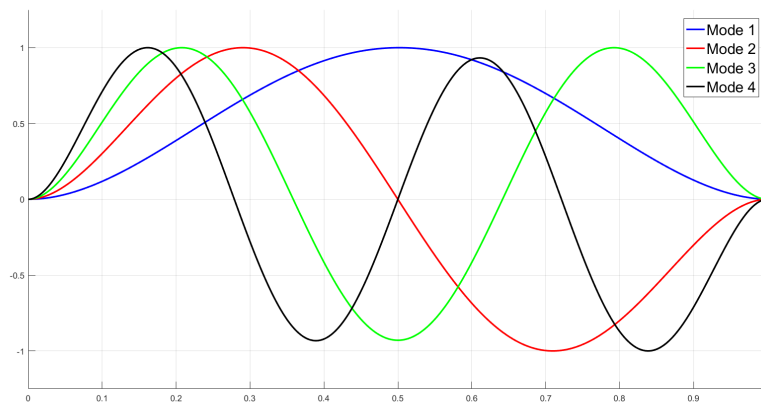


Figure 7.3: The first four eigenmodes of a simply supported beam with a constant cross section

JRC and Bachmann with 'stationary'-moving (see 7.2b and 7.2c)

As already known, there is a big reduction when the 'Stationary' case is compared with the moving case for the same load case. For the JRC as well as the Bachmann load there is a reduction of $(1 - 0.26) \cdot 100 = 74\%$ when the moving case is considered compared to the stationary case.

It must be noted that this depends highly on the time the jogger is on the bridge. When the bridge length increases while the jogger speed remains 3 m/s, the loading time will increase and therefore the amplitude of the oscillation will increase.

For the 'stationary' jogger, the load is always applied at the location of biggest displacement. This leads to the biggest response for the prescribed load. For the moving jogger the location changes, so the maximum acceleration will always be lower than the 'stationary' jogger.

Different designs are made to show how the length influences the maximum acceleration. The same cross section is used, but larger HEA profiles are applied to increase the cross sectional stiffness and in that way achieve a bigger span length.

The increasing size of the HEA profiles also mean an increase in mass. This results in a reduction in the maximum acceleration during resonance (see equation 4.7). To quantify the influence of the different lengths the acceleration during the moving load case is normalized with the maximum acceleration for the 'Stationary' load case with the same design.

The three designs are:

- HEA 320 ; L = 23.5 m
- HEA 600 ; L = 33.5 m
- HEA 1000 ; L = 43.5 m

The accelerations normalized with the acceleration from the stationary case for the three designs are shown in figure 7.4. It can be seen that the ratio of the maximum acceleration of the moving over 'stationary' case increases when the length increases. The biggest possible profile HEA 1000 with a

length of $L = 43.5$ m results in a ratio of 0.41. When the cross section using HEA profiles is used, the maximum acceleration by applying a 'stationary' load case will overestimate the maximum acceleration by at least 2.4 times.

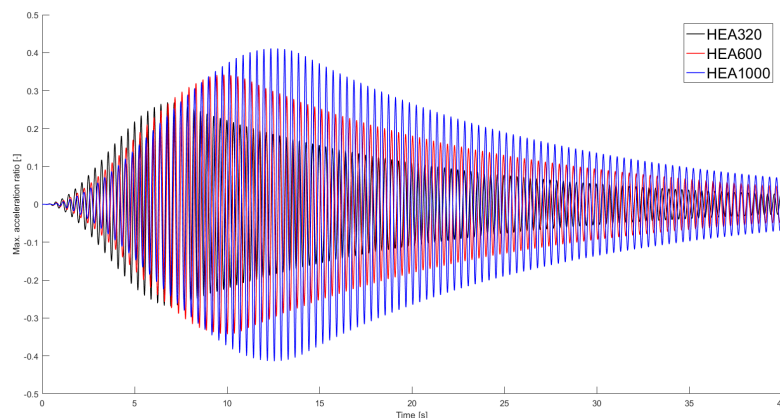


Figure 7.4: Ratio between maximum acceleration of 'Stationary' and moving jogger case for three different designs with increasing length

Moving with JRC-Bachmann (see 7.2d)

For the Moving jogger case, the Bachmann load results in a reduction of $(1 - 0.82) \cdot 100 = 18\%$ compared to the JRC load. This is again dependent on the time jogger is on the bridge. The acceleration over time is also a bit different. The Bachmann load model shows a higher frequency vibration at the beginning, which fades out further in time.

7.3. Sub-conclusions

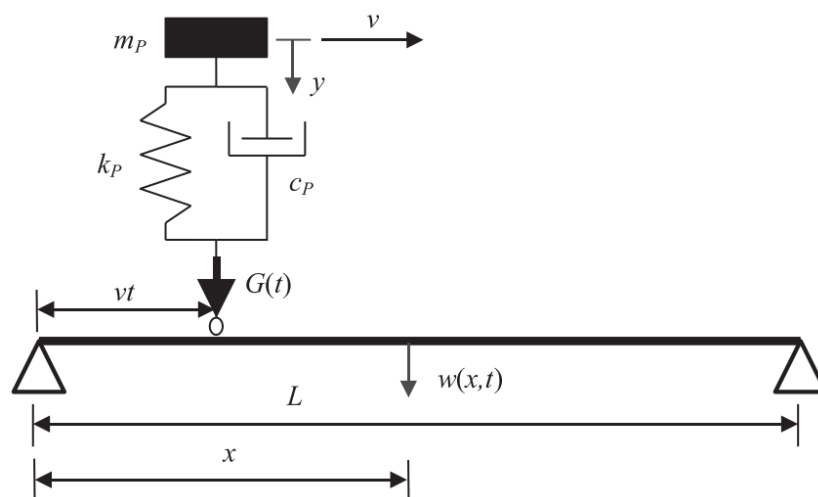
The first question that needs to be answered is considering the 'stationary' simplification: 'What is the influence of applying a 'stationary' jogger compared to the moving case'?

It can be concluded that the simplification of the 'stationary' case always overestimates the maximum accelerations. The degree of overestimation decreases when the span length increases. For the current bridge design, a constant cross section with 4 HEA320 profiles and a span length of 23.5 m, the 'stationary' approximation results in a maximum acceleration 3.8 times larger than the moving load case.

The second question considers the difference between the JRC and Bachmann load: 'What is the influence of neglecting the separation when applying the jogger load'?

It can be seen that the Bachmann load results in a lower maximum acceleration for both the 'stationary' and moving case, even though the impulse is higher than that of the JRC load. Therefore, it can be concluded that neglecting the separation increases the maximum acceleration found. For the 'stationary' and moving case the Bachmann load model results in 17% and 18% lower acceleration compared to the JRC load, respectively. So there is a relation between the speed of the jogger and the influence of neglecting the separation.

Jogger load case - Including Human-Structure Interaction



8.1. Mass-Spring-Dashpot model - Input

The most important input parameters of this MSD model are the mass, stiffness, and damping of the pedestrian oscillator. As described in the state-of-art (see chapter 2) these can change quite significantly. Therefore, it may be useful to model these parameters stochastically. To have a more complete knowledge of the HSI during the jogger load case these deviations are neglected initially. In this chapter the mean values will be used to see what the influence of the HSI is on the 'stationary' jogger and moving jogger cases. Both with and without separation of the bridge and pedestrian. Therefore, a complete comparison with the MF model can be made.

For the calculations done in this chapter the mean values will be used:

- $m_p = 78.2$ kg
- $c_p = 957.9$ Ns/m
- $k_p = 32.9$ kN/m

In chapter 9 the probability distributions of these parameters are explained.

Note that the step frequency is (as was done for the MF model) set equal to the fundamental frequency of the bridge in this chapter, which is 2.86 Hz for the used design. The speed of the jogger is also again equal to 3 m/s.

8.2. Mass-Spring-Dashpot model - Results

In this chapter the same four combinations as for the MF model 7 are used for the MSD model (including the HSI). These are shown in figure 8.1. First the four combination for the MSD model will be compared. The comparison between MF and MSD model is done directly after that.

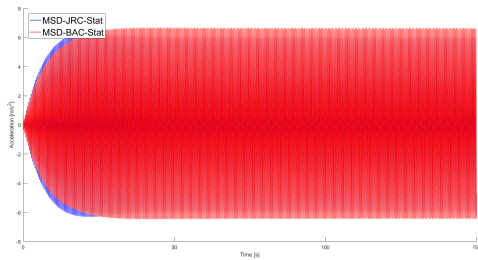
It is important to keep in mind that the mass-spring-dashpot oscillator representing the HSI is disconnected from the beam when the force is zero for the Bachmann load. This means that difference in the result originates from the difference in loading and difference in HSI.

The four combinations result in four maximum accelerations:

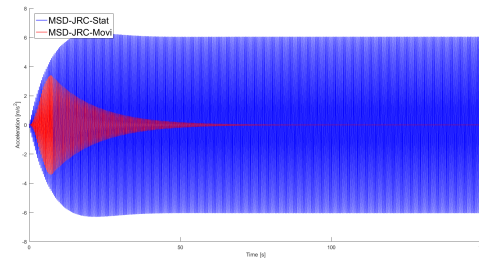
- JRC load - 'Stationary' jogger
→ $a_{max} = 6.31 \text{ m/s}^2$
- JRC load - Moving jogger
→ $a_{max} = 3.41 \text{ m/s}^2$
- Bachmann load - 'Stationary' jogger
→ $a_{max} = 6.70 \text{ m/s}^2$
- Bachmann load - Moving jogger
→ $a_{max} = 2.87 \text{ m/s}^2$

Table 8.1: Difference in maximum acceleration for **MSD** models = $a_{max}(\text{model } i)/a_{max}(\text{model } j)$

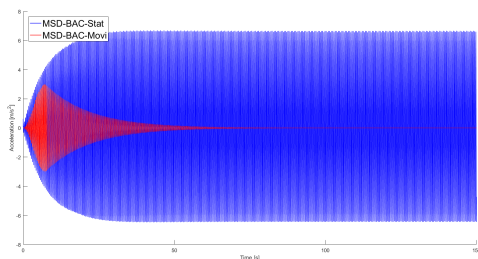
model i	model j			
	JRC - Stat	BAC - Stat	JRC - Movi	BAC - Movi
JRC - Stat	1.00	0.94	1.85	2.20
BAC - Stat	1.06	1.00	1.96	2.33
JRC - Movi	0.54	0.51	1.00	1.19
BAC - Movi	0.45	0.43	0.84	1.00



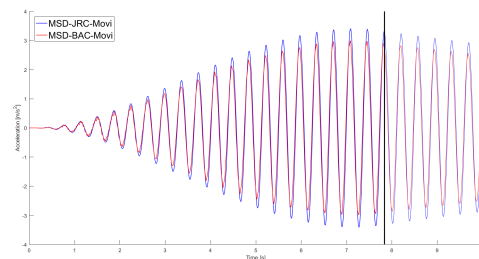
(a) JRC and Bachmann load for a 'stationary' jogger



(b) JRC load for a 'stationary' and moving jogger



(c) Bachmann load for a 'stationary' and moving jogger



(d) JRC and Bachmann load for a moving jogger. Vertical line indicates the time where the jogger has left the bridge

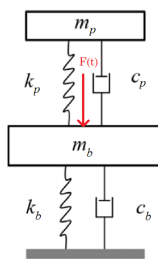
Figure 8.1: Comparison of accelerations over time according to the **MSD** model for the initial design

‘Stationary’ jogger with JRC-Bachmann (see 8.1a)

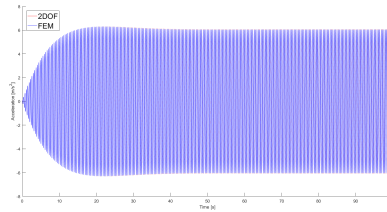
For the ‘stationary’ jogger at midspan the maximum acceleration is 6% higher for the Bachmann case. The behaviour for reaching the steady-state response is not the same for both load cases. The Bachmann increases before reaching a constant maximum response. However, for the JRC load something remarkable can be seen. The acceleration increases past the maximum steady-state acceleration and then decreases towards the steady-state response.

To confirm that this result is correct a simplified model is made. The ‘stationary’ case of the MSD model is similar to a bridge with a Tuned Mass Damper at midspan. The only difference is that the mass-Spring-Dashpot oscillator of the jogger is not tuned to optimize the energy absorption. A good simplified model describing the situation is therefore a 2 degree of freedom system (see figure 8.2a). The bridge response is governed by the fundamental vibrational mode. Using modal analysis the bridge is modelled as a single degree of freedom system with the following parameters:

- $m_b = \frac{\mu L}{2} = 10879 \text{ [kg]}$
- $k_b = m_b (2\pi f_n)^2 = 9.87^2 \frac{EI}{2L^3} = 3095.4 \text{ [kN/m]}$
- $c_b = 2\xi\sqrt{k_b m_b} = 1468.1 \text{ [Ns/m]}$



(a) 2DOF model representation of the fundamental modal behaviour of a bridge with damper at midspan [29]



(b) Accelerations due to ‘stationary’, JRC, MSD model calculated

Figure 8.2: A comparison between the FEM and 2DOF model representing a ‘stationary’ jogger load case

Solving this two degree of freedom problem using numerical integration, results in almost exactly the same accelerations as the FEM model. The difference between the two is approximately 0.03 m/s^2 , which is negligible. Thus the somewhat remarkable result can be described by seeing the jogger as a poorly tuned mass damper. However, this result requires a long time period (> 50 seconds) of perfect synchronization between the step load and the bridge fundamental frequency. It can be questioned if the MSD model is appropriate for the ‘stationary’ case in which the separation is neglected. The Matlab code made for the calculation can be found in annex B

JRC and Bachmann with ‘stationary’-moving (see 8.1b and 8.1c)

The difference between the ‘stationary’ and moving jogger is as expected big for both load models. The accelerations increase less fast for the moving case compared with the ‘stationary’ model. The reduction of the maximum acceleration due to the JRC load model $\rightarrow (1 - 0.54) \cdot 100 = 46\%$ and Bachmann load model $\rightarrow (1 - 0.43) \cdot 100 = 57\%$. It is important to note that there is a difference between the reductions of both models. The length dependency as described in the MF chapter 7 of the reduction also holds here.

Moving with JRC-Bachmann (see 8.1d)

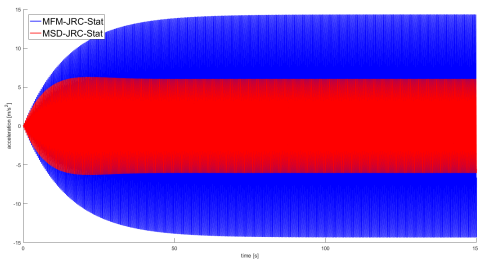
The difference between the JRC and Bachmann loading for the moving jogger case is found to be $(1 - 0.84) \cdot 100 = 16\%$. As we already have seen for the MF model, the Bachmann model results in higher vibrational response. These higher vibrations fade out further in time, but not completely. The higher vibrations are damped out quickly when the jogger has left the bridge. Note that the line is less thick when the jogger has left the bridge.

8.3. Comparison between MF and MSD model results

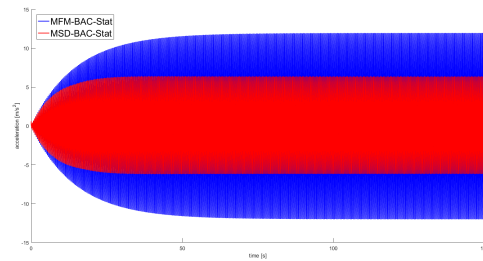
To conclude what influence the Human-Structure Interaction may have, the results of the MF and MSD models for the 4 combinations are directly compared. The maximum accelerations and the differences are shown in table 8.2 and the accelerations over time for the four combination can be found in figure 8.3.

Table 8.2: Difference in maximum acceleration for the MF and MSD model

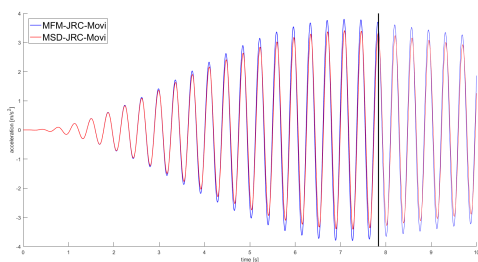
load - location	a_{\max} [m/s^2]		difference [m/s^2]	difference [%]
	MFM	MSD		
JRC - Stat	14.36	6.31	8.05	56.1%
BAC - Stat	11.96	6.70	5.26	44.0%
JRC - Movi	3.81	3.41	0.40	10.4%
BAC - Movi	3.13	2.87	0.26	8.3%



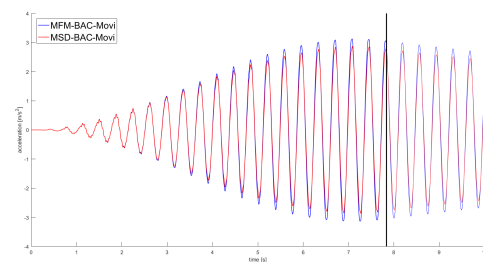
(a) JRC load for a 'stationary' jogger



(b) Bachmann load for a 'stationary' jogger



(c) JRC load for a moving jogger. Vertical line indicates the time where the jogger has left the bridge



(d) Bachmann load for a moving jogger. Vertical line indicates the time where the jogger has left the bridge

Figure 8.3: Comparison of accelerations over time according to the MF and MSD model

'Stationary':

The MSD model results in significantly lower maximum acceleration for the 'stationary' jogger at midspan. The reduction is 56.1% for the JRC load model and 44.0% for the Bachmann load. It is important to note that the reduction for the Bachmann load case is smaller, which results in a larger maximum acceleration for the MSD model in that case. Looking at the accelerations over time in figures 8.3a and 8.3b the only difference that can be seen is the amplitude.

Moving:

The differences for the moving jogger cases are smaller than the 'stationary' case. For the JRC load model the reduction is found to be 10.4% and for the Bachmann load model 8.3%. Similar to the 'stationary' case, the Bachmann load results in a lower reduction here. Looking at the accelerations over time for the JRC load (see figure 8.3c) no difference except the amplitude can be seen. For the Bachmann load (see figure 8.3d) both the MF and the MSD model show the high frequency vibrations. For the MF model this behaviour reduces, but for the MSD model they are not damped out completely.

Influence of separation on the Human-Structure Interaction:

The difference between the results of the MF and MSD model using the Bachmann load is caused by the separation of the MSD oscillator and the beam when Bachmann load equals zero. To be able to quantify the influence of the separation on the HSI a additional model is made: The bachmann load but the MSD oscillator is always connected with the beam. This resulted in a maximum accelerations:

- 'Stationary' MSD model, Bachmann load **without** separation

$$a_{\max} = 5.37 \text{ m/s}^2$$

- Moving MSD model, Bachmann load **without** separation

$$a_{\max} = 2.86 \text{ m/s}^2$$

Neglecting the separation results in a lower maximum acceleration, so an increase in the effect of the HSI. For the 'stationary' case a reduction of $6.70 - 5.37 = 1.33 \text{ m/s}^2$ and for the moving case $2.87 - 2.86 = 0.01 \text{ m/s}^2$.

8.4. Sub-conclusions

First considering the 'stationary' load cases, it is found that the Bachmann load leads to larger accelerations. This is the opposite of what was found for the Moving Force model. This means that neglecting of the separation in the MSD model results in lower accelerations for the MSD model. When the separation is neglected for the Bachmann load MSD model the maximum acceleration is decreased by 1.33 m/s^2 for the initial design. Neglecting the separation for the moving jogger case also resulted in a lower maximum acceleration, but the reduction is only 0.01 m/s^2 . It is therefore possible to conclude that the neglecting of the separation leads to an increase in the Human-Structure Interaction. Since the separation is part of the running behaviour, it is expected that neglecting the separation underestimates the maximum acceleration. However, for the moving case, which is more realistic compared to the 'stationary' case, the influence of the separation on the HSI is limited for the initial bridge design. This may change for different designs, due to a lower self weight or a longer span.

Looking at the difference between the 'stationary' and moving load it can be seen that the moving cases result in lower accelerations as expected. The difference is larger for the Bachmann load model. This can be explained by looking at the most effective location of a mass-spring-dashpot oscillator. Since the motion of the bridge is mainly the first mode, the maximum displacement is at midspan which is therefore the location where the oscillator has the largest effect. During the moving jogger case the effect of the oscillator is therefore lower. This means that neglecting the separation has less influence for the moving case, resulting in a bigger difference for the Bachmann load model.

The higher frequency response for the Bachmann load during the moving case does not completely fade out during the time the jogger is on the bridge. This can be explained by the separation of the MSD oscillator of the jogger every step. This influences the frequency and damping of the system and this can be seen in the acceleration behaviour.

The comparison between the MF and MSD model for the four combinations (load-location) showed that the MSD model always resulted in a lower maximum acceleration. This result is less relevant for the 'stationary' case, since this case is unrealistic and was only used for investigation of the separation in the MSD model. For the most realistic MSD model which consist of a Bachmann load model for a moving jogger the reduction due to Human-Structure Interaction is 8.3%.

Jogger load case - Stochastic analysis

Since joggers are subjected to variability, it may be useful to consider this into a stochastic analysis. In this research a Monte-Carlo analysis is done. The MSD model introduces new parameters which have significant variability: stiffness k_p and damping c_p . Since the influence of the MSD oscillator is depending on these parameters it is needed to add them into the stochastic analysis. This results in the following two Monte-Carlo analyses with the stochastic parameters:

Moving Force model

(1) step frequency f_s and (2) mass m_p

Mass-Spring-Dashpot model

(1) step frequency f_s , (2) mass m_p , (3) stiffness k_p and (4) damping c_p

In this analysis the Bachmann load model is used for both models, which means the mass of the human directly influences the force magnitude (see equation 7.1). The research of [33] showed that the pedestrian mass variance was too small to have a significant influence. However, in the MSD model the mass is an important parameter of the oscillator so it needs to be modelled as a stochastic parameter. To make a good comparison between the two models the mass will also be modelled stochastically for the MF model.

The Monte-Carlo analysis is done with a sample size of 200 joggers. These joggers are used for both the MF and the MSD model. So this results in 200 maximum acceleration values for both models. The result of the analysis will be more accurate when the sample size is increased, but due to the computational time this is limited.

9.1. Stochastic analysis - Input

Starting with the step frequency during running. This parameter determines the loading frequency and so the probability of occurrence of resonance. As already seen in the JRC document [17] it is found that the step frequency during running mostly is between 1.9 and 3.5 Hz. This slightly changes for other recommendations: SETRA [10] tells 2 to 3.5 Hz and Occhiuzzi et al [22] 1.9 to 3.0 Hz. Nothing is mentioned about the probability density for these ranges. The probability is assumed to be normal distributed, the same as for walking behaviour. To range between 1.9 and 3.5 Hz is chosen to hold 95% of the probability distribution. So the mean $\mu = \frac{(3.5-1.9)}{2}$ and the standard deviation $\sigma = \frac{(3.5-\mu)}{2}$ results in the step frequency distribution $f_s = \mathcal{N}(2.7, 0.4)$ Hz.

Different researchers tried to find the dynamic parameters of humans for different behaviours. Currently it is still unclear what the best way is to describe the dynamic properties of the human body. Due to the different researches it is now known that the stiffness depends on the step frequency and the velocity of the subject [9, 14]. In this thesis the dynamic characteristics of the human body during running are used. However, the relations stiffness and step frequency as well as stiffness and velocity are not found in the earlier research. Therefore, in this thesis these relations are neglected.

In this thesis it is tried to combine the different recommendations. There are two fundamental reasons why the recommendations of previous researches differ from each other. First of all, not all measurements are done during running of a subject [27, 31]. In these researches they assumed the stiffness of a human body to be similar during standing still and jogging. The second fundamental reason why the recommendations differ is the sample size. For example the research by Zhang et al [31] is done with 3 subjects. Due to the low number of subject this may lead to differences in recommendations. Next to the different recommended values for the parameters, it differs which parameters are given as an output. There are two options: 1) recommended values for k_p and c_p or 2) recommended f_p and ξ_p . Note that both recommendations depend on the mass m_p . Since the information about the mass of a subject is commonly known, this is not mentioned.

The following recommendations are relevant for running behaviour. First Arampatzis et al [9] did research on the leg stiffness of running humans for different speeds and found a range of 21.09 to 39.5 kN/m, but no damping was considered. Zhang et al. [31] gave a mean value of 28.5 kN/m for the leg stiffness combined with 950 Ns/m for the damping coefficient. More recently Van Nimmen [27] proposed distributions for the (undamped) frequency and damping of the human body with a standing posture with bent legs. The mass of the human body is sampled using a log-normal distribution with a standard deviation of 21% [25] and a mean of 78.2 kg [2] for humans in The Netherlands.

Combining these recommendations leads to the following input for the stochastic analysis in this research:

- Human body eigenfrequency, $f_p = \mathcal{N}(3.25, 0.32)$
- Human body damping, $\xi_p = \mathcal{N}(0.3, 0.05)$
- Human body mass, $m_p = \text{Lognormal}(78.2, 16.4)$

The stiffness k_p and damping c_p of the human oscillator are calculated using equation 9.1. In figure 9.1, it can be seen that the stiffness and damping ranges are similar as given by the different researches.

$$\begin{aligned} c_p &= 4\pi m_p \xi_p f_p \\ k_p &= m_p (2\pi f_p)^2 \end{aligned}$$

with: (9.1)

f_p = Eigenfrequency of the human body

ξ_p = Damping ratio of the human body

m_p = Mass of the human body

NOTE: The distribution of the dynamic properties of the joggers are based on results different researches. Therefore, it is not possible to say these are correct, but it covers the range of the parameters. Therefore, it is assumed that these values represent a conservative range of the dynamic properties of the jogger including the inter-subject variability.

9.2. Stochastic analysis - Results

Results of the 'fully' stochastic analysis

With 'fully' stochastic the analysis described here fore is meant. The important thing to note is that the step frequency is based on a normal distribution and is not set equal to the fundamental frequency of the bridge. This means the resonance will not always occur, which will lower the maximum acceleration significantly.

The 'fully' stochastic analysis result in a somewhat scattered result. The maximum accelerations are found in a large range between 0.1 and 3.1 m/s². For both models the mean of the maximum acceleration is close to 1.1 m/s². As seen chapter 7 and 8 the maximum acceleration when the step frequency is set equal to the fundamental frequency of the bridge are 3.13 and 2.87 m/s², respectively. This is roughly 3 times higher than the found mean values.

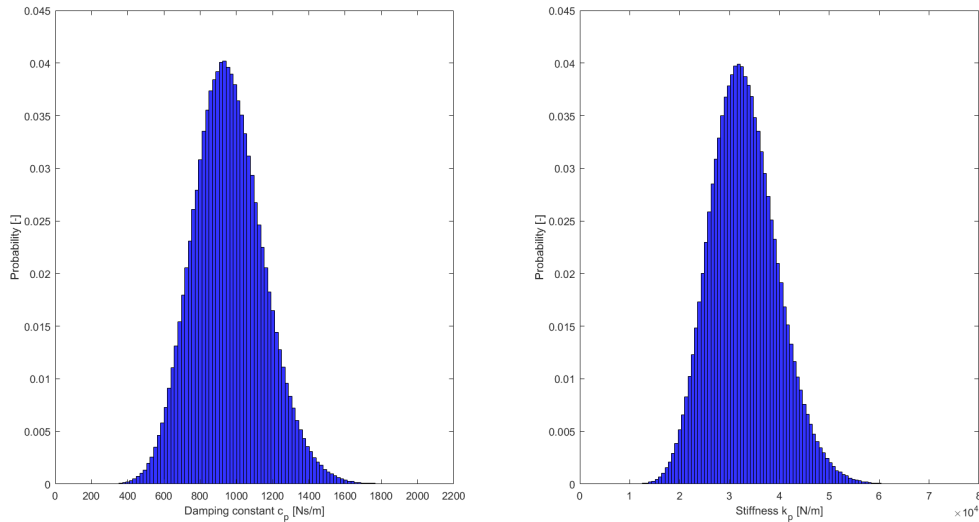
Figure 9.1: Histogram of stiffness and damping for 10^6 sampled joggers

Table 9.1: Mean and standard deviation of the maximum acceleration resulting from the 'fully' stochastic analysis for the MF and MSD model

a_{\max} [m/s ²]	MF	MSD
mean μ	1.16	1.10
std. dev. σ	0.92	0.85
95th percentile	2.80	2.58

When the results of the MF and MSD models are compared it can be seen that the difference is not constant. The reduction in the maximum acceleration according to the MSD model is larger towards the more extreme cases. The mean values of the maximum accelerations for the MF and MSD model show a reduction $(1.16 - 1.10)/1.16 \cdot 100 = 5.2\%$ for the MSD model. This is lower than the reduction calculated in chapters 7 and 8 which showed a reduction of 8.3%. The standard deviation is also lower for the MSD model, compared to the MF model. Since the mean value is similar, this means that the probability of a higher maximum acceleration is lower when the MSD model is used. This can be seen in figure 9.2a.

To check the results of a stochastic analysis the 95th percentile value is used. In this case this value is the found maximum acceleration corresponding to the probability of exceeding that acceleration of 5%. Note: Since a stochastic analysis is used the found 95th is an approximation that will be more accurate when more joggers are sampled. When the 95th percentile of the maximum acceleration due to both models are compared, the difference is $(2.80 - 2.58)/2.80 \cdot 100 = 7.9\%$.

Results of the 'semi' stochastic analyses

In the 'fully' stochastic analysis a large range of maximum accelerations was found. This was found for both the MF and the MSD model. Therefore, it is expected that this is mainly caused by the variance in the step frequency and not by the mass, stiffness and/or damping. To check this two 'reduced' stochastic analyses are done: one where the step frequency is set constant and equal to the bridge fundamental frequency while human properties are stochastic parameters (see figure 9.2b and table 9.2). The second 'semi' stochastic analysis used the human properties mean values while the step frequency is stochastic (see figure 9.2c and table 9.3).

When the step frequency is set constant and equal to the fundamental frequency the maximum accelerations are increased. The mean values were already found in chapter 7 and 8. The standard deviation is 0.17 and 0.14 m/s^2 . So despite the increase in stochastic parameters for the MSD model, the variance of the maximum acceleration decreases.

When the dynamic properties of the jogger are set constant to the mean values the results are almost identical. This holds for the mean, standard deviation and also for the 95th percentile.

Table 9.2: Mean, standard deviation and 95th of the maximum acceleration resulting from the 'Human properties' stochastic analysis for the MF and MSD model

a_{\max} [m/s^2]	MF	MSD
mean μ	3.13	2.87
std. dev. σ	0.17	0.14
95th percentile	3.43	3.11

Table 9.3: Mean, standard deviation and 95th of the maximum acceleration resulting from the 'step frequency' stochastic analysis for the MF and MSD model

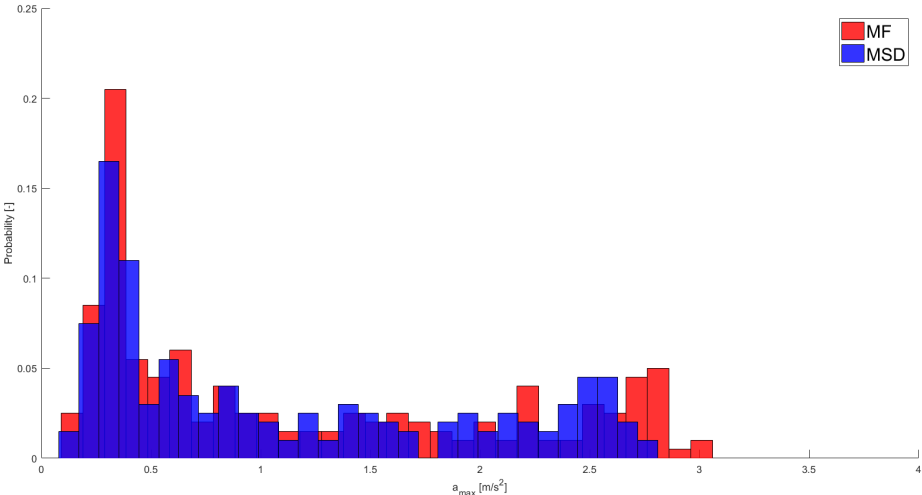
a_{\max} [m/s^2]	MF	MSD
mean μ	1.17	1.10
std. dev. σ	0.92	0.84
95th percentile	2.79	2.57

9.3. Sub-conclusions

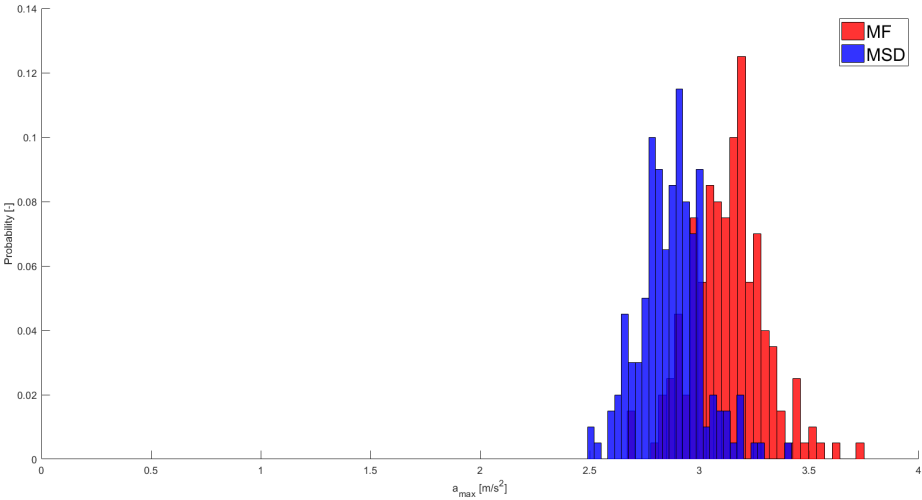
Since the step frequency and dynamic properties of the jogger show significant variability it may be useful to perform a stochastic instead of a deterministic analysis. For the Moving force model this means that the step frequency and mass of the jogger must be sampled. For the Mass-Spring-Dashpot model the stiffness and damping of the jogger during running must be sampled additionally.

The stochastic analysis with 200 sampled joggers showed that for both the MF and MSD model the variance in maximum acceleration is mainly originated by the variance in step frequency. The variance of the dynamic properties has almost no effect on the results of both models.

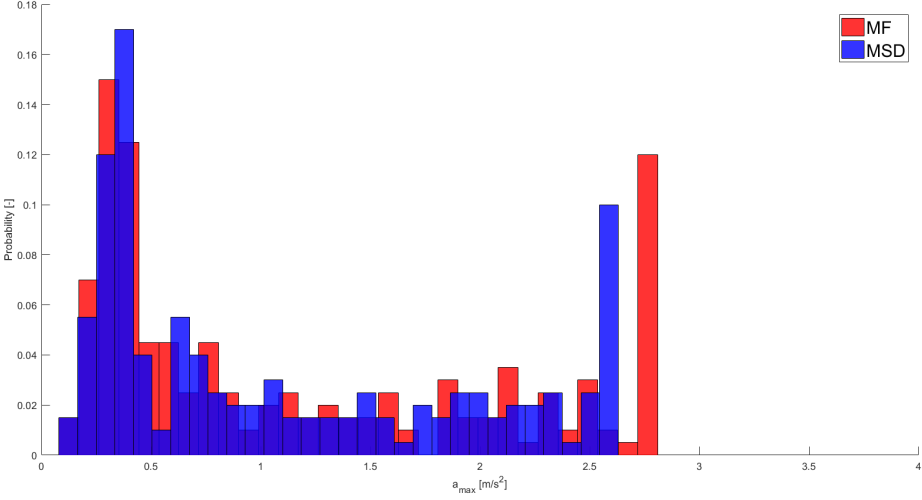
When the 95th percentile is used for the comfort criteria the MSD model results in a reduction of 7.9% compared to the MF model. This is slightly lower than the reduction found with the mean values and step frequency equal to the fundamental frequency of the bridge.



(a) 'fully' stochastic analysis



(b) 'human properties' stochastic analysis



(c) 'Step frequency' stochastic analysis

Figure 9.2: Histogram of the maximum acceleration as a result of different stochastic parameters

10

Jogger load case - Multiple joggers

Up till now all results are based on 1 jogger on the bridge. In the dutch national annex of Eurocode NEN-EN 1991-2 it is prescribed that not just 1 jogger needs to be used in the load model. Depending on the length of the largest span the following number of joggers needs to be applied:

$$\begin{cases} L < 20 & N_{\text{jog}} = 5 \\ L \geq 20 & N_{\text{jog}} = 10 \end{cases} \quad (10.1)$$

For the initial design that is used throughout this thesis with a length of 23.5 m it is prescribed that 10 joggers need to be considered.

In this chapter the influence of the Human-Structure Interaction of joggers will be investigated for the case of multiple joggers. A lot of different research can be done, but due to time limitations only the first few steps will be done. The purpose of this chapter is to predict if the Human-Structure Interaction effect will be higher or lower when multiple joggers are on the bridge. This is done with three different distributions of joggers for both the MF and MSD model. Based on the results a recommendation can be made if more research needs to be done on the MSD model for multiple joggers.

10.1. Multiple joggers - Model description

When the MF model is used to describe multiple joggers on the bridge, the model described in section 6.1 is sufficient. In the MF model the jogger is represented as a force that results in equivalent nodal forces in the force vector \mathbf{P} , see equation 6.1. Therefore, the force vector is constructed by a summation of the nodal forces of each jogger:

$$\begin{aligned} \mathbf{M}\ddot{\mathbf{u}} + \mathbf{C}\dot{\mathbf{u}} + \mathbf{K}\mathbf{u} &= \mathbf{P} \\ \text{with:} & \\ \mathbf{P} &= \sum_{j=1}^{N_{\text{jog}}} \mathbf{N}^T(x_j)F_j(t) \end{aligned} \quad (10.2)$$

Since each jogger has a corresponding location every jogger has a shape function vector to transfer the forces to the nodes of the bridge. They are constructed in exactly the same way and are denoted as $\mathbf{N}(x_j)$ for the j^{th} jogger. Note that the location of the jogger depends on the start location and velocity.

To be able to implement multiple joggers including Human-Structure Interaction using the MSD model some changes are needed. In section 6.3 the model including HSI is described for 1 jogger. This resulted in two equivalent matrix describing the coupled equation of motion, 6.24 and 6.29. Both these equation can be expended for multiple joggers. Here equation 6.24 will be used, since this equation gives a direct expression for the force between jogger and bridge, see equation 6.17.

When multiple joggers are considered in the MSD model every jogger will be an additional degree of freedom. So the combined system now has $(N+N_{\text{jog}})$ degrees of freedom. The vector \mathbf{u} is now defined as a column vector with the degree of freedoms of the bridge and the degrees of freedom of the joggers:

$$\begin{Bmatrix} \mathbf{u}_{N \times 1} \\ \mathbf{y}_{N_{\text{jog}} \times 1} \end{Bmatrix} \quad (10.3)$$

For every jogger the interaction force will be similar: a part for the force $G(t)$, a part for the leg stiffness k_p and a part for the leg damping c_p . Therefore, every jogger has an influence on the damping and stiffness matrix \mathbf{C} and \mathbf{K} . This results in the following equation of motion:

$$\begin{bmatrix} \mathbf{M}_b & \mathbf{0}_{N \times N_{\text{jog}}} \\ \mathbf{0}_{N_{\text{jog}} \times N} & \mathbf{m}_p \end{bmatrix} \begin{Bmatrix} \ddot{\mathbf{u}} \\ \ddot{\mathbf{y}} \end{Bmatrix} + \begin{bmatrix} \mathbf{C}_b + \mathbf{c}^* & \mathbf{C}_{12} \\ \mathbf{C}_{21} & \mathbf{c}_p \end{bmatrix} \begin{Bmatrix} \dot{\mathbf{u}} \\ \dot{\mathbf{y}} \end{Bmatrix} + \begin{bmatrix} \mathbf{K}_b + \mathbf{k}^* & \mathbf{K}_{12} \\ \mathbf{K}_{21} & \mathbf{k}_p \end{bmatrix} \begin{Bmatrix} \mathbf{u} \\ \mathbf{y} \end{Bmatrix} = \begin{Bmatrix} \mathbf{P}_b(t) \\ \mathbf{0}_{N_{\text{jog}} \times 1} \end{Bmatrix} \quad (10.4)$$

The pedestrian mass matrix \mathbf{m}_p is described as (the same holds for the the pedestrian damping \mathbf{c}_p and stiffness \mathbf{k}_p matrices):

$$\mathbf{m}_p = \text{diag}[m_{p,j}] \quad \text{for } j = 1, \dots, N_{\text{jog}} \quad (10.5)$$

The additional parts added to the damping and stiffness of the bridge are the summation of each jogger. So these are described as:

$$\begin{aligned} \mathbf{c}^* &= \sum_{j=1}^{N_{\text{jog}}} c_{p,j} \mathbf{N}^T(x_j) \mathbf{N}(x_j) \\ \mathbf{k}^* &= \sum_{j=1}^{N_{\text{jog}}} c_{p,j} v_j \mathbf{N}^T(x_j) \mathbf{N}_x(x_j) + k_{p,j} \mathbf{N}^T(x_j) \mathbf{N}(x_j) \end{aligned} \quad (10.6)$$

The cross terms of the stiffness and damping matrices describe the coupling between the bridge and each jogger. For the upper right quadrants, parts $\mathbf{C}_{12}, \mathbf{K}_{12}$, this means that every column of the $(N \times N_{\text{jog}})$ matrix is corresponding to a specific jogger. So these are defined as:

$$\begin{aligned} \mathbf{C}_{12}[1, \dots, N; j] &= -c_{p,j} \mathbf{N}^T(x_j) \\ \mathbf{K}_{12}[1, \dots, N; j] &= -k_{p,j} \mathbf{N}^T(x_j) \end{aligned} \quad (10.7)$$

For the lower left quadrants, parts $\mathbf{C}_{21}, \mathbf{K}_{21}$, this means that every row of the $(N_{\text{jog}} \times N)$ matrix is corresponding to a specific jogger. Resulting in:

$$\begin{aligned} \mathbf{C}_{21}[j; 1, \dots, N] &= -c_{p,j} \mathbf{N}(x_j) \\ \mathbf{K}_{21}[j; 1, \dots, N] &= -c_{p,j} v_j \mathbf{N}_x(x_j) - k_{p,j} \mathbf{N}(x_j) \end{aligned} \quad (10.8)$$

The force vector is also expended to the new degrees of freedom. In this model no force is acting on the mass of the joggers. Therefore, the forcing vector consists of the nodal forces due to the load of the joggers on the bridge, $\mathbf{P}_b(t)$, and zeros for the degrees of freedom of the joggers.

10.2. Multiple joggers - Input

For this multiple jogger cases a deterministic analysis is done, similar to that of chapter 8. Every jogger has the same dynamic properties that are defined as the mean value of the probability distributions. The most unfavourable case will be considered where all joggers have a step frequency equal to the fundamental eigenfrequency of the bridge. So for each jogger:

- $m_{p,j} = 78.2 \text{ kg}$
- $c_{p,j} = 957.9 \text{ Ns/m}$
- $k_{p,j} = 32.9 \text{ kN/m}$
- $f_{s,j} = f_n \text{ Hz}$
- $v_j = 3 \text{ m/s}$
- $F(t)$, Bachmann load model

According to the Dutch national annex it is allowed to model all joggers at the same location. This can be seen as a giant jogger moving along the bridge, which can be modelled by 1 mass-spring-damper

combined with a force. This is a unrealistic load cases, but it is a simplification that lowers the amount of calculation cost. However, this simplification will have an effect on the response of the bridge. To see what effect the distribution of joggers on the bridge has on the response the following three cases will be considered:

1. 1 giant jogger, representing 10 joggers at the same location
2. 5 jogger pairs, 2 side-by-side with a gap of 1.5 m to the next two joggers
3. 10 single joggers, one after the other with a gap of 1.5 m between every jogger

10.3. Multiple joggers - Result

Results of MF model

The maximum accelerations due to the three different load cases are:

- 1 giant jogger
→ $a_{max} = 31.32 \text{ m/s}^2$
- 5 jogger pairs
→ $a_{max} = 30.07 \text{ m/s}^2$
- 10 single joggers
→ $a_{max} = 28.13 \text{ m/s}^2$

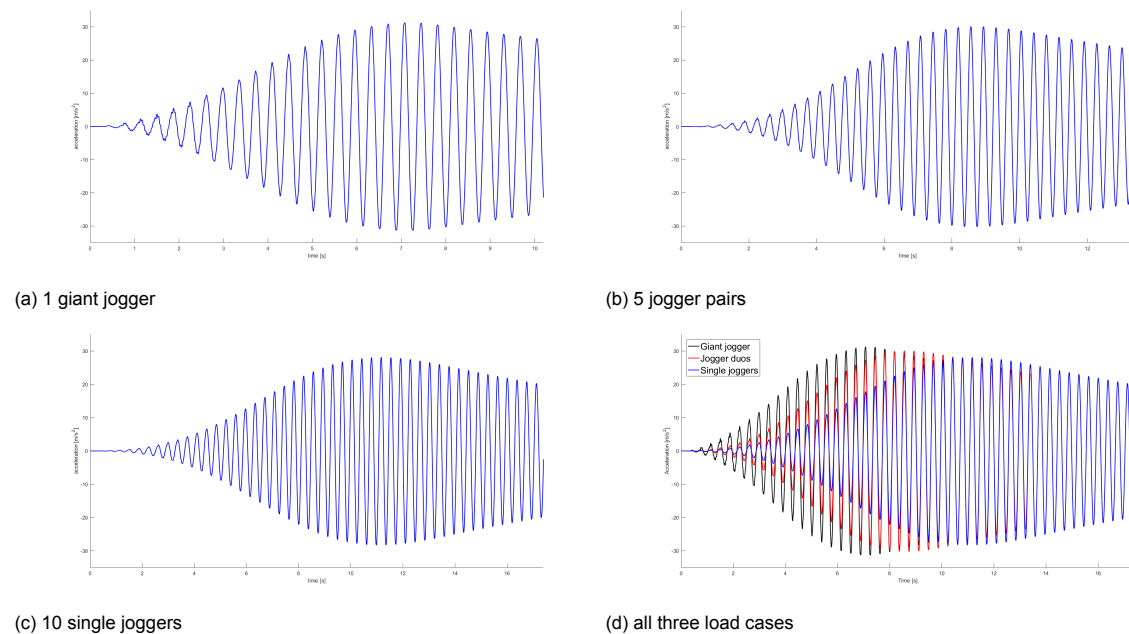


Figure 10.1: acceleration due to the **MF** model for three different distributions of 10 joggers (NOTE: the time axis of the three cases differ)

Looking at the maximum acceleration, it can be seen that it decreases when the joggers are more widely distributed along the length of the bridge. Compared to the 10 joggers at one location, so the giant jogger, the reduction in maximum is 4.0% for the jogger pairs and 10.2% for the single joggers. Looking at the accelerations over time, the global behaviour is similar. Due to the distribution along the length of the bridge it takes more time for the bridge to reach the maximum acceleration, this can be seen in figure 10.1d. For the single jogger case investigated in chapter 8 high frequency vibrations where visible at the beginning. For the giant jogger case, this is again visible. When the 10 joggers are more widely distributed these high frequency vibrations decrease.

Results of the MSD Model

For the MSD model the maximum accelerations for the three cases are:

- 1 giant jogger
→ $a_{max} = 14.76 \text{ m/s}^2$
- 5 jogger pairs
→ $a_{max} = 13.75 \text{ m/s}^2$
- 10 single joggers
→ $a_{max} = 13.10 \text{ m/s}^2$

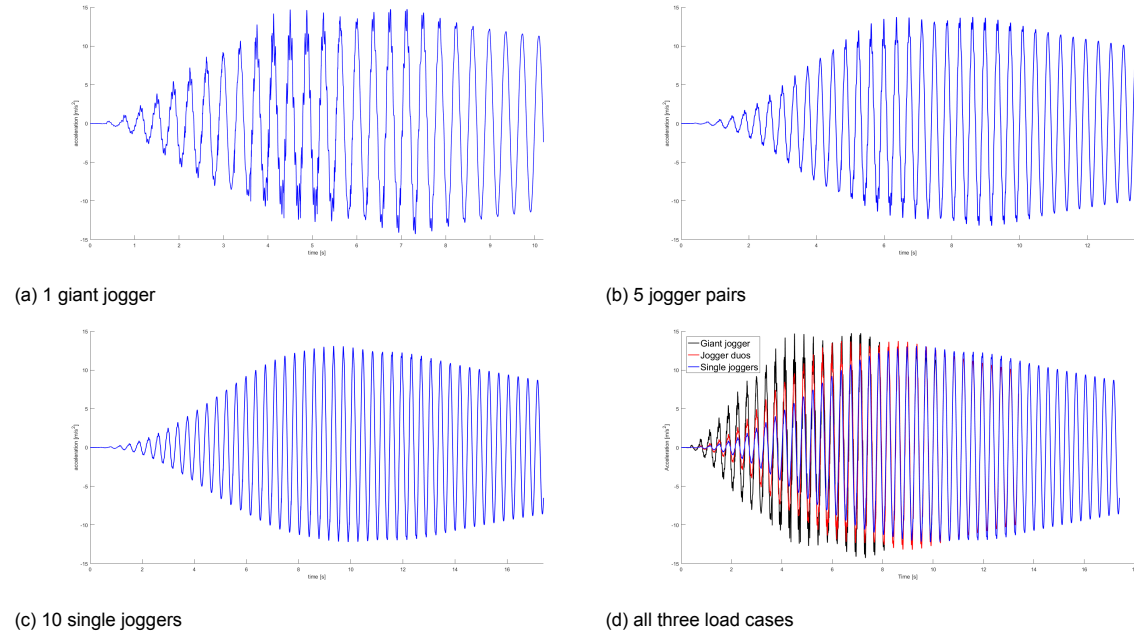


Figure 10.2: acceleration due to the **MSD** model for three different distributions of 10 joggers (NOTE: the time axis of the three cases differ)

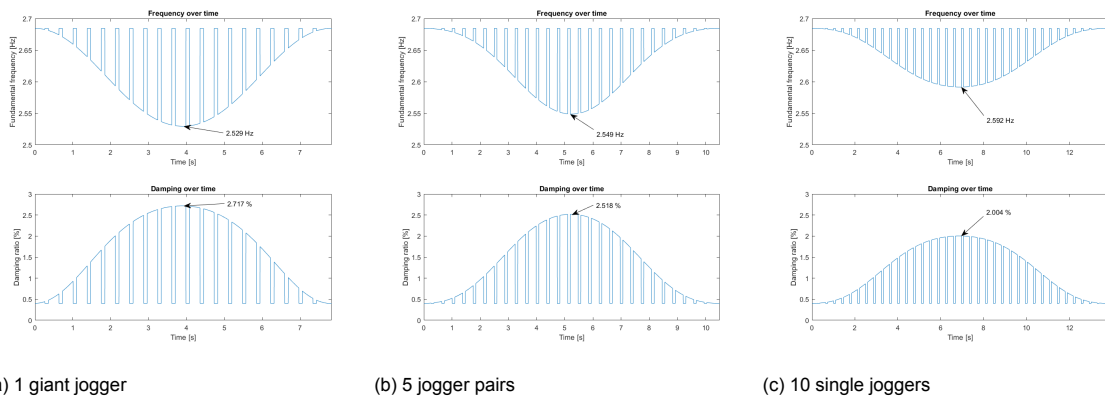


Figure 10.3: Damping and Frequency over time for the fundamental mode for three different distributions of 10 joggers according to the **MSD** model, plotted until the last jogger crossed the bridge.

For the MSD model it can also be seen that the maximum acceleration reduces when the joggers are more distributed. Comparing with the joggers at one location, the reduction is 6.2% for the jogger pairs and 11.8% for the single joggers. The maximum is also found later in time as was the case in the MF model.

Looking at the time history of the accelerations it can be seen that the patterns are different for the three distributions. For the giant jogger case (see figure 10.2a) two observation are noticeable. Firstly, in the global behaviour 2 maxima can be seen in the accelerations. Secondly, large high frequency

vibrations can be seen. This raises the question if the model is acting correctly in describing this load case. Therefore, some additional research is done to check the results. This can be found in 10.3.1. For the 5 jogger pairs distribution (see figure 10.2b), again the two maxima and the high frequency vibrations can be seen. However, the two effects are smaller compared to the giant jogger case. For the 10 single joggers, the two maximum are almost completely gone and the pattern is similar to the MF model result. Only a small disturbance around $t = 12$ seconds can be seen. The high frequency vibrations that was found for the other two distributions is not present any more.

The MSD model also influences the frequency and damping of the bridge. The distribution of the joggers will have an influence on this effect. In figure 10.3 the effect on the first eigenmode of the bridge is shown. For all three cases the frequency is lowered and the damping is increases when the joggers are on the bridge. It can be seen that if the joggers are spaced more along the bridge length the lower the effect on the frequency and damping is. For all three cases the increase in damping is significant knowing that the modal damping without joggers is 0.4%.

10.3.1. Research to check MSD model results

Since the results of the MSD model for the giant jogger and the 5 jogger pairs shows unexpected results some more research is done to check if it is correct. The first step is to make sure the numerical ordinary differential equation solver, ODE45, is working sufficiently. This was done by reducing the tolerance of the solver, but this did not change the results. Another solver of Matlab, ODE113, is also considered since this is a multi-step solver. This solver is capable of reaching higher precisions compared to ODE45. However, using this the higher accuracy numerical solver also resulted in the same large high frequency vibrations.

The separation and reconnecting of the Mass-Spring-Dashpot oscillator representing the jogger may be a problematic event. To see if this causes the high frequency behaviour the following is done and resulted in figure 10.4:

- Mass-Spring-Dashpot model
- Bachmann load model
- moving jogger
- MSD oscillator always connected to the bridge

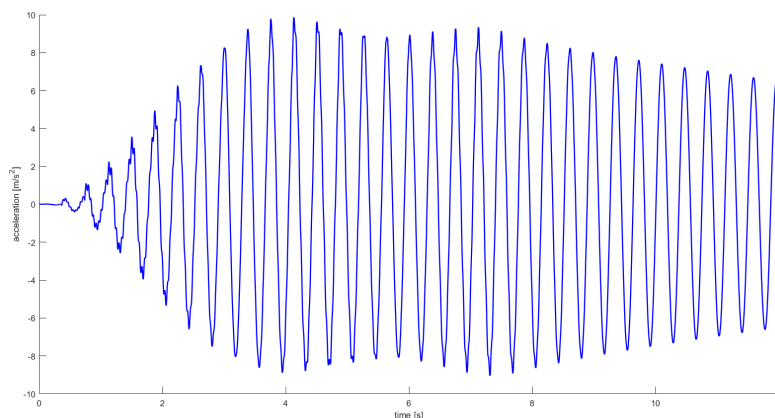


Figure 10.4: Accelerations due to the MSD model with **Bachmann** load model without separation of the MSD oscillator describing 1 giant jogger moving across the bridge

Note that neglecting the separation leads to an decrease in maximum acceleration of $14.76 - 9.87 = 4.89$ m/s^2 , which is 33% lower.

It can be seen that the large high frequency vibrations are not present when the MSD oscillator of the jogger is not separated from the bridge. Therefore, this behaviour is caused by the dis- and reconnecting of the two systems. In the model this separation is made by eliminating the cross terms in the \mathbf{M} , \mathbf{C} and \mathbf{K} matrices. Which is done by setting the global shape vector to zero. This means we have decoupled the bridge and the joggers. No constraints are made on the behaviour of the jogger and no load is applied on the jogger, this means that it will keep moving until the connection is made again (if the force is not equal to zero). This means that the relative distance and velocity between the bridge and the jogger can be different at the beginning of each step.

It is important to keep in mind that the Mass-Spring-Dashpot oscillator does not represent the complete jogger. This model is based on the assumption that the force of each step is not influenced by the movement of the bridge. The MSD oscillator only describes the effect of the jogger on the movement of the bridge. To put it in the correct terms, it describes the H2SI and not the S2HI.

It is possible that the unrestricted behaviour of the disconnected jogger causes the large high frequency behaviour. However, it is unclear how to model the behaviour of the jogger when it is separated from the bridge. A 'restricted' model is made to still be able to see if the unrestricted behaviour results in the large high frequency vibrations. In this 'restricted' model the MSD oscillator is separated from the bridge when the force is zero, as was also done for the unrestricted model. At that point the velocity of the jogger is set to zero and the displacement is set equal to the displacement of the bridge. Physically this is the same as that every step a 'new' oscillator is added. This means that the additional forces due to the relative displacement and velocity at the time of reconnection is zero. For a single jogger with mean values for the mass, damping and stiffness this two different models result in the following accelerations over time:

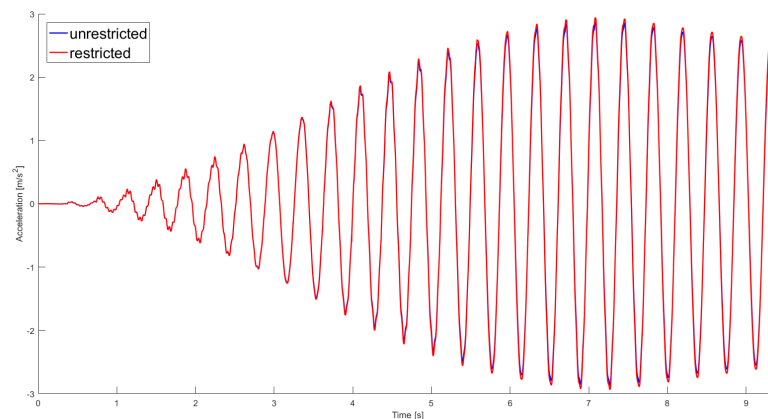


Figure 10.5: The accelerations due to the unrestricted and restricted model describing the behaviour of the jogger when separated from the bridge

As can be seen in the midspan acceleration of the model with and without the restriction of the joggers behaviour there are no large differences. The maximum acceleration of the unrestricted model is 2.87 m/s^2 as found in chapter 8. For the restricted model (every step a new MSD oscillator) this is changed to 2.90 m/s^2 , so it increased about 1%. The difference in maximum displacement of the jogger for the unrestricted and 'restricted' model is about 0.005 m , so the difference is limited. Therefore, it can be said that this influence is negligible for the 1 jogger load cases that were used in this research.

It is now found that the influence of the 'restricted' behaviour is limited, but it may still cause the large high frequency behaviour. Therefore the giant jogger cases is also modelled with the restricted behaviour of the joggers during separation (see figure 10.6). This result still shows the large high frequency vibrations. This means that these vibrations are not caused by the unrestricted behaviour of the jogger oscillator during separation. The only explanation is the accuracy of the numerical solver. Changing the tolerance or using another ODE solver within Matlab was not the solution to this problem. However, the assumption of small vibrations is highly questionable for multiple joggers.

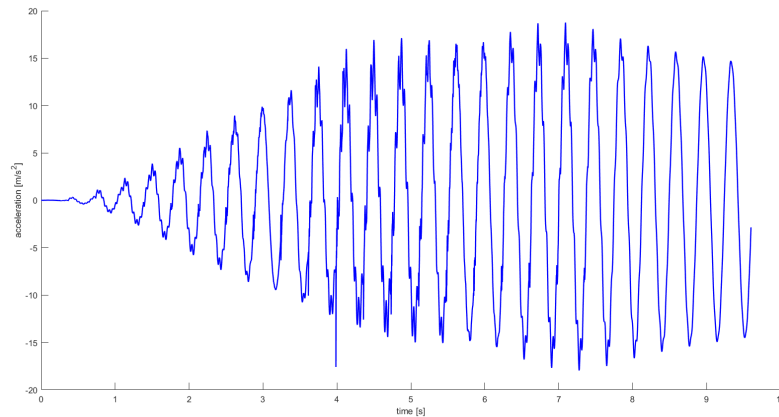


Figure 10.6: The giant jogger load case with restricted behaviour during separation

Looking at figure 10.6 larger acceleration are noted compared to the unrestricted model. An increase in maximum acceleration of $18.75 - 14.76 = 3.99 \text{ m/s}^2$. This difference can not be neglected as could be done for the single jogger case. It is not possible to consider one of the two models (restricted or unrestricted) to be better than the other, since it is unclear what behaviour is most realistic for the MSD oscillator to represent the Human-to-Structure Interaction.

The goal of the multiple jogger analysis in this chapter is to see what influence the distribution of joggers (along the length of the bridge) has on the response of the bridge. This is still relevant even though it is not completely sure what behaviour of the mass of the jogger during separation needs to be used.

The two global maxima are still found when the oscillator is not separated (see figure 10.4) and some small high frequency vibrations are still visible, especially in the beginning. These small high frequency vibrations are a result of the Bachmann load model, which was already found in chapter 7. To make sure the two global maxima are not a result of the Bachmann load model the MSD model without separation is also preformed with the JRC load model. This leads to the following result for the giant jogger case (10 joggers at the same location):

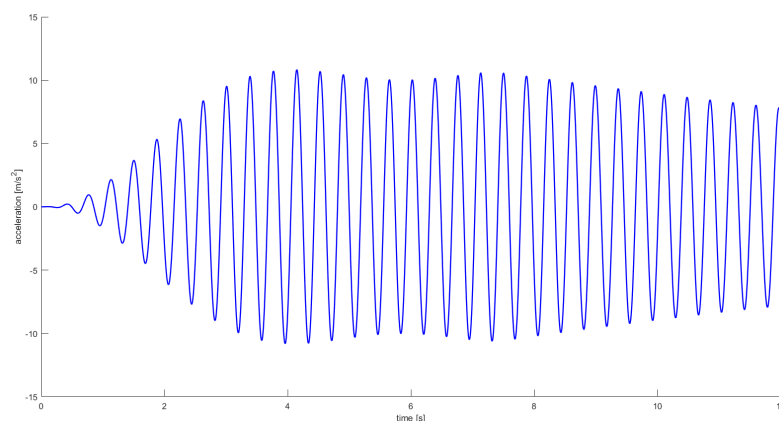


Figure 10.7: Accelerations due to the MSD model with **JRC** load model without separation of the MSD oscillator describing 1 giant jogger moving across the bridge

Applying the JRC load model shows that all high frequency vibrations are gone. So the two global maxima in the accelerations are not caused by the separation of the MSD oscillator or the load model.

The explanation of the two maxima can be found in the change in property due to the MSD model of the joggers (see figure 10.3). Due to the presence of the 10 joggers the eigenfrequency and damping change over time. The influence is maximal if the joggers are at midspan. For the 1 giant jogger case, considered here, the fundamental frequency is reduced from 2.681 to 2.529 Hz. However, the step frequency is set equal to the fundamental frequency of the empty bridge. This means that load is not acting with the fundamental eigenfrequency of the bridge, which reduces the response. This effect causes the two global maxima in the time history of the accelerations.

The acceleration results show that the response shows a decrease in the two maxima behaviour. For the 10 single joggers, one after the other, this behaviour was almost not visible. This corresponds with the smaller change in fundamental frequency for these load cases.

10.4. Comparison between MF and MSD model for multiple joggers

To investigate if the MF and MSD models are affected differently by the distribution of joggers a comparison is made. The maximum accelerations can be found in table 10.1. For all the three distribution an large decrease in maximum acceleration can be seen, around 53% reduction. It is important to note that the reduction is similar for every jogger distribution. This means that both the MF and MSD model are affected in a similar manner by the spatial distribution.

Table 10.1: Difference in maximum acceleration for different distributions of 10 joggers for the MF and MSD model

load case	a_{\max} [m/s ²]		difference [m/s ²]	difference [%]
	MF	MSD	MF - MSD	(MF-MSD)/MF
1 giant jogger	31.32	14.76	16.56	52.9%
5 jogger pairs	30.07	13.75	16.32	54.3%
10 single joggers	28.13	13.10	15.03	53.4%

10.5. Sub-conclusions

Three different distributions for 10 joggers were made to investigate what influence the distribution of joggers has on the HSI: the giant jogger, 5 jogger pair and 10 single joggers. The giant jogger case, where 10 joggers are modelled at the same location, is a simplification that has no realistic physical meaning. The joggers are all modelled equally and the step frequencies are all equal to the fundamental frequency of the empty bridge.

It can be concluded that for both the MF and MSD model the maximum acceleration decreases when the joggers are more widely distributed along the length of the bridge. A reduction between the giant jogger and the 10 single joggers was 10.2% and 11.4% for the MF and MSD, respectively.

For MSD model the distribution of the joggers also effects the fundamental frequency and damping of the bridge. As also seen for the single jogger case the frequency decreases and damping increases when the jogger is moving towards the middle of span. This influence is lowered when the joggers are more widely distributed. For the giant jogger and jogger pairs load cases these resulted in two global maxima in the accelerations time history, because the step frequency was always equal to the fundamental frequency of the bridge.

Applying the MSD model reduces the maximum acceleration compared to the MF model. For the different distributions the difference is between 53.9 and 54.3%. This is a large reduction, but the maximum acceleration according to the Dutch national annex comfort check of 0.7 m/s² exceeded with more than 14 m/s². The reduction for to the MSD model compared to the FM model is similar for all distributions of joggers. It can be concluded that for these conditions the Human-Structure Interaction is not effected by the distribution of joggers.

The MSD model shows large frequency vibrations for the giant jogger load case. The same can be seen in the results for the 5 jogger pairs but smaller. It was found that the separation of the MSD os-

illator causes these high frequency vibrations. Due to the large influence of the oscillators for these load cases, the numerical solver has problems finding realistic values.

For the MSD model including the separation between jogger and bridge, it is unclear what to do with the behaviour of the jogger during separation. As described in chapter 8, the separation is made by eliminating the cross terms of the mass, damping and stiffness matrix by setting the global shape vectors to zero. This means the jogger degree-of-freedom keeps moving after separation. This is called the unrestricted model. The second possibility is to add a new oscillator at the beginning of every step, without an initial relative displacement or velocity. The so called restricted model. For the single jogger case there is a negligible difference between the results of this unrestricted and 'restricted' model. However, for the giant jogger case there is a significant difference of 3.99 m/s^2 , which is 27% of the maximum acceleration of the unrestricted model. Since it is unclear what behaviour represents the Structure-to-Human Interaction the best, it is impossible to judge at this point which model is most appropriate.

Neglecting the separation, which overestimates the HSI, results in a decrease of 4.89 m/s^2 on the maximum acceleration for the giant jogger case, which is 33%. For the single jogger case the decrease due to neglecting the separation was found to be negligible. Therefore, it can be concluded that modelling the separation is of increasing importance when the mass ratio of the jogger and bridge increase.

IV

Conclusions

11

Discussion

In this discussion the following points will be considered: 1) The limitations due to the 'initial' design, 2) the limitations of the Mass-Spring-Dashpot model in describing the Human-Structure Interaction and 3) the processing of the results.

Initial design limitation

The overall aim of this research is to contribute to the knowledge about dynamic jogger loading, so footbridges may be designed more slender. Therefore, a design basis which consists out of standard size girders and a constant cross section is chosen. This was chosen for the straight forward structural system, so a realistic combination of mass, stiffness and length was found for the design. However, due to the relatively low loads, compared to road traffic bridge, more different structural designs may be possible. The results found in this research are based on 1 design type, which means that they are not directly applicable for every footbridge. However, when a structural design can be estimated with a single span, simply supported bridge, the results are applicable. The amount of influence of the Human-Structure Interaction may be different since the mass, stiffness and dimensions of a design might change.

In the initial design only the global checks, the maximum stress due to global bending, the maximum deformation of global bending and vertical vibrations are considered. This is possible by simplifying the bridge in a 1-dimensional beam. This means that the transverse direction is not considered, statically and dynamically. For the static checks, the design must also be capable of supporting non-uniform loads. For the considered design this will be done using cross girders that distribute the forces towards the main girders. The presence of these additional girders is added in the self weight and so added to the vertical checks considered. However, the 1-dimensional simplification results in neglecting the torsional dynamical modes. The distribution of the joggers will have an effect on the bridge response when it is modelled as a 2-dimensional problem, since the torsional modes will also be affected by the loading. The 1-dimensional simplification is conservative for the vertical vibrations, but the torsional dynamic checks are not considered. If the torsional modes have a eigenfrequency that may coincides with the step frequency, they must be checked additionally.

Limitations of the Mass-Spring-Dashpot model

The Mass-Spring-Dashpot model is made to add the Human-Structure Interaction to the dynamical problem. However, it is based on the assumption that bridge vibrations are relatively small. This assumption is made so that the force induced by the pedestrian is equal to the force on a rigid floor. This means that the jogger mass acceleration is constant and therefore not affected by the motion of the bridge. Generally, when a pedestrian is walking on a flexible structure, the walking forces may be affected by the movement of the bridge. This is the so called Structure-to-Human Interaction. During small vibrations this effect is negligible. In that way the Mass-Spring-Dashpot oscillator can be added to simulate the Human-Structure Interaction. The assumption of small vibrations is plausible for a single jogger, but for multiple joggers the response of the bridge is found to be higher than the gravitational acceleration. It is highly questionable that the assumption still holds for multiple joggers. To check this

a model needs to be made where the Structure-to-Human Interaction is also considered. This can be done by a model where the force is applied on or a displacement is prescribed to the degree-of-freedom of the jogger. On a rigid floor this model should give the same result as the force models, but on a flexible structure the complete Human-Structure Interaction is implemented. It is important to keep in mind that both models are only applicable when the pedestrian is not altering the way walking due to large vibrations.

Whilst running a separation between the jogger and the bridge occurs. The Human-Structure Interaction will therefore be limited to the time the jogger is connected to the bridge. In the Mass-Spring-Dashpot model the separation is added by disconnecting the two dynamical systems when the applied force is zero. However, it is unclear if any restrictions on the movement of the joggers degree-of-freedom during separation needs to be added. It was found that for a single jogger, this restriction has a negligible influence on the behaviour of the bridge. However, when multiple joggers where on the bridge this effect can cause deviations in the response of the bridge. It is not possible to measure this displacement for a real jogger, since the model only represents the Human-to-Structure interaction. This problem can be solved using the model including the Structure-to-Human Interaction as described in the previous paragraph.

The Mass-Spring-Dashpot model shows large high frequency vibrations for the multiple jogger cases. This behaviour decreases when the joggers are more widely distributed along the length of the bridge. It is found that the separation of the MSD oscillator causes these high frequency vibrations. Due to the large influence of the oscillators for these load cases, the numerical solver has problems with finding realistic values. In this study the standard implemented numerical solver in Matlab is used. With the minimum tolerance and maximum refinement of the solver it still produces questionable large high frequency vibrations. Thus, the multiple jogger cases require additional research into the numerical solvers in order to obtain more confident results.

Processing of the results

As a result of the stochastic analysis a large variance in the maximum acceleration is found. The mean maximum acceleration for both models, including and excluding the Human-Structure Interaction, is significantly lower than the 95th percentile value. This is an effect of the step frequency variance and the sensitivity of resonance occurring. The 95th percentile is considered to be the design value to check the comfort criteria. In the Dutch national annex the comfort criteria states that the maximum vertical acceleration $a_{\max} = 0.7 \text{ m/s}^2$. This is the mid value of the comfort class CL2 defined in the Eurocode, which is a relatively strict criteria. Due to the large variance in the maximum acceleration caused by the subject variability, it might be more reasonable to use a less strict comfort class for the jogger load case.

The step frequency is set equal to the fundamental frequency of the bridge in the dynamic analysis of a footbridge under pedestrian loading. This is the most unfavourable situation for the bridge and leads to the largest response. A result of the Human-Structure Interaction is the decrease of the fundamental frequency of the bridge. The step frequency however, is kept equal to the fundamental frequency of the empty bridge. This means that the loading frequency is not equal to the eigenfrequency of the bridge, thus resulting in a lower amplitude of the response. So for the model including the Human-Structure Interaction the most unfavourable situation has a step frequency that changes over time, equal to the eigenfrequency of the bridge. This is extremely unlikely to happen. It is possible to imagine a realistic case where the step frequency is constant and slightly lower than the fundamental frequency of the empty bridge. This case can result in a larger response compared to the case where step frequency is equal to the frequency of the empty bridge.

12

Conclusion

As a conclusion of this research the main research question will be answered, after which other conclusions based on this research are mentioned. The main research question is:

”Is it possible to increase the maximum slenderness for a typical single span steel foot-bridge design when the dynamic jogger load case is considered as a moving model including separation and Human-Structure Interaction?”

In the Eurocode combined with the Dutch National annex a jogger load case must be considered for a design of a footbridge. In these documents a prescription is made on the load that needs to be applied, but nothing is mentioned about the dynamic interaction between the vertical movement of the bridge and the human body. So the human structure interaction is not considered in the code whilst the jogger load case is often governing for the maximum overall height over length ratio of a design. Based on a one-dimensional Finite Element beam model it can be concluded that the Human-Structure Interaction reduces the maximum acceleration. However, the reduction does not result in a maximum acceleration below the comfort criteria. Note that there is a steep increase in the maximum acceleration when the eigenfrequency is within the step frequency range. So the cases where the reduction due to the Human-Structure Interaction leads to acceptable maximum accelerations are extremely limited. Therefore, it can be concluded that including the Human-Structure Interaction generally does not lead to an increase in maximum slenderness of the design.

Other conclusions that can be drawn from this research are listed below. The numbers and percentages are based on the used initial design. This initial design is a 'typical' slender design for a span 23.5 m. The constant cross section consists out of 4 HEA320 profiles with a 15 mm steel structural deck. These numbers serve as an example to get a better feeling of the conclusions. All the results are based on jogger properties (mass, damping and stiffness) equal to mean values of their probability distribution and the step frequency is equal to the fundamental frequency of the empty bridge, except for the stochastic analysis.

- The simplified load model in which the jogger load is applied stationary at midspan overestimates the response for a jogger running across the bridge. For the initial design the maximum acceleration is 2.4 times larger than the moving load case. This overestimation reduces when the span length of the bridge increases, since the loading time increases.
- When a single jogger load case is modelled including the separation between jogger and bridge whilst running, the Human-Structure Interaction reduces the maximum acceleration. For the initial design an reduction of 8.3% was found.
- There is a reduction in the Human-Structure Interaction due to the separation between jogger and bridge whilst running. Since this separation is part of the running behaviour an underestimation of the maximum acceleration can be made when this is not considered. For the initial design, the single jogger case showed a negligible underestimation, but for the giant jogger case,

representing 10 joggers at the same location, a underestimation of 33% has been made. Thus, it is concluded that when the jogger-to-bridge mass ratio increases, the underestimation of the maximum acceleration becomes bigger. Therefore, it is important to consider the separation for lightweight bridges and load cases with multiple joggers when the Human-Structure Interaction is included.

- The human variability results in a large variance of maximum acceleration of the bridge deck. This is mainly caused by the step frequency, not by the human dynamic properties (mass, stiffness and damping). Therefore, it is acceptable to do a stochastic analysis with the step frequency as the only stochastic parameter. For the initial design this reduced stochastic analysis resulted in a 95th percentile acceleration of 2.57 m/s² compared to 2.58 m/s² for the 'fully' stochastic analysis. The 95th percentile acceleration is considered for the comfort criteria check. This means that the probability of exceeding that value is 5%.
- The spatial distribution of joggers along the length of the bridge results in a decrease of the maximum acceleration, both for the models with and without Human-Structure Interaction. For the model including Human-Structure interaction the fundamental frequency decreases and damping of the bridge increases. These changes are smaller when the joggers are more widely distributed. The Human-Structure Interaction reduces the maximum acceleration for multiple joggers. This was expected, since this was seen for a single jogger case. The reduction is increased significantly when multiple joggers are on the bridge. For the initial design the MSD model result in a reduction of approximately 53%. The spatial distribution of the joggers has a negligible effect on the Human-Structure Interaction.

13

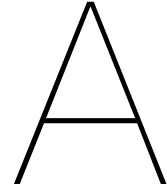
Recommendations

Based on the discussion and conclusion the following recommendations for further research can be made:

- The results and conclusions in this research are all based on a numerical model. This model is verified only for walking behaviour, so without separation between the jogger and the bridge deck. Therefore, it is important to verify the results of the jogger numerical model with measurements. Further research is recommended so that the different parameters can be verified. Therefore, a measurement research should be conducted on a constructed bridge. The first step is to calibrate a Finite Element model with the measured characteristics of the bridge. Different joggers will be running over the bridge measuring the response of the bridge and the behaviour of the human. Based on the human information the damping and stiffness parameters during running can be estimated. Using these parameters, the MSD model can be verified with the acceleration measurements of the bridge.
- It is recommended to add a Mass-Spring-Dashpot oscillator into available FEM programs. This will result in more practical implementation of the Mass-Spring-Dashpot model into engineering practise. Allowing to easily implement it in more dimensional finite element models. It will also result in easier implementation of different numerical solvers to investigate the accuracy. Another beneficial result will be an increase of the calculation speed.
- In this research the assumption was made that the response of the bridge remains small so that the force of the pedestrian is not changed. For the multiple jogger load case this assumption is highly questionable due to the large accelerations. Therefore, it is recommended to construct a model that is not based on this assumption. This can be done by a model where the force is applied on or a displacement is prescribed to the degree-of-freedom of the jogger. On a rigid floor this model should give the same result as the force models, but on a flexible structure the complete Human-Structure Interaction is implemented.
- It is recommended to do more research on the multiple jogger load cases including Human-Structure Interaction. The stochastic analysis for the single jogger case shows a large variance in the response. It is expected that this variance will increase when a stochastic analysis is done for the multiple jogger cases. It is recommended that the step frequency and a phase shift will be modelled as stochastic parameters.

V

Appendices



Impulse of force models

Impulse is defined as the integral of a force, F , over the time interval, T . To compare the JRC and Bachmann load model, both are calculated with a step frequency of 3 Hz. Therefore, the time interval will be set to be the period of the step frequency $T = 1/f_s = 1/3$ seconds.

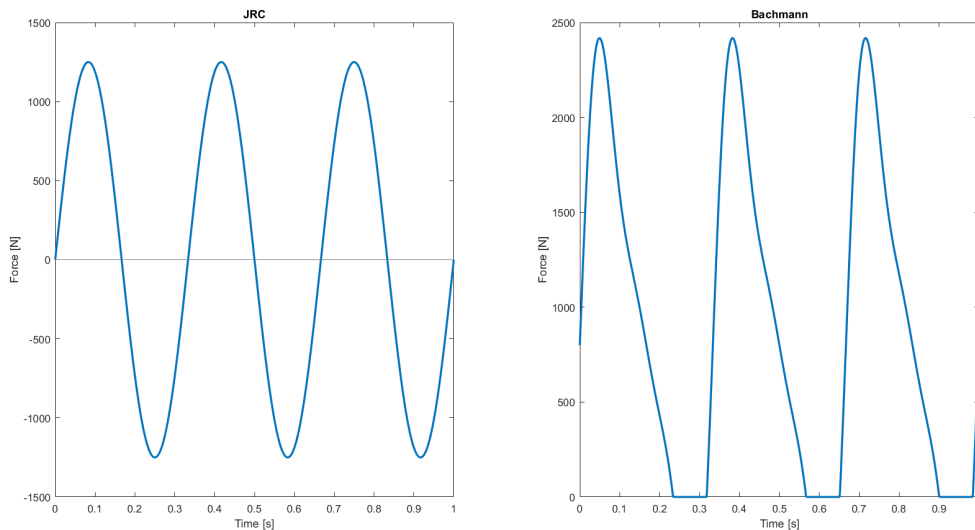


Figure A.1: JRC and Bachman load for a step frequency of 3 Hz

JRC load model The JRC load model is defined to be:

$$F_{\text{JRC}}(t) = 1250 \sin(2\pi f_s t) \quad (\text{A.1})$$

Since the force of the JRC load is negative over half of the period (see figure A.1), the integral is calculated for $0 < t < T/2$ and multiplied by 2. This results in the following

$$2 \cdot \int_0^{T/2} F_{\text{JRC}}(t) dt = 2 \cdot \int_0^{1/6} 1250 \sin(2\pi f_s t) dt = 265.3 \text{ N} \cdot \text{s} \quad (\text{A.2})$$

Bachmann load model The Bachmann load model is defined to be:

$$F_{\text{Bachmann}}(t) = \max \{ 800 \cdot (1 + 1.6 \sin(2\pi f_s t) + 0.9 \sin(4\pi f_s t) + 0.2 \sin(6\pi f_s t)) ; 0 \} \quad (\text{A.3})$$

The force of the Bachmann load model truncates all negative value to zero and has a value of 800 N at $t=0$ s (see figure A.1). To make a correct comparison, the Bachmann load first needs to be translated so that the $F=0$ N at $t=0$ s. Solving the equation $Bachmann = 0$ is found to result in a needed translation of $t_1 = 0.01548$ s. Using this updated Bachmann equation the impulse is found to be:

$$\begin{aligned}
 \int_0^T F_{Bachmann}(t) dt &= \\
 \int_0^{1/3} \max \{ 800 \cdot (1 + 1.6 \sin(2\pi f_s(t - t_1)) + 0.9 \sin(4\pi f_s(t - t_1)) + 0.2 \sin(6\pi f_s(t - t_1))), 0 \} dt & \\
 = 309.0 \text{ N} \cdot \text{s} &
 \end{aligned}
 \tag{A.4}$$

B

2DOF MSD model stationary - JRC load

Here the dynamical problem of a 'stationary' jogger at midspan with a Mass-Spring-Dashpot oscillator to account for the Human-Structure-Interaction is investigated. This is done by a modal analysis for the bridge to end up with a 2 degree-of-freedom problem.

The modal analysis for the bridge with a constant cross section leads to straight forward parameters. Since the jogger is located at midspan the fundamental mode will be used for modal analysis. The modal mass is described by:

$$m_b = \int_L \mu(\Phi(x))^2 dx = \frac{\mu L}{2} \quad [\text{kg}] \quad (\text{B.1})$$

The modal stiffness is described by:

$$k_b = m_b(2\pi f_n)^2 = 97.42 \frac{EI}{2L^3} \quad [\text{N/m}]$$

with:

$$f_n = \frac{9.87}{2\pi} \sqrt{\frac{EI}{\rho AL^4}} \quad [\text{Hz}] \quad (\text{B.2})$$

The modal damping is described by:

$$c_b = 2\xi\sqrt{k_b m_b} \quad [\text{Ns/m}] \quad (\text{B.3})$$

Note: In this these a damping ratio of 0.4% is used.

The coupled system of equations will then be:

$$\begin{bmatrix} m_b & 0 \\ 0 & m_p \end{bmatrix} \begin{Bmatrix} \ddot{u} \\ \ddot{y} \end{Bmatrix} + \begin{bmatrix} c_b & -c_p \\ -c_p & c_p \end{bmatrix} \begin{Bmatrix} \dot{u} \\ \dot{y} \end{Bmatrix} + \begin{bmatrix} k_b & -k_p \\ -k_p & k_p \end{bmatrix} \begin{Bmatrix} u \\ y \end{Bmatrix} = \begin{Bmatrix} 1250 \sin(2\pi f_s t) \\ 0 \end{Bmatrix} \quad (\text{B.4})$$

Similar to what is done for the complete analysis of the bridge, numerical integration is used to calculate the response at the next time step and so solving the system of equations.

Bibliography

- [1] Epoxy slijtlagen - smits neuchatel b.v. <https://www.smitsneuchatel.nl/nl/productensystemen/slijtlagen/epoxy-sn-ep-slurry>. Accessed: 04-05-2020.
- [2] Open data cbs: Lengte en gewicht sinds 1981. <https://opendata.cbs.nl/#/CBS/nl/dataset/81565NED/table?searchKeywords=lengte>. Accessed: 10-06-2020.
- [3] Footbridge ljubljana. <https://www.dezeen.com/2014/10/05/architektura-d-o-o-ribja-brv-footbridge-ljubljana-minimalist/>. Accessed: 05-11-2019.
- [4] Footbridge tuinveld. <https://www.nationalestaalprijs.nl/archief/2012/projecten/karakteristieke-stalen-bouwdelen/bruggen-tuinveld>. Accessed: 05-11-2019.
- [5] Venette dam footbridge. <https://structurae.net/en/structures/venette-dam/photos>. Accessed: 05-11-2019.
- [6] Lecture notes cie4140 tu delft. 2018.
- [7] Ehsan Ahmadi, Colin C. Caprani, and Amin Heidarpour. An equivalent moving force model for consideration of human-structure interaction. *Applied Mathematical Modelling*, 51, 2017. ISSN 0307904X. doi: 10.1016/j.apm.2017.06.042.
- [8] Ehsan Ahmadi, Colin Caprani, Stana Živanović, Neil Evans, and Amin Heidarpour. A framework for quantification of human-structure interaction in vertical direction. *Journal of Sound and Vibration*, 432:351–372, 2018. ISSN 10958568. doi: 10.1016/j.jsv.2018.06.054.
- [9] Adamantios Arampatzis, Gert Peter Brüggemann, and Verena Metzler. The effect of speed on leg stiffness and joint kinetics in human running. *Journal of Biomechanics*, 32(12):1349–1353, 1999. ISSN 00219290. doi: 10.1016/S0021-9290(99)00133-5.
- [10] Association Française de Génie Civil. Technical Guide: Footbridges. Assesment of vibrational behaviour of footbridges under pedestrian loading. *Sétra*, (october):127, 2006.
- [11] Colin C. Caprani and Ehsan Ahmadi. Formulation of human–structure interaction system models for vertical vibration. *Journal of Sound and Vibration*, 377:346–367, 2016. ISSN 10958568. doi: 10.1016/j.jsv.2016.05.015. URL <http://dx.doi.org/10.1016/j.jsv.2016.05.015>.
- [12] Hiep V. Dang and Stana Živanović. Modelling pedestrian interaction with perceptibly vibrating footbridges. *FME Transactions*, 41(4):271–278, 2013. ISSN 14512092.
- [13] B. R. Ellis and T. Ji. Floor vibration induced by dance-type loads: Verification, 1994. ISSN 00392553.
- [14] Claire T. Farley and Octavio González. Leg stiffness and stride frequency in human running. *Journal of Biomechanics*, 29(2):181–186, 1996. ISSN 00219290. doi: 10.1016/0021-9290(95)00029-1.
- [15] Marta García-Diéguez and Jose Zapico-Valle. Sensitivity of the Vertical Response of Footbridges to the Frequency Variability of Crossing Pedestrians. *Vibration*, 1(2):290–311, 2018. doi: 10.3390/vibration1020020.
- [16] Greish. Voetbruggen in lourdes. <https://www.greisch.com/nl/projet/voetbruggen-in-lourdes/>. Accessed: 05-11-2019.

- [17] Christoph Heinemeyer, Christiane Butz, Andreas Keil, Mike Schlaich, Arndt Goldack, Stefan Trometer, Mladen Lukić, Bruno Chabrolin, Arnaud Lemaire, Pierre-Olivier Martin, Álvaro Cunha, and Elsa Caetano. Design of Lightweight Footbridges for Human Induced Vibrations. Technical report.
- [18] Javier Fernando Jiménez-Alonso and Andres Sáez. Motion-based optimum design of a slender steel footbridge and assessment of its dynamic behaviour. *International Journal of Steel Structures*, 17(4):1459–1470, 2017. ISSN 20936311. doi: 10.1007/s13296-017-1215-8.
- [19] Klaus Lievens, Geert Lombaert, Guido De Roeck, and Peter Van den Broeck. Robust design of a TMD for the vibration serviceability of a footbridge. *Engineering Structures*, 2016. ISSN 18737323. doi: 10.1016/j.engstruct.2016.05.028.
- [20] Klaus Lievens, Geert Lombaert, Guido De Roeck, and Peter Van Den Broeck. Comparison of TMD designs for a footbridge subjected to human-induced vibrations accounting for structural and load uncertainties. In *Procedia Engineering*, 2017. doi: 10.1016/j.proeng.2017.09.381.
- [21] Y.-H. Lin and M. W. Trethewey. Finite Element To Analysis Moving of Elastic Dynamic Beams Loads. *Journal of Sound and Vibration*, 136(2):323–342, 1990.
- [22] Antonio Occhiuzzi, Mariacristina Spizzuoco, and Francesco Ricciardelli. Loading models and response control of footbridges excited by running pedestrians. *Structural Control and Health Monitoring*, (May 2011):n/a–n/a, 2011. ISSN 15452255. doi: 10.1002/stc.248. URL <http://dx.doi.org/10.1002/stc.456>.
- [23] Lars Pedersen and Christian Frier. Sensitivity of footbridge vibrations to stochastic walking parameters. *Journal of Sound and Vibration*, 2010. ISSN 0022460X. doi: 10.1016/j.jsv.2009.12.022.
- [24] V Ā Racic, A Pavic, and J M W Brownjohn. Experimental identification and analytical modelling of human walking forces : Literature review. 326:1–49, 2009. doi: 10.1016/j.jsv.2009.04.020.
- [25] Erfan Shahabpoor, Aleksandar Pavic, and Vitomir Racic. Interaction between Walking Humans and Structures in Vertical Direction: A Literature Review. *Shock and Vibration*, 2016:12–17, 2016. ISSN 10709622. doi: 10.1155/2016/3430285.
- [26] Federica Tubino and Giuseppe Piccardo. Serviceability assessment of footbridges in unrestricted pedestrian traffic conditions. *Structure and Infrastructure Engineering*, 12(12):1650–1660, 2016. ISSN 17448980. doi: 10.1080/15732479.2016.1157610. URL <http://dx.doi.org/10.1080/15732479.2016.1157610>.
- [27] Katrien Van Nimmen, Pieter Verbeke, Geert Lombaert, Guido De Roeck, and Peter Van Den Broeck. Numerical and experimental evaluation of the dynamic performance of a footbridge with tuned mass dampers. *Journal of Bridge Engineering*, 21(8):1–14, 2016. ISSN 10840702. doi: 10.1061/(ASCE)BE.1943-5592.0000815.
- [28] Felix Weber, Glauco Feltrin, and Olaf Huth. Guidelines for structural control. *Structural Engineering Research Laboratory, Swiss Federal Laboratories for Materials Testing and Research. Dübendorf, Switzerland*, (March):1–155, 2006. URL <http://citeseerx.ist.psu.edu/viewdoc/download?doi=10.1.1.121.3774{%&}rep=rep1{%&}type=pdf>.
- [29] Xiaojun Wei and Stana Živanović. Frequency response function-based explicit framework for dynamic identification in human-structure systems. *Journal of Sound and Vibration*, 422(March):453–470, 2018. ISSN 10958568. doi: 10.1016/j.jsv.2018.02.015.
- [30] S. Yao, J. R. Wright, A. Pavic, and P. Reynolds. Forces generated when bouncing or Jumping on a flexible structure. *Proceedings of the 2002 International Conference on Noise and Vibration Engineering, ISMA*, (September 2014):563–572, 2002.
- [31] Li-Qun Zhang, Dali Xu, Mohsen Makhsoos, and Fang Lin. Stiffness and viscous damping of the human leg. Technical report. URL <http://asbweb.org/conferences/2000/pdf/144.pdf>.

-
- [32] S. Živanović, I. M. Díaz, and A. Pavić. Influence of walking and standing crowds on structural dynamic properties. *Conference Proceedings of the Society for Experimental Mechanics Series*, (January), 2009. ISSN 21915644.
- [33] Stana Živanović. Probability-Based Estimation of Vibration for Pedestrian Structures due to Walking. (February):–, 2006.